Quantitative Texture Analysis

D. Chateigner
CRISMAT-ENSICAEN; IUT-UCBN
6 bd. M. Juin 14050 Caen

Outline

- Qualitative aspects of crystallographic textures
  - Grains, Crystallites and Crystallographic planes
  - Normal diffraction
- Effects on diffraction diagrams, their limitations
  - θ-2θ scans
  - Asymmetric scans
  - ω-scans (rocking curves)
- Representations of texture: pole figures
  - Pole Sphere
  - Stereographic projection
  - Equal-area projection: Lambert/Schmidt projection
- Pole figures
  - Localisation of crystallographic directions from pole figures
  - Direct and normalised pole figures
  - Normalisation
  - Incompleteness and corrections of pole figures
  - Single texture component
  - Multiple texture components
  - Pole figures and $(hk\ell)$ multiplicity
  - A real example

- Pole figure types
  - Random texture
  - Planar textures
  - Fibre textures
  - Three-dimensional texture
- Pole Figures and Orientation spaces
  - Mathematical expression of diffraction pole figures and ODF
  - From pole figures to the ODF
  - Orientations g and pole figures
  - Euler angle conventions
  - From f(g) to pole figures
  - Deal with ODF in the $\mathcal{G}$ space
  - Plotting the ODF
- Inverse pole figures
- ODF refinement
  - Generalised spherical harmonics
  - WIMV
  - Entropy modified WIMV and Entropy maximisation
  - ADC, Vector and component methods
  - ODF coverage
  - Reliability and texture strength estimators
- Magnetic QTA

Why needing QTA !!

- correcting texture effects
  - powder XRD
  - spectroscopic methods (P-EXAFS, ESR, Raman …)
- mollusc phylogeny, fossils
- predicting texture effect on macroscopic anisotropic properties
  - average to get macroscopic tensors
  - simulating elasticity, electric polarisation
  - Bulk Acoustic Waves
  - anisotropic magnetisation
- correlation texture - macroscopic anisotropic properties
  - Thermoelectric Power Factor
  - Pyroelectric coefficients
  - Tauc gap
  - Jc in superconductors
  - Levitation forces and trapped flux

But why classical QTA vanishes

Why needing Combined analysis

Minimum experimental requirements ….

Qualitative aspects of texture

- Polycrystal: aggregate of grains, different phases, sizes, shapes, orientations, stress state, crystallinity, faults …

- Diffraction:
  - probes lattice planes: crystallites, not grains
  - x-rays, neutrons or electrons

- SEM:
  - grains, not crystallites (coherent, single crystal domains)
  - shape vs crystallographic texture (EBSD)

Grains, crystallites, crystallographic planes

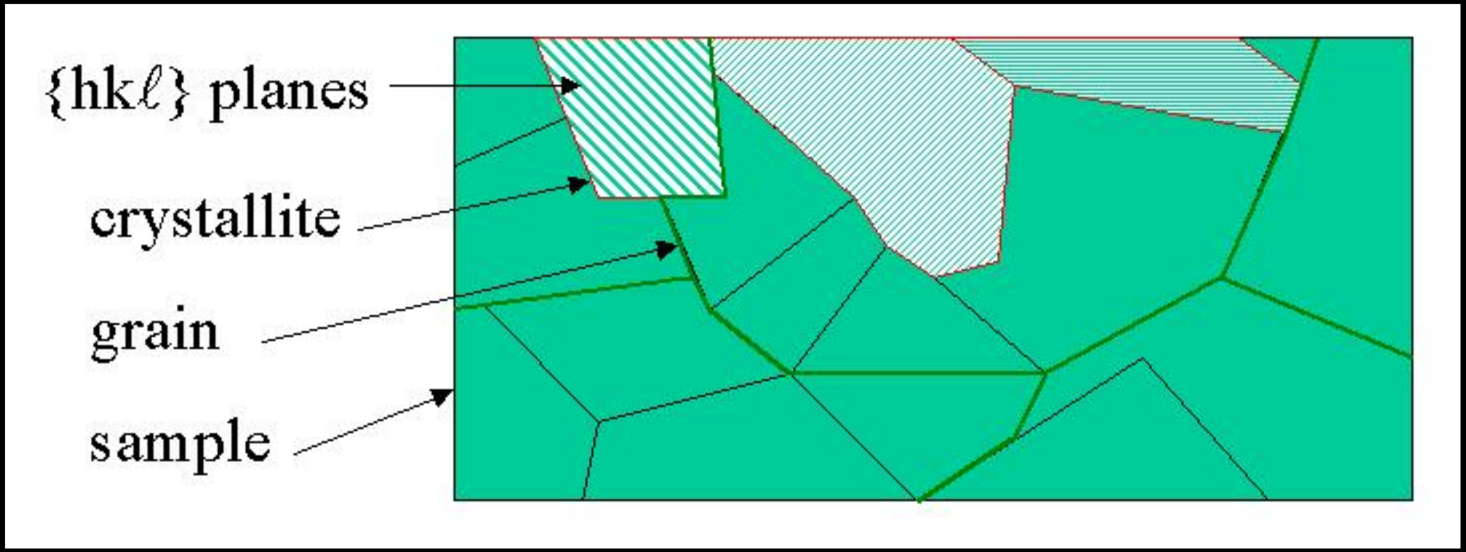

Friedel's law: $I_{hk\ell} = I_{-h-k-\ell}$ using normal diffraction
+ or - directions not distinguished

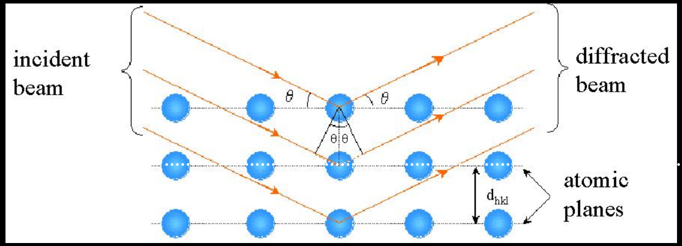

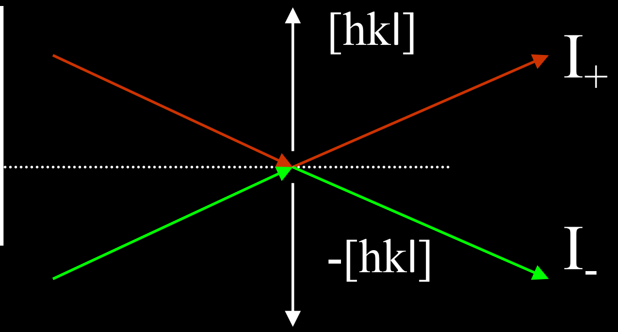

Texture effects on diffraction diagrams

θ-2θ scan: probes only parallel planes

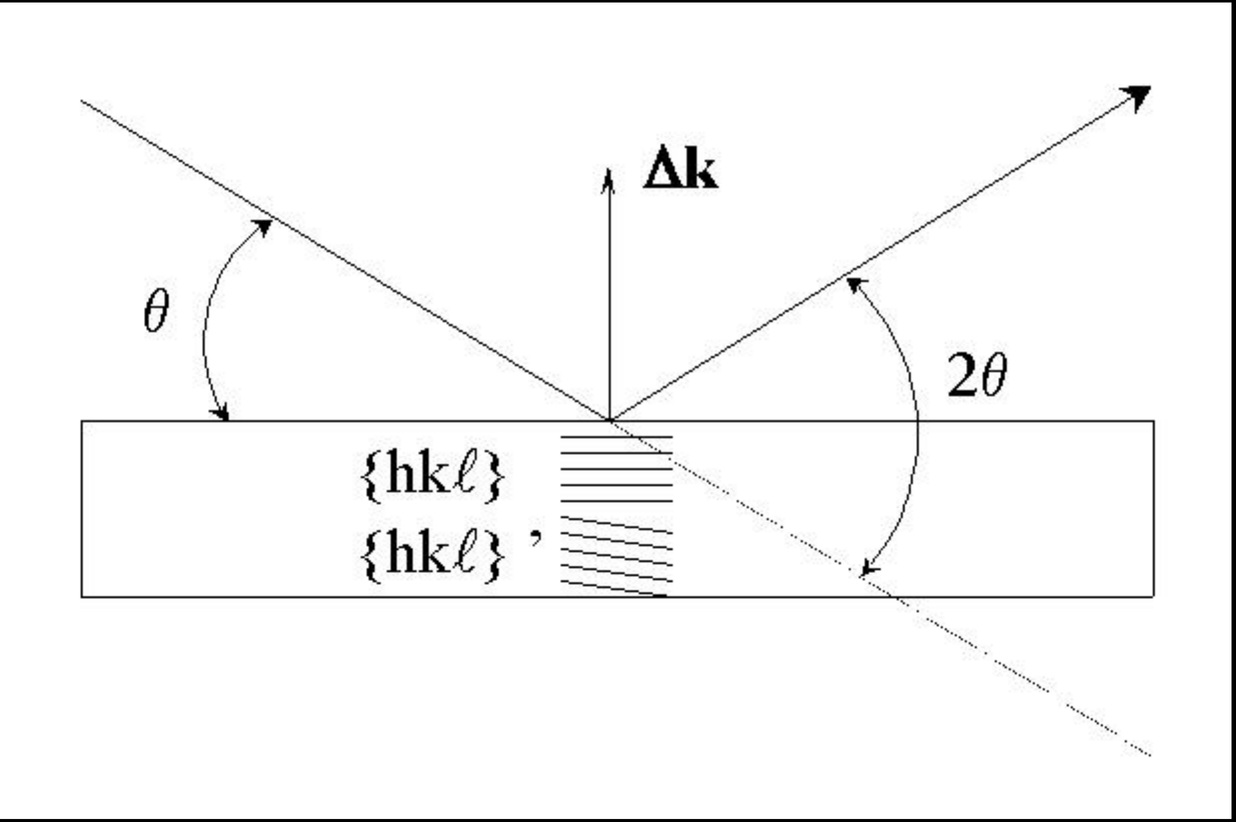

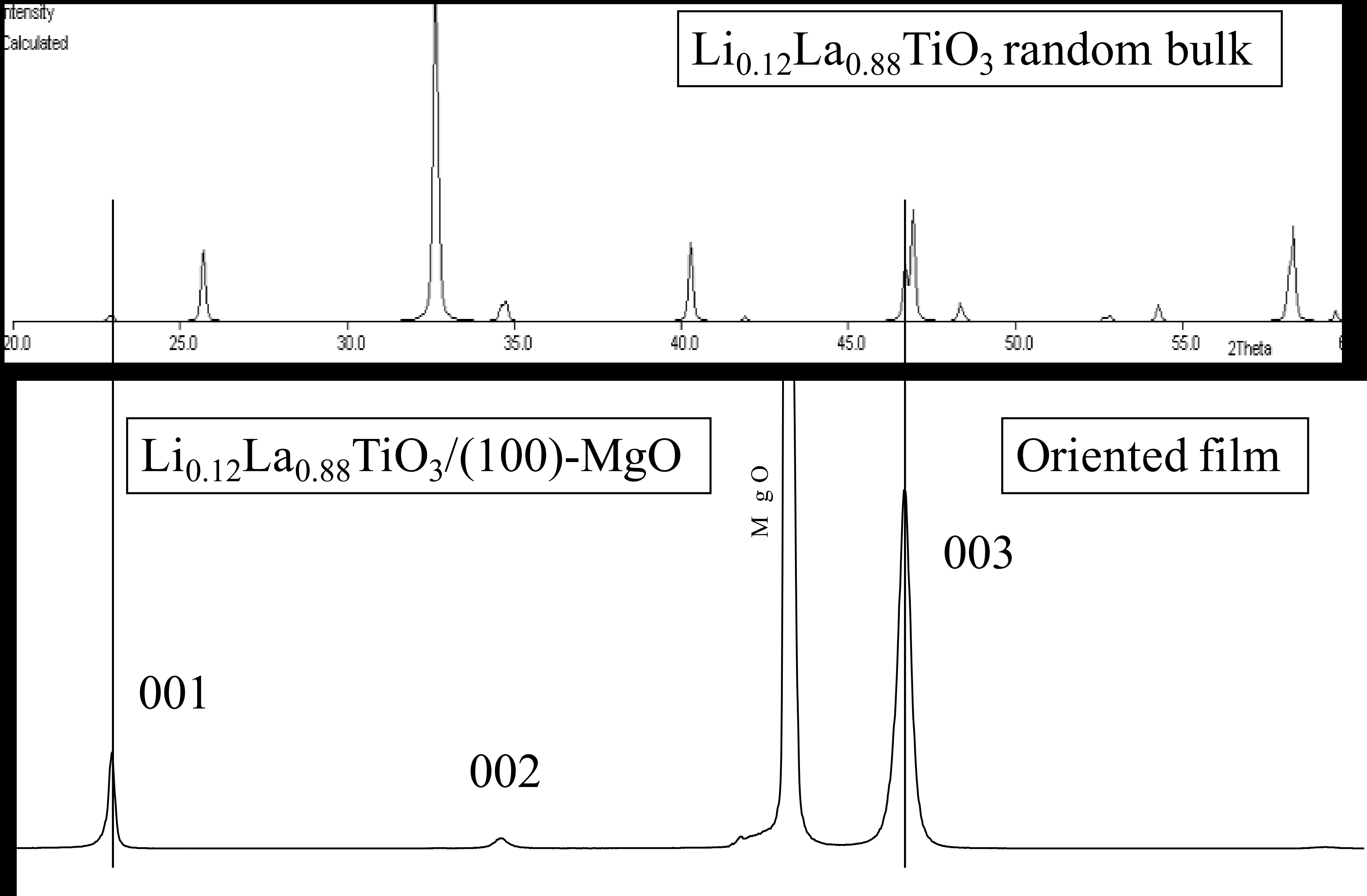

Intensity
Calculated
Li0.12La0.88TiO3 random bulk
20.0
25.0
30.0
35.0
40.0
45.0
50.0
55.0
2Theta
Li0.12La0.88TiO3/(100)-MgO
Oriented film
MgO
001
002
003

asymmetric scan: probes only inclined planes

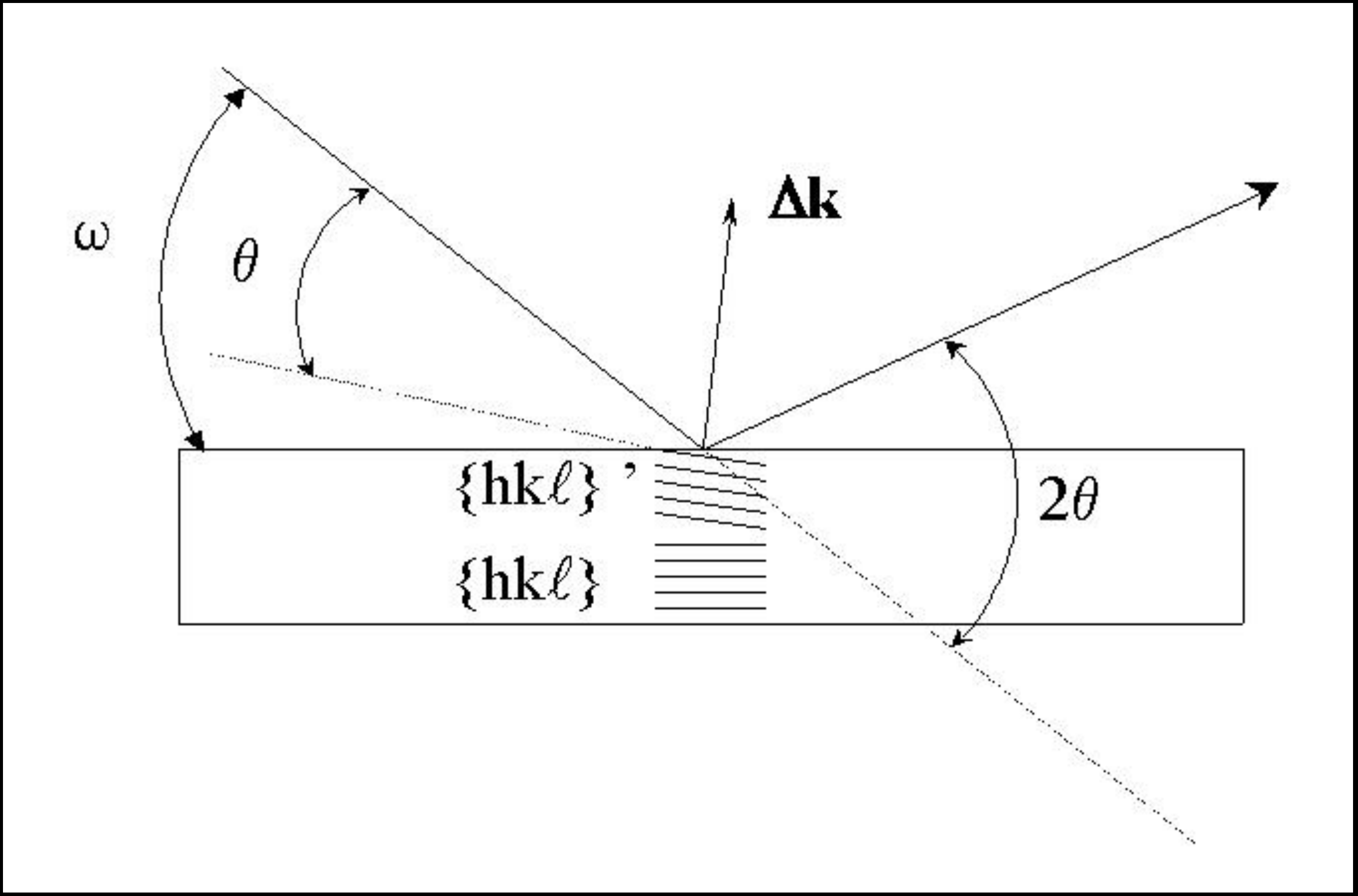

mixed scan: probes specific planes for specific orientations

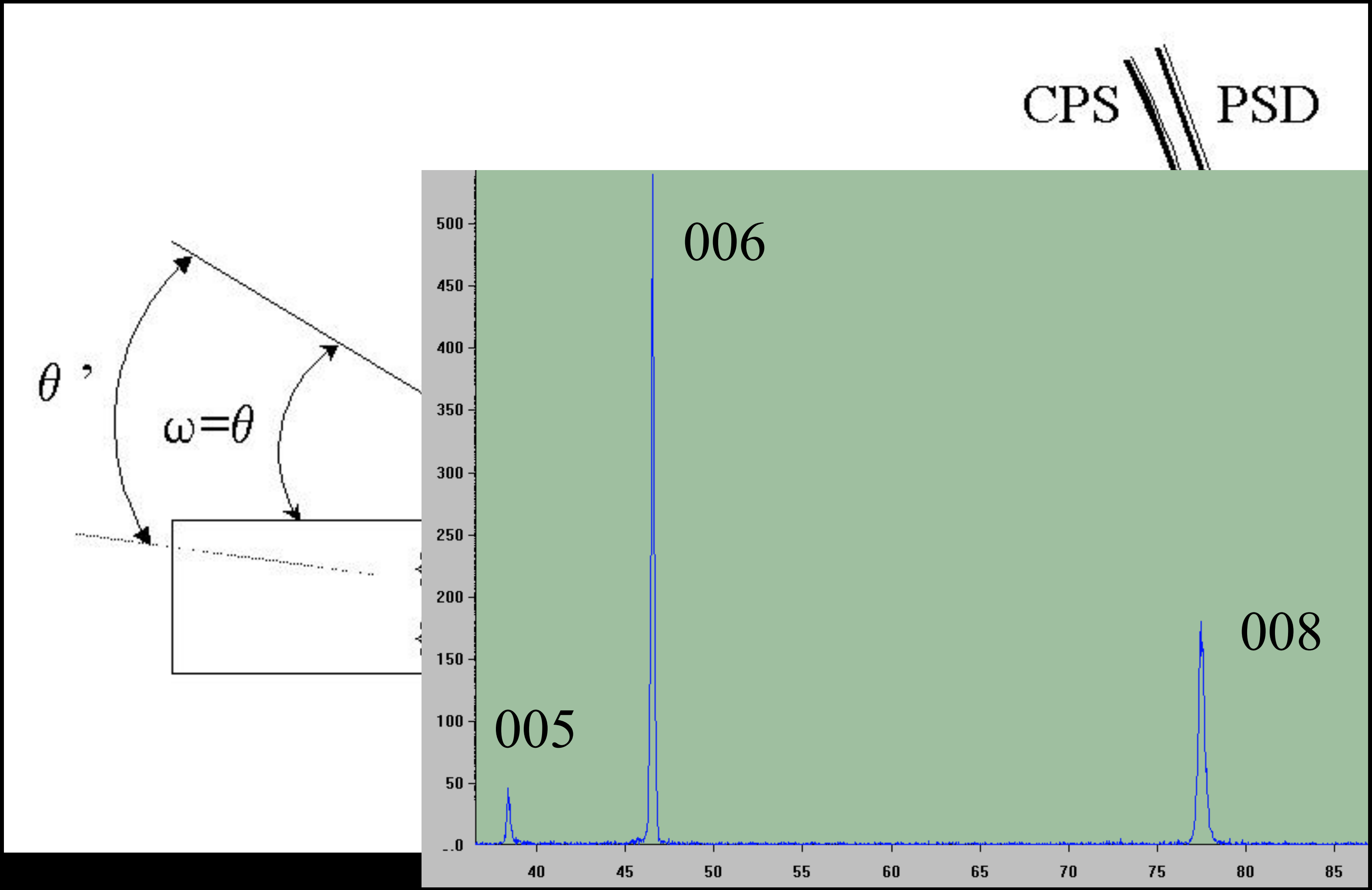

ω scan: probes orientation of only one plane type (fixed θ), only for small ω-θ

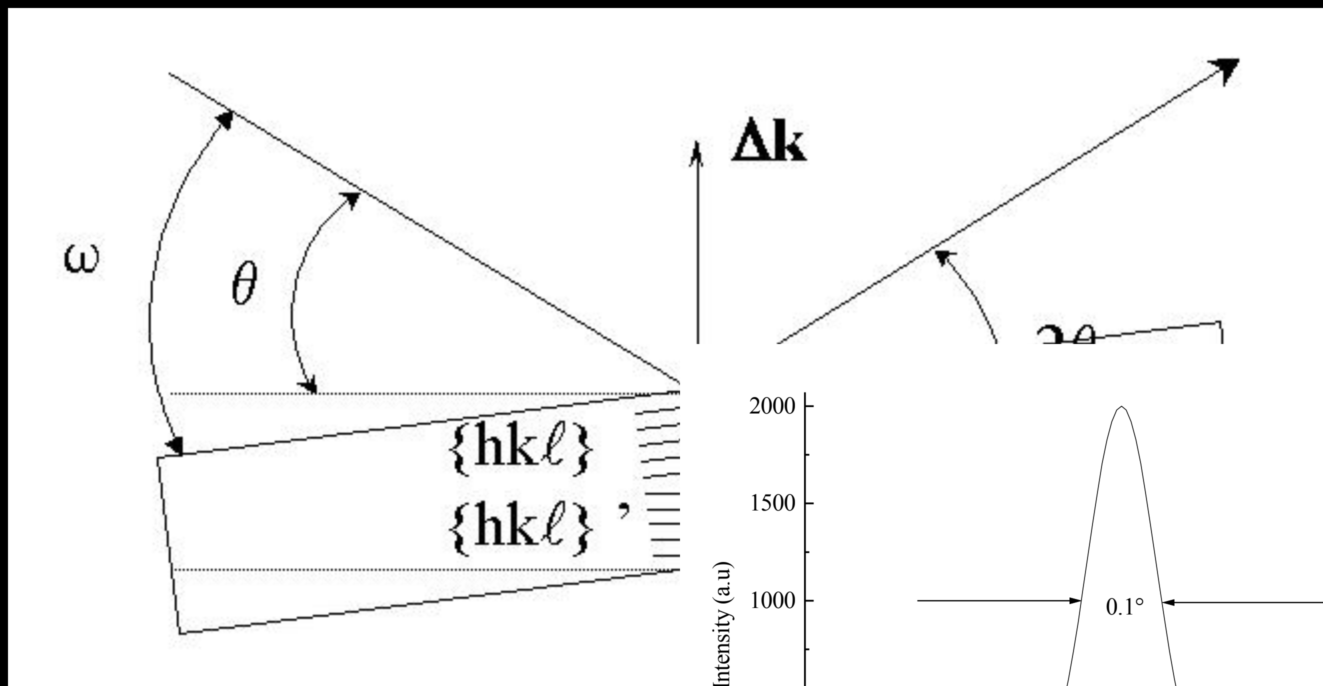

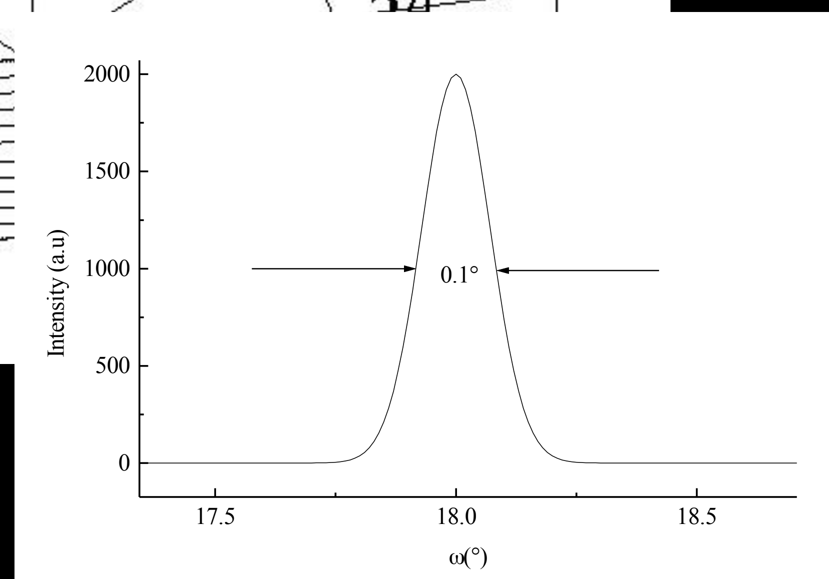

limitations: available θ (or other) range

diamond (Fd3m), 2.52 Å neutrons, up to 2θ = 150˚

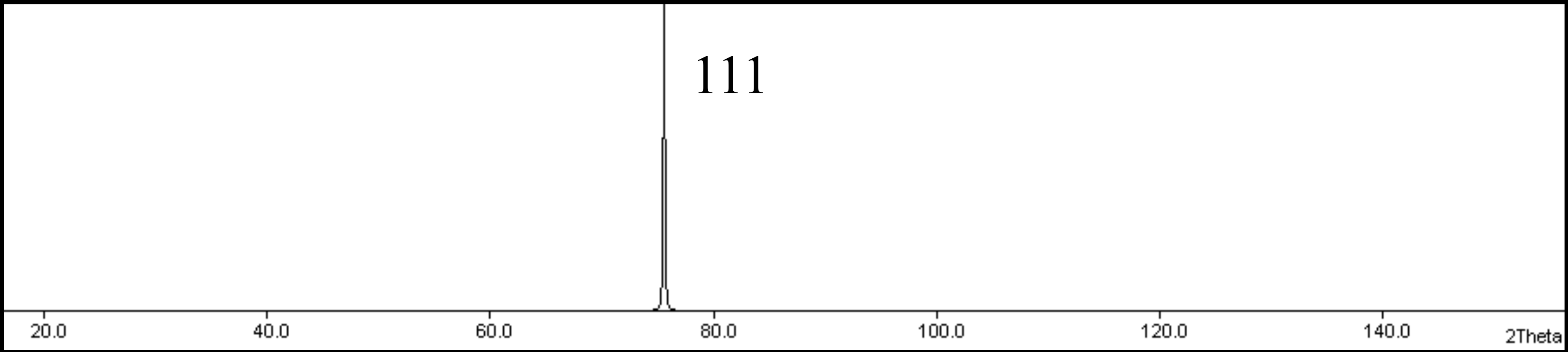

limitations: 2 texture components

same c-axes direction, but not same a-axes orientation

$$L_{hk\ell} = \frac{p - p_0}{1 - p_0} ; p_0 : random$$

$$p = \frac{\sum_i I\{00\ell\}_i}{\sum_{hk\ell} I\{hk\ell\}} = 1 = L_{00\ell}$$

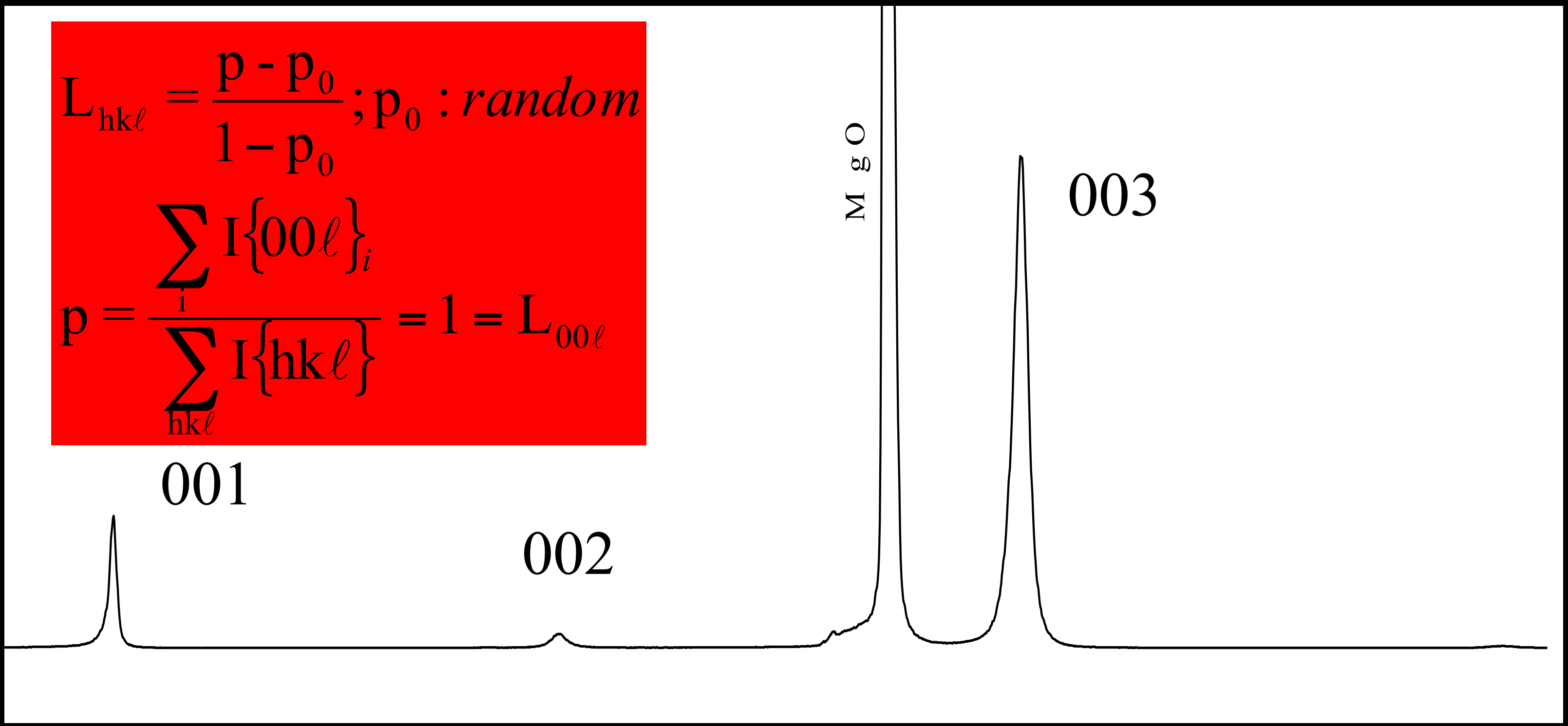

limitations: 2 texture components, one inclined

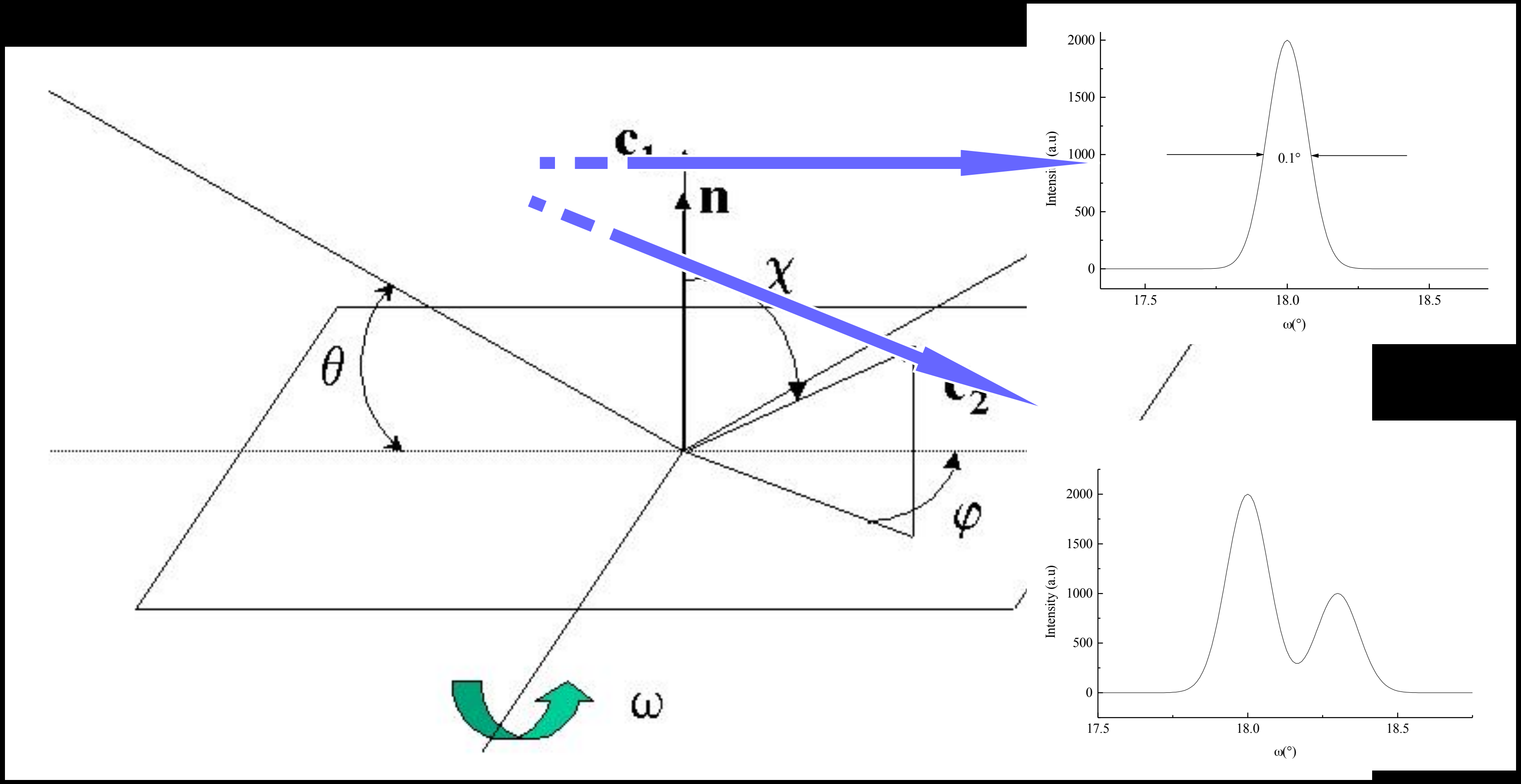

Representations of texture: pole figures

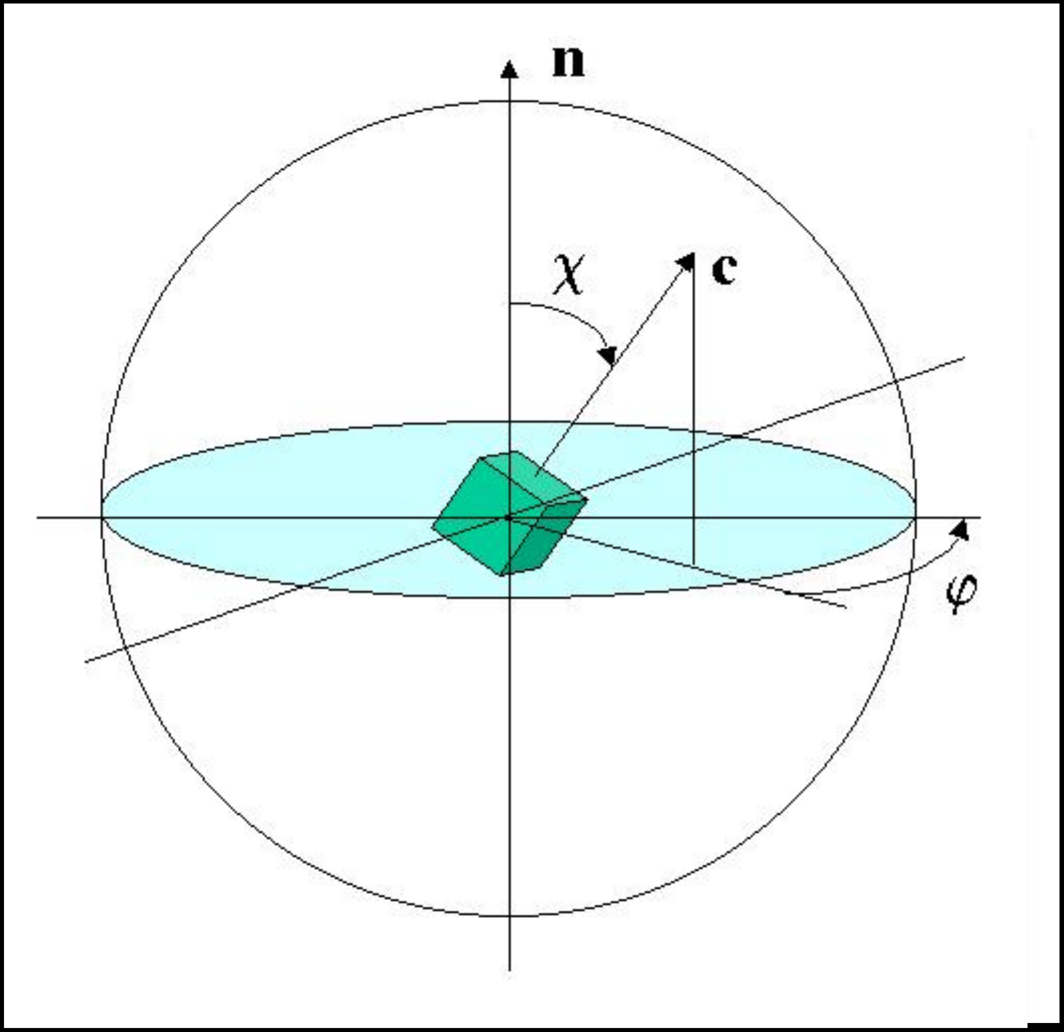

One crystallite oriented in the <u>Pole sphere:</u>

- location of all [hkl] ∈ unit sphere
- $dS = \sin\chi \, d\chi \, d\varphi$
- (χ,φ): angles in the <u>diffractometer space S</u>

Hard to visualise: needs <u>pole figures</u>

Stereographic projections: equal angle

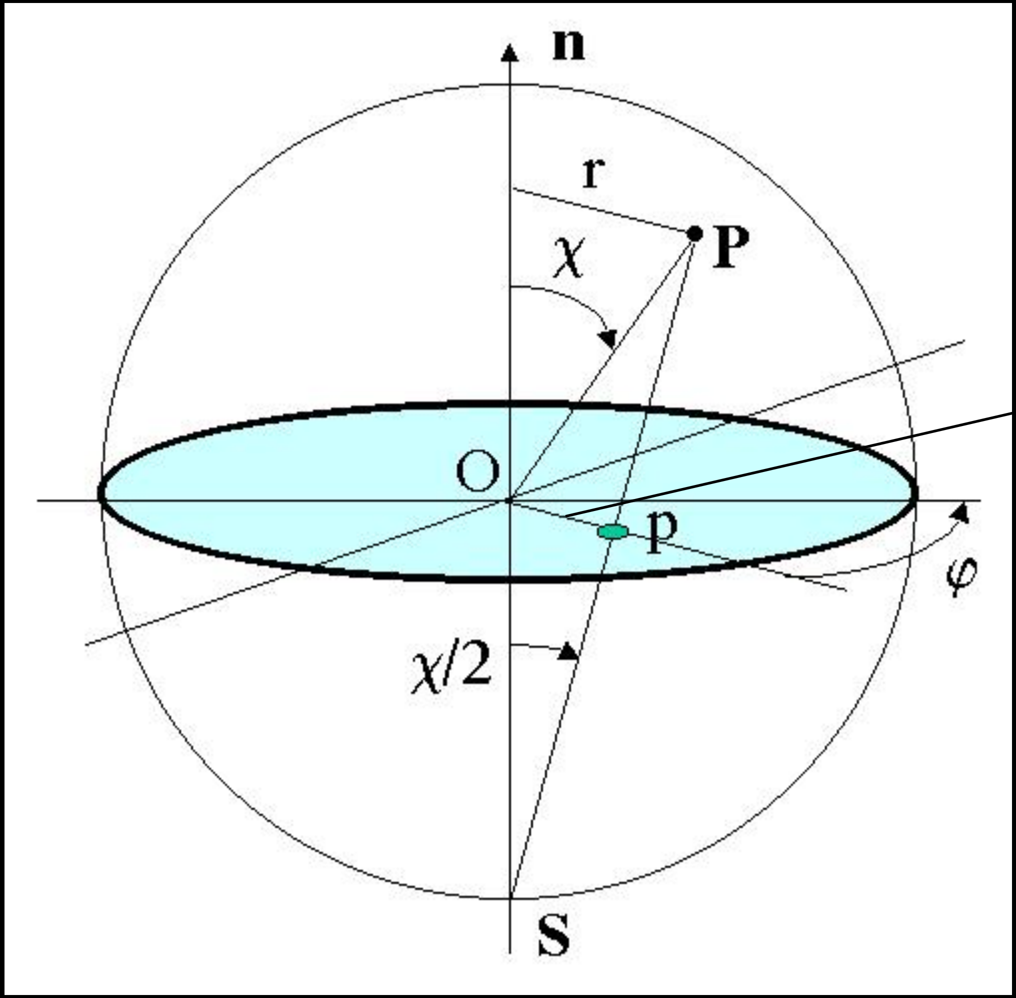

Poles: p(r',φ):

$r' = R \tan(\chi/2)$

Lambert projections (equal area)

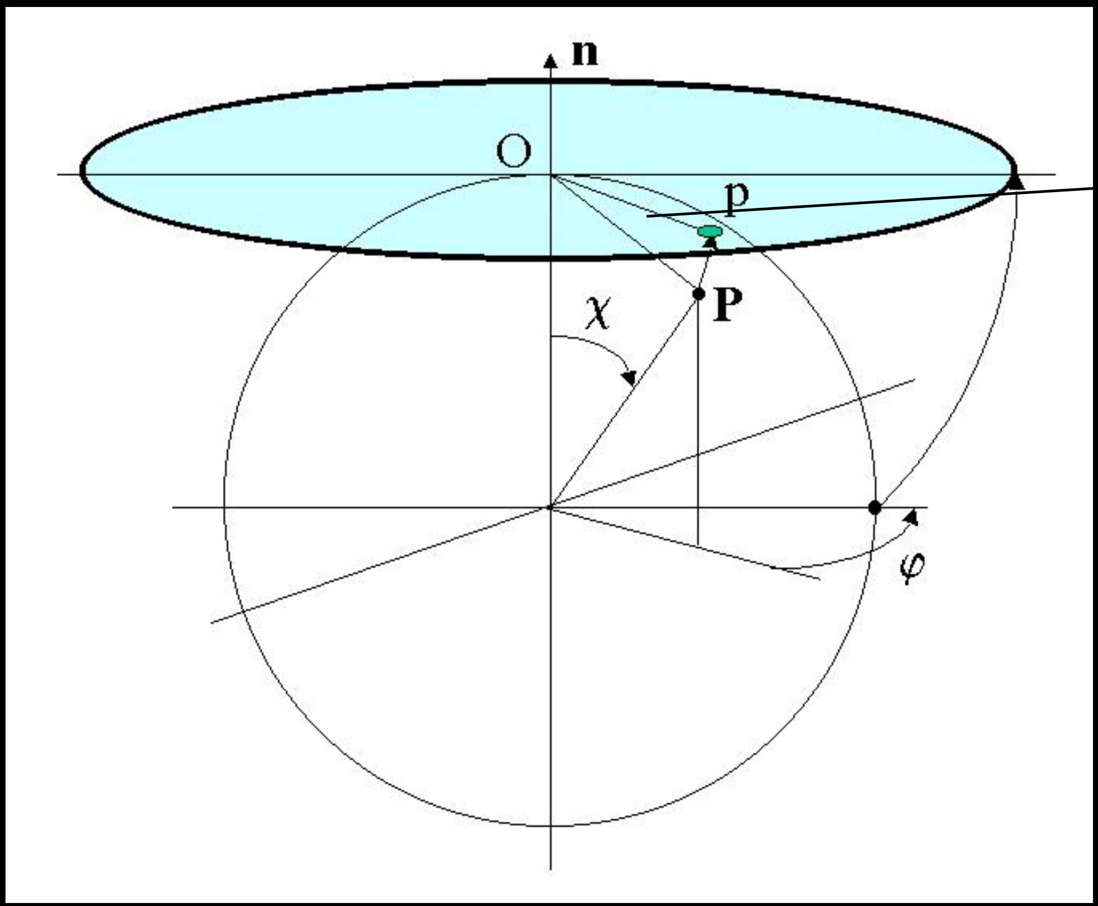

Poles: p(r',φ):

r' = 2R sin(χ/2)

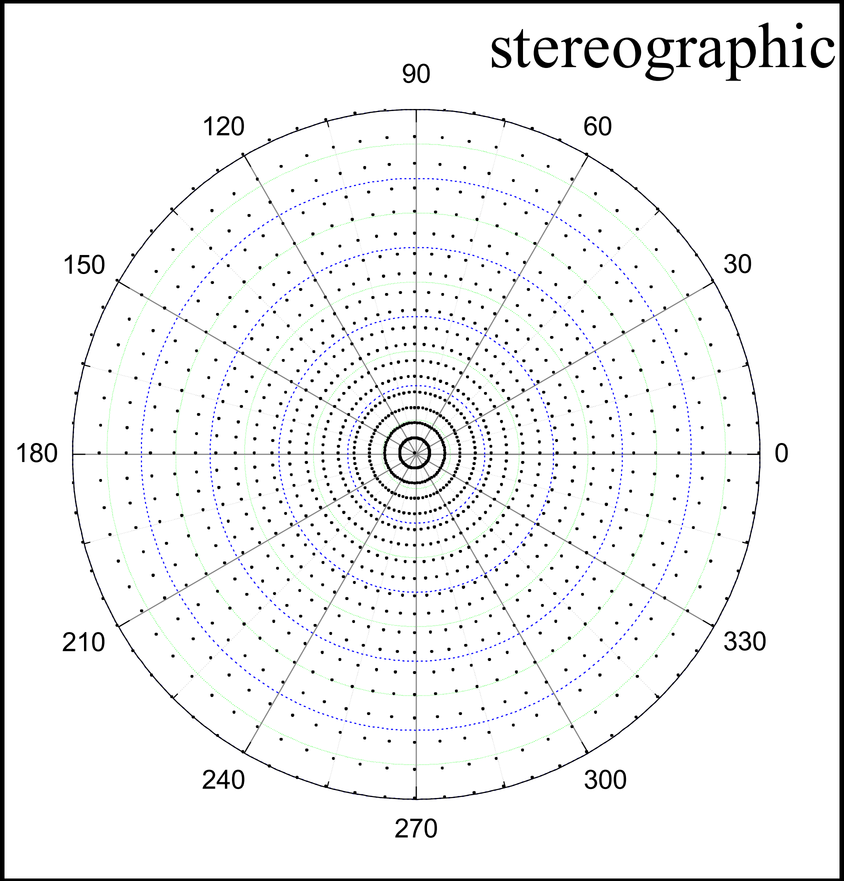

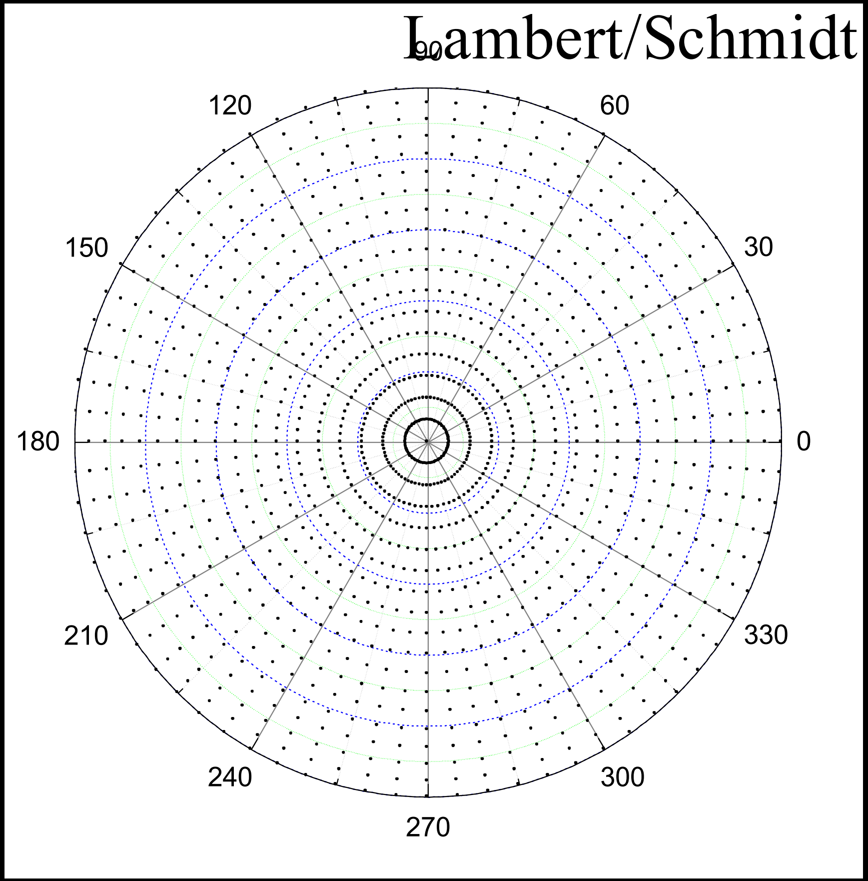

5° x 5° grid: 1368 points

Pole figures

{hkl}-Pole figure: location of distribution densities, for the {hkl} diffracting plane, defined in the crystallite frame K_B, relative to the sample frame K_A.

Pole figures space: Y, with $\mathbf{y} = (\vartheta_y, \varphi_y) = [hkl]^*$

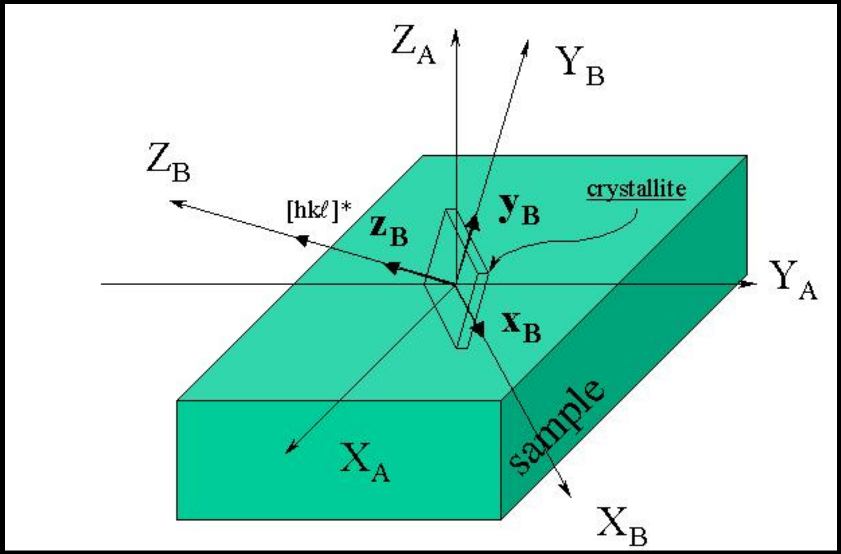

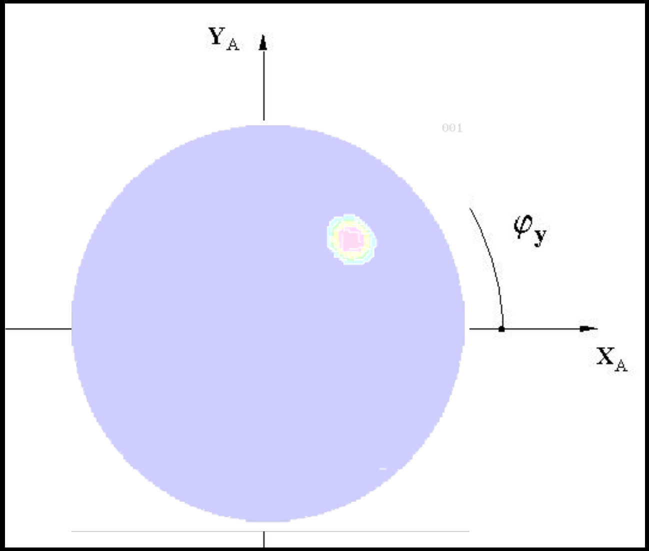

<u>Direct Pole Figure:</u> built on diffracted intensities $I_\mathbf{h}(\mathbf{y})$, $\mathbf{h} = \langle hk\ell \rangle^*$
<u>Normalised Pole Figure:</u> built on distribution densities $P_\mathbf{h}(\mathbf{y})$

Density unit: the "<u>multiple of a random distribution</u>", or "m.r.d."

Usual pole figure frames K_A

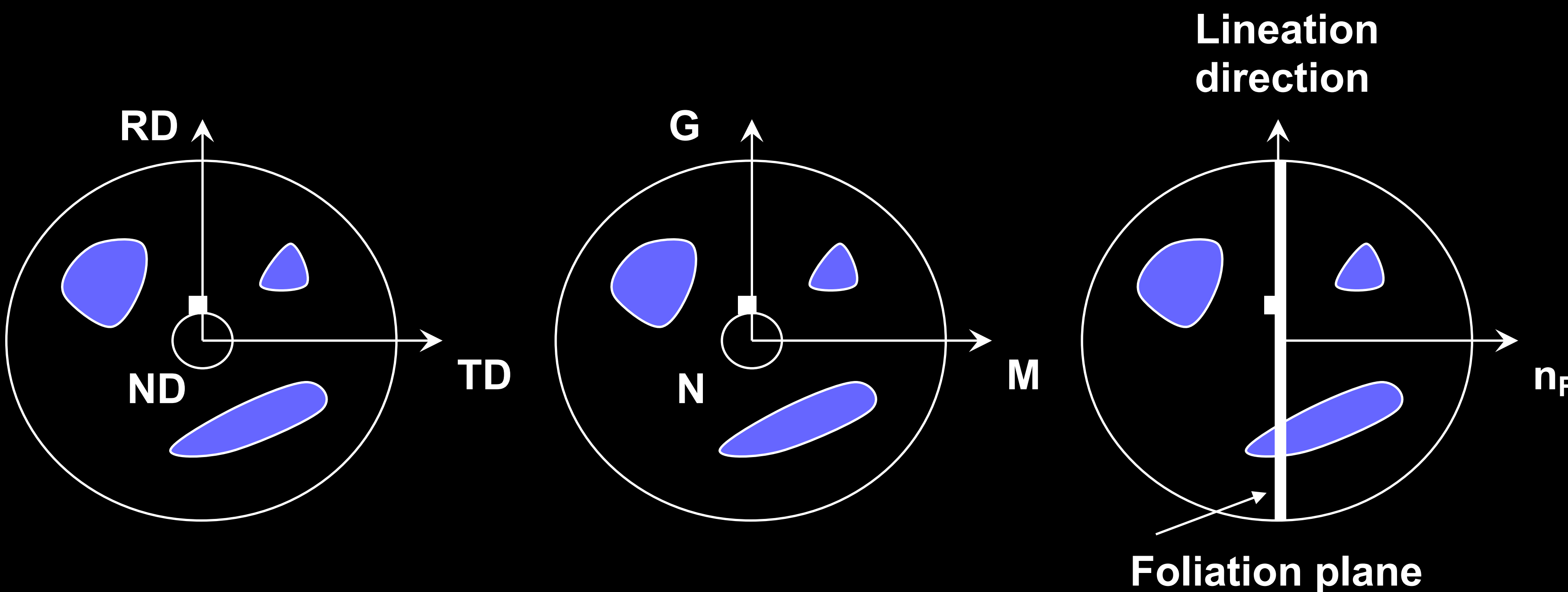

metallurgy

malacology

geophysics

Thin films: substrate directions … X_A, Y_A, Z_A

Normalisation

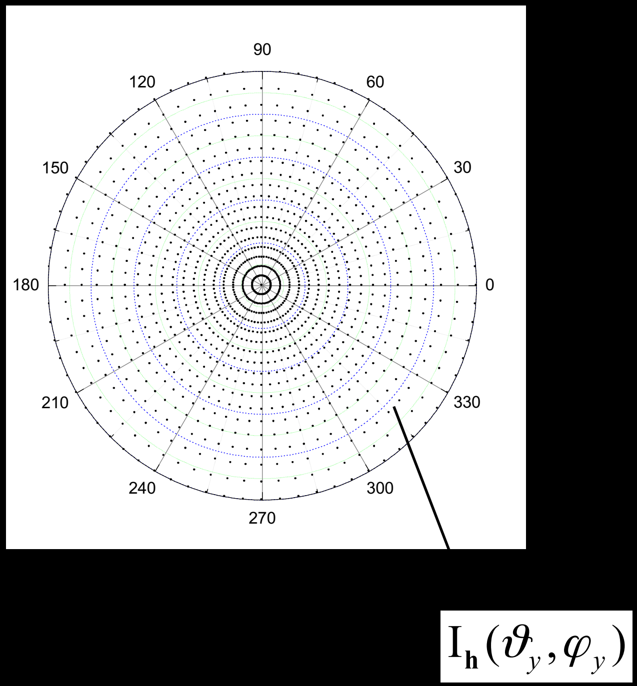

$$I_{\mathbf{h}}^{\text{total}} = \int_{\varphi_y=0}^{2\pi} \int_{\vartheta_y=0}^{\pi/2} I_{\mathbf{h}}(\vartheta_y, \varphi_y) \sin\vartheta_y \, d\vartheta_y d\varphi_y$$

$$I_{\mathbf{h}}^{\text{random}} = I_{\mathbf{h}}^{\text{total}} / \int_{\varphi_y=0}^{2\pi} \int_{\vartheta_y=0}^{\pi/2} \sin\vartheta_y \, d\vartheta_y d\varphi_y$$

$$P_{\mathbf{h}}(\mathbf{y}) = \frac{I_{\mathbf{h}}(\mathbf{y})}{I_{\mathbf{h}}^{\text{random}}}$$

- Only valid for complete pole figures:

neutrons in symmetric geometry

- Needs a refinement strategy to get I^{random} for all **h**'s

Incompleteness and corrections of pole figures

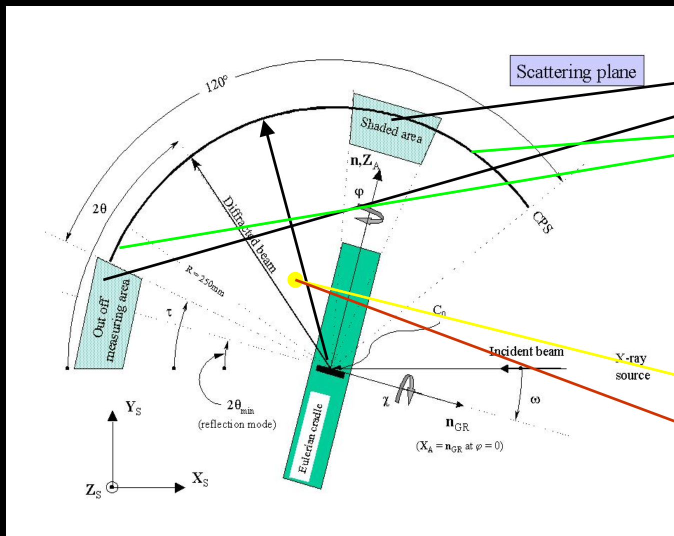

Missing Bragg peaks

Absorption + volume

Defocusing (x-rays)

Blind area

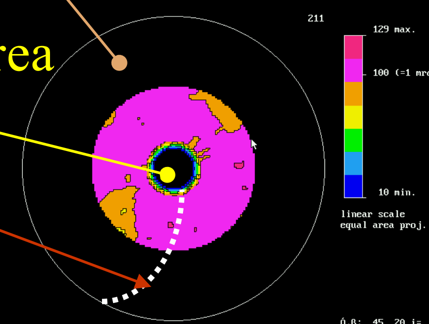

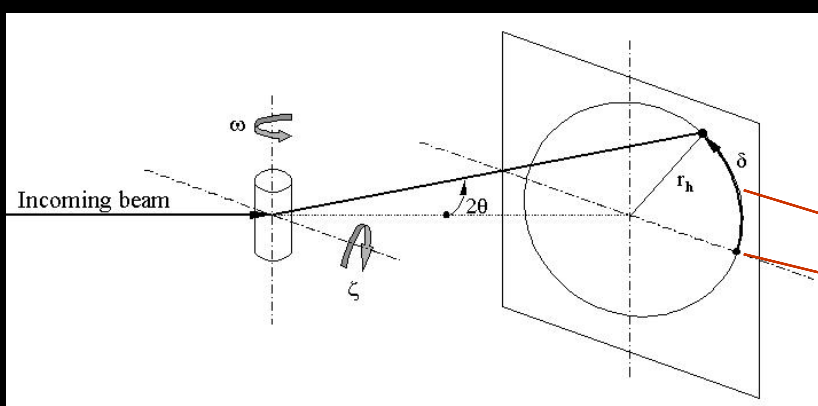

Localisation

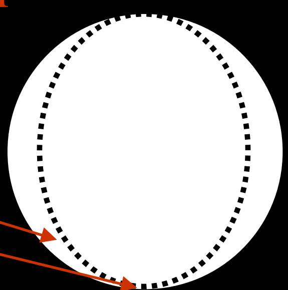

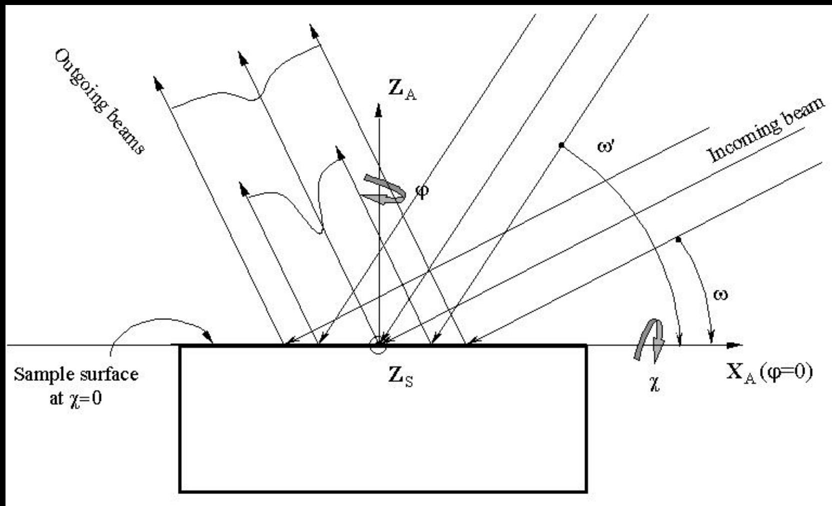

ω-defocusing

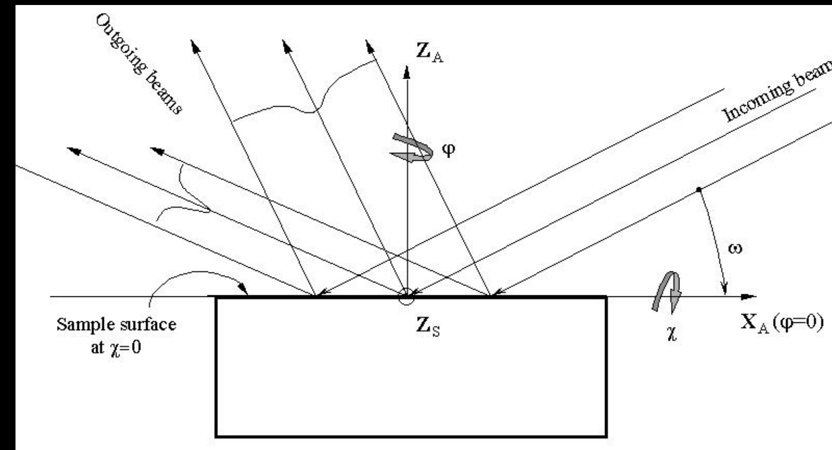

2θ-defocusing

χ-defocusing

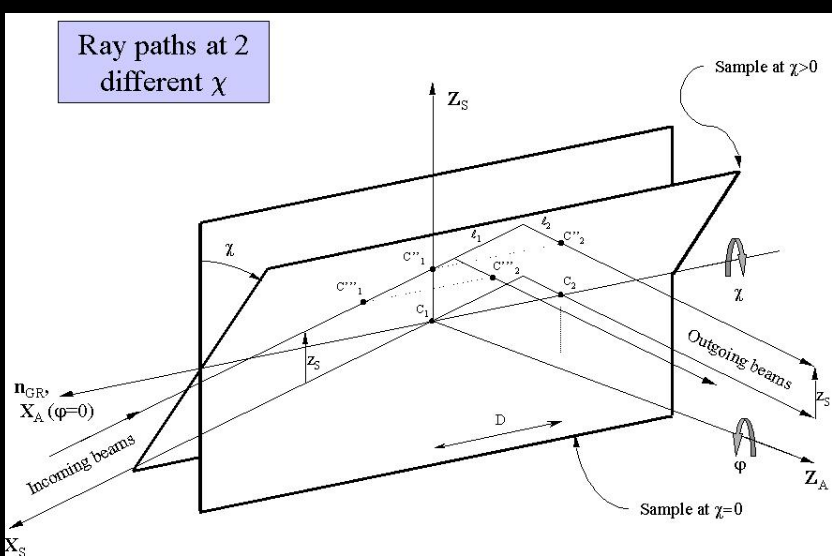

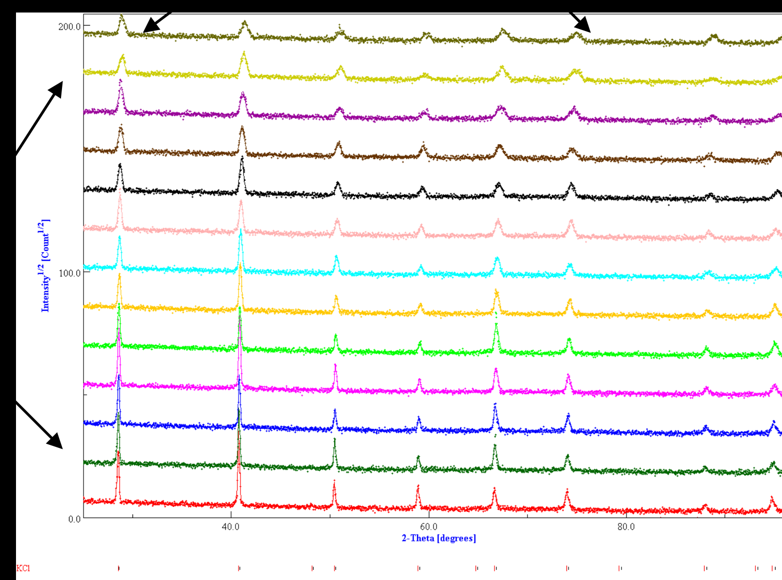

Defocusing corrections:

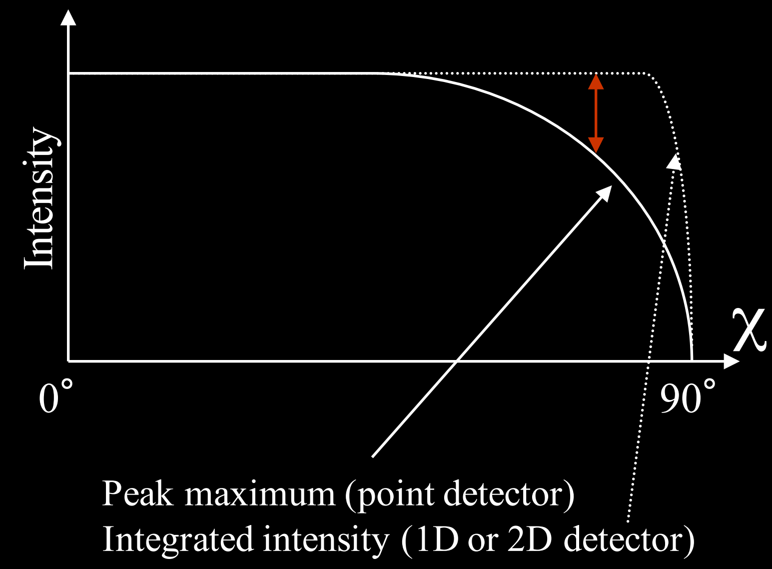

- Calibration on a random powder

$$I^{cor}_{\chi,\varphi,\omega,\theta} = I^{meas}_{\chi,\varphi,\omega,\theta}\frac{I^{rand}_{0,\omega,\theta}}{I^{rand}_{\chi,\omega,\theta}}$$

Net intensities (point detector)

$$= \left[I^{meas}_{\chi,\varphi,\omega,\theta} - I^{bkg}_{0,\omega,\theta}\frac{I^{b}_{\chi,\omega,\theta}}{I^{bkg}_{0,\omega,\theta}}\right]\frac{I^{rand}_{0,\omega,\theta}-I^{bkg}_{0,\omega,\theta}}{I^{rand}_{\chi,\omega,\theta}-I^{bkg}_{0,\omega,\theta}}$$

- Total integration of the peak (direct integration or fit)

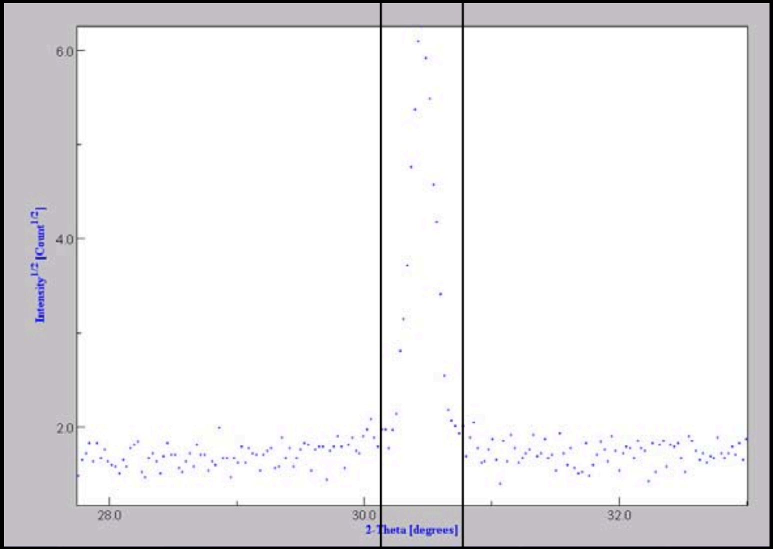

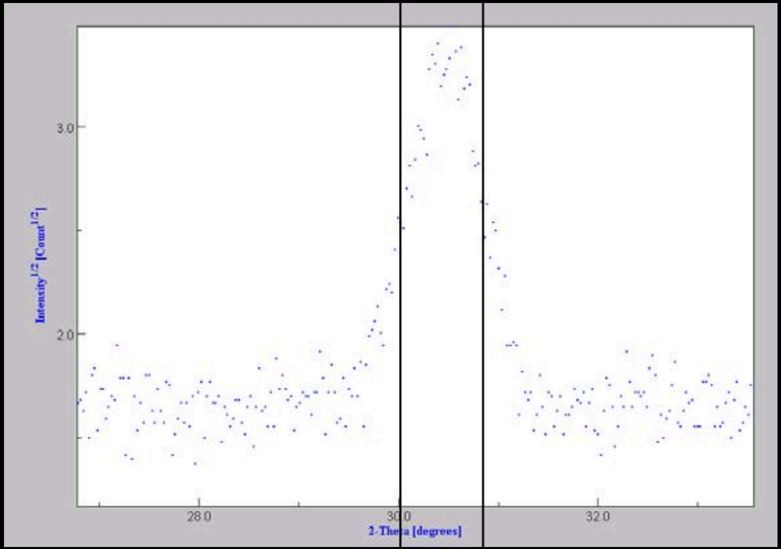

Overlaps enhance the problems !

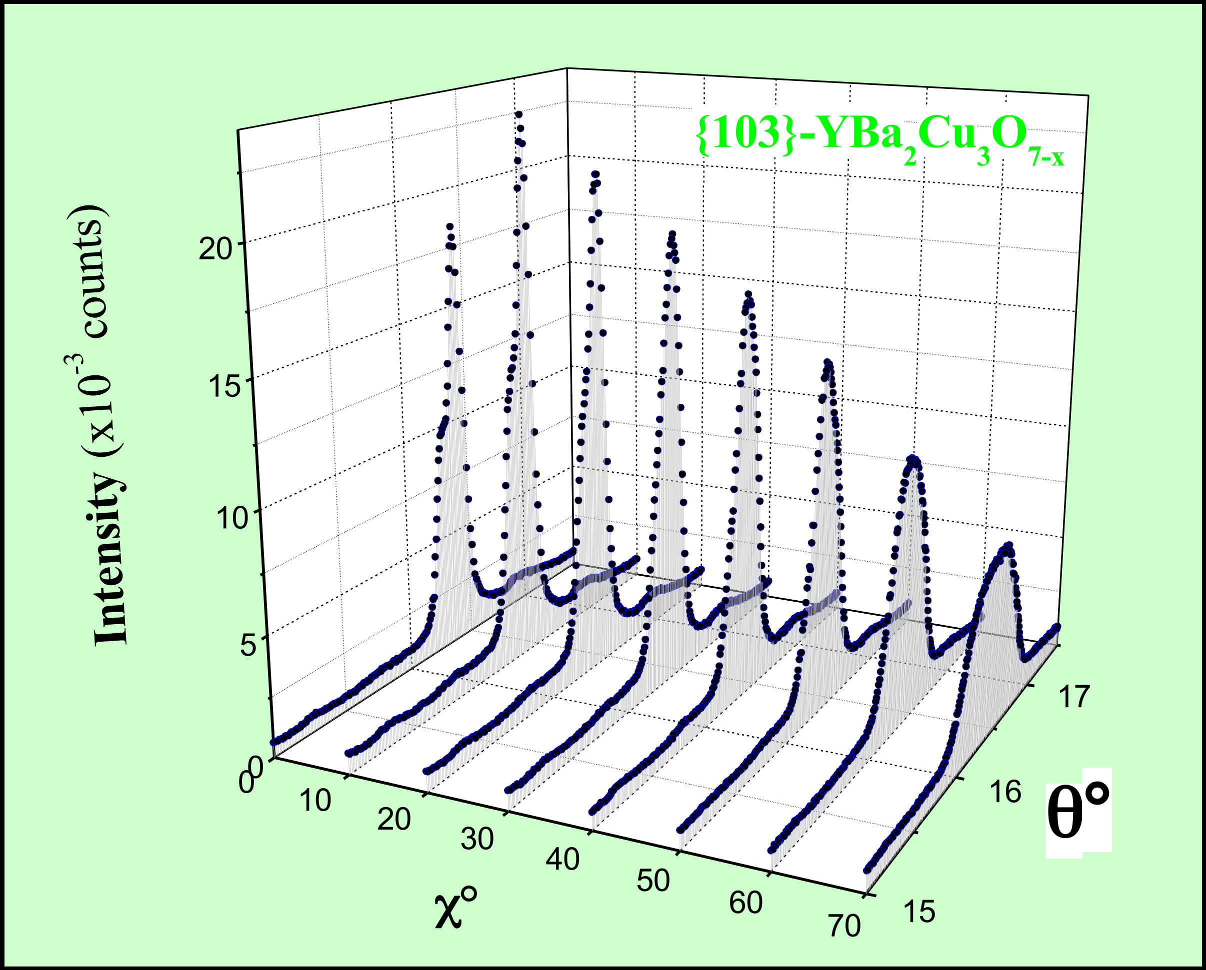

Absorption/Volume corrections:

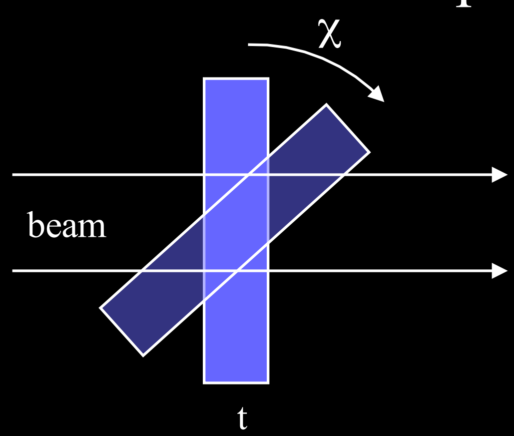

Specific to each instrumental geometry
Sample dependent (films, multilayers …)
Modifies the defocusing curves
Can be integrated in fitting procedures

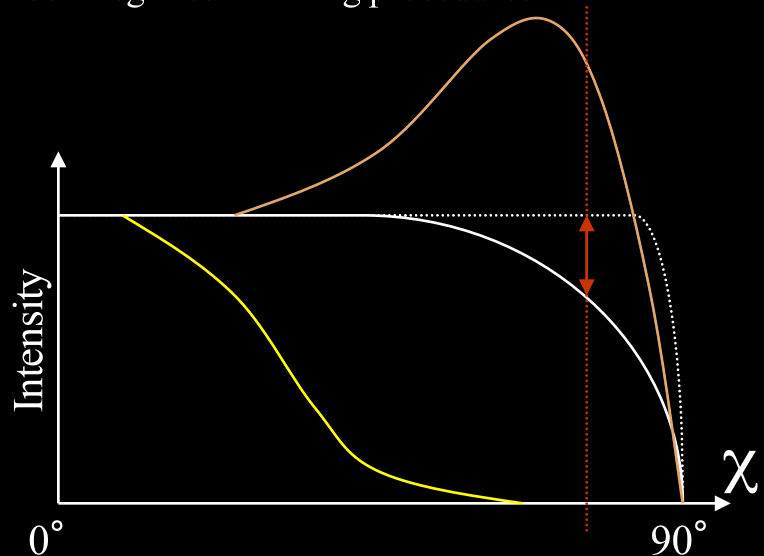

Top film

$$I(0) = I(\chi)\frac{\left(1-\exp\left(-2\mu T/\sin\theta_i\right)\right)}{\left(1-\exp\left(-2\mu T/\sin\theta_i\cos\chi\right)\right)}$$

Covered layer

$$I(0) = I(\chi)\frac{\left(1-\exp\left(-2\mu T/\sin\theta_i\right)\right)\exp\left(\dfrac{-2\sum_j \mu_j T_j}{\sin\theta_i}\right)}{\left(1-\exp\left(-2\mu T/\sin\theta_i\cos\chi\right)\right)\exp\left(\dfrac{-2\sum_j \mu_j T_j}{\sin\theta_i\cos\chi}\right)}$$

Single or multiple texture components, multiplicity

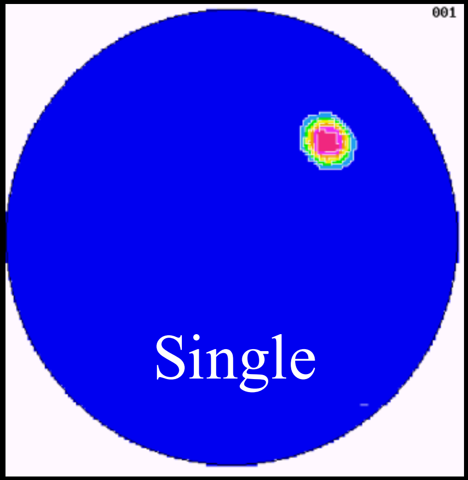

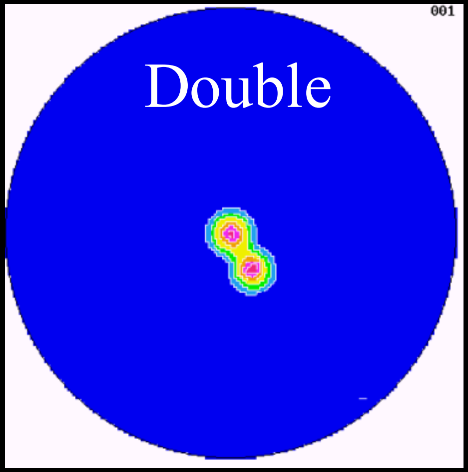

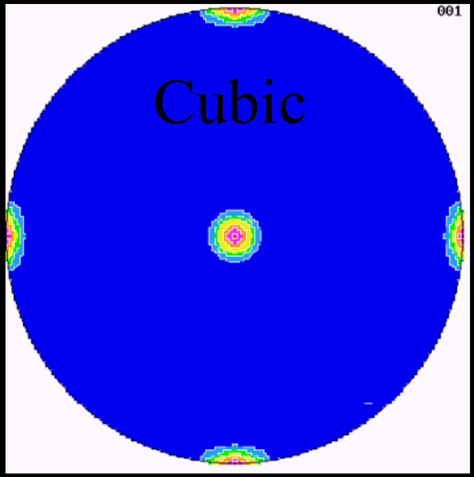

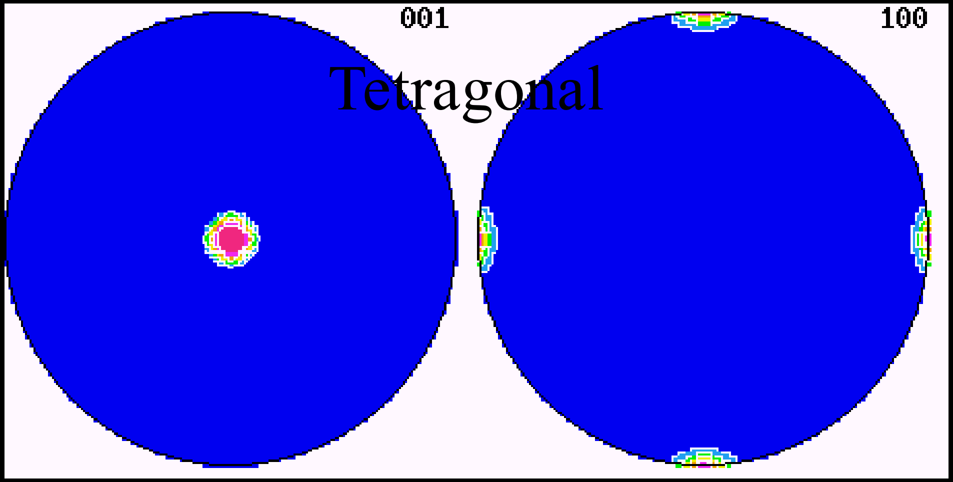

Program convention !
orientations are … oriented objects

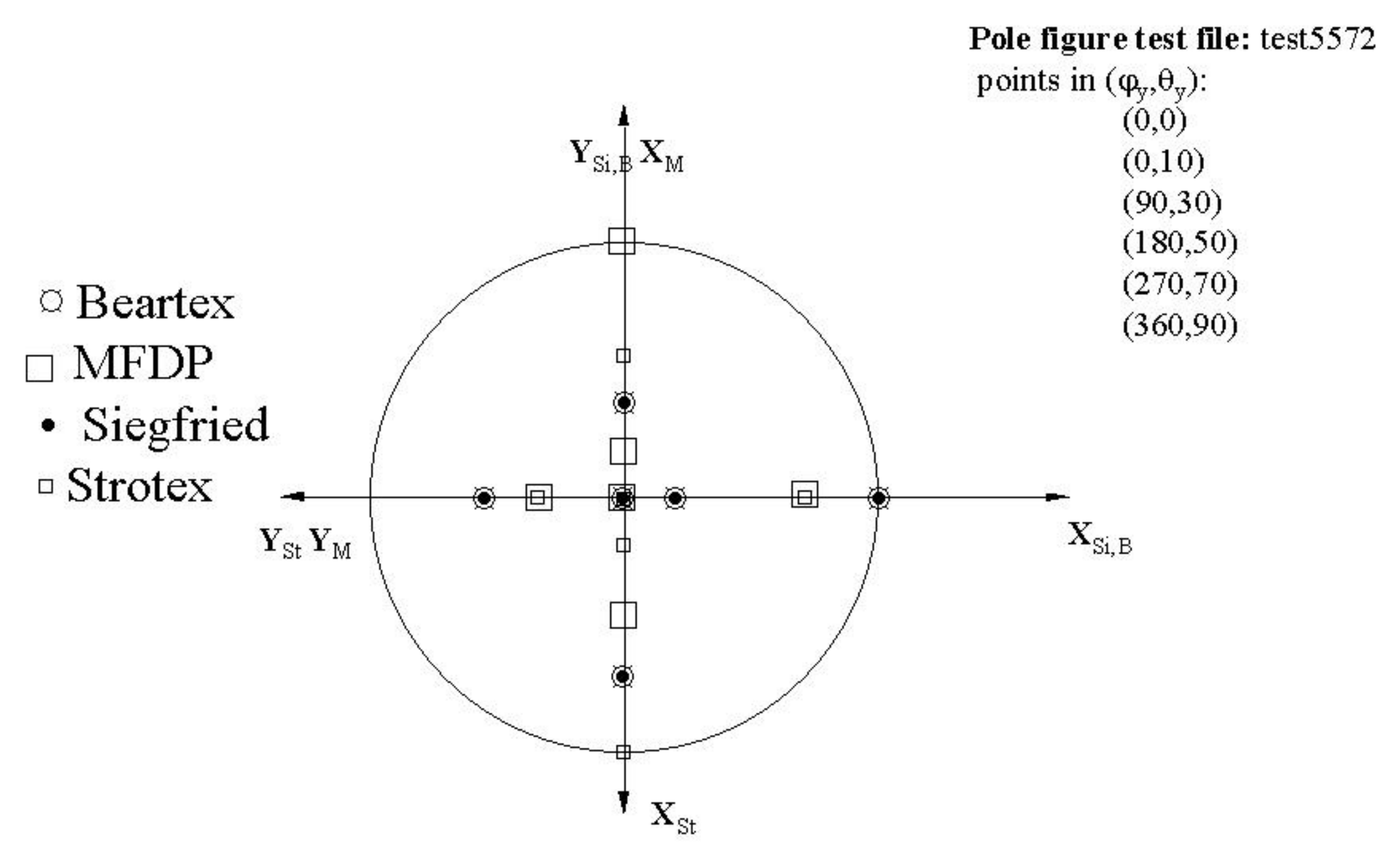

Pole figure plot programs correspondences

A real example

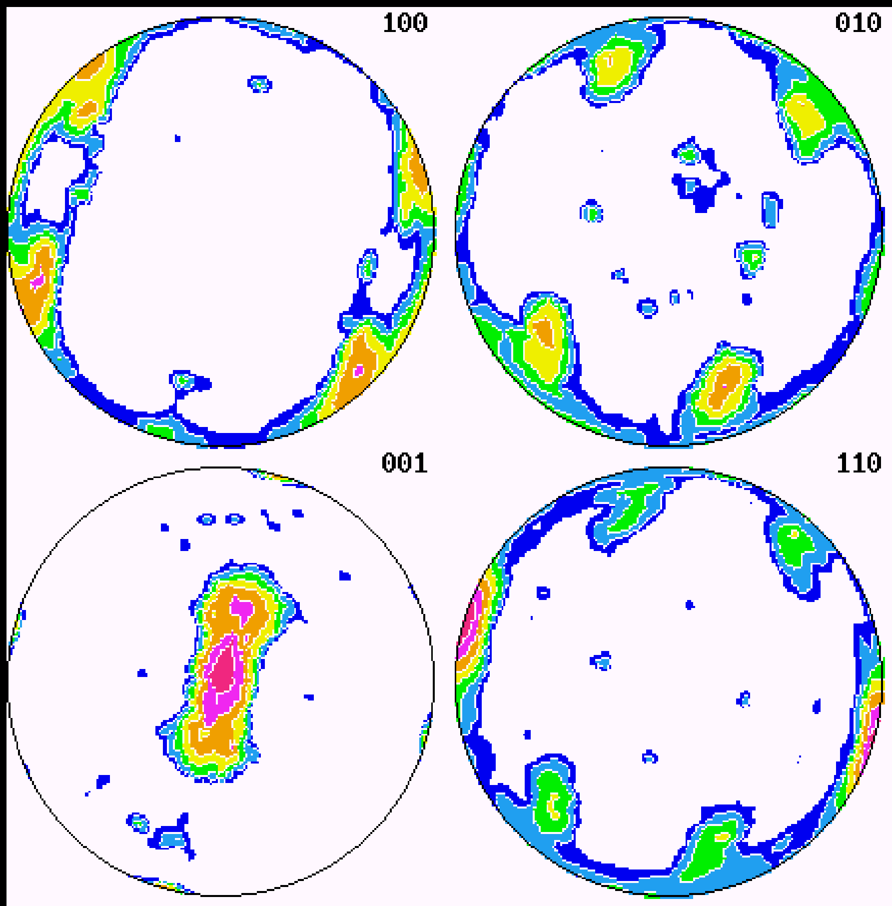

Cypraea testudinaria

Outer aragonite layer
Pnma space group

Texture types

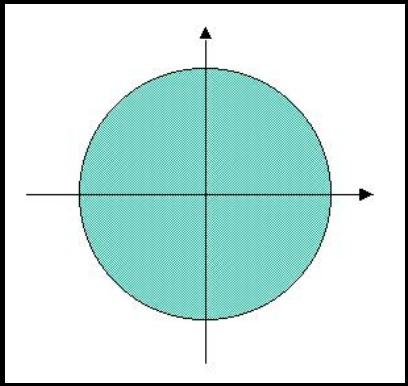

Random texture

3 degrees of freedom
All $P_{\mathbf{h}}(\mathbf{y})$ homogeneous
1 m.r.d. density whatever $\mathbf{y}$

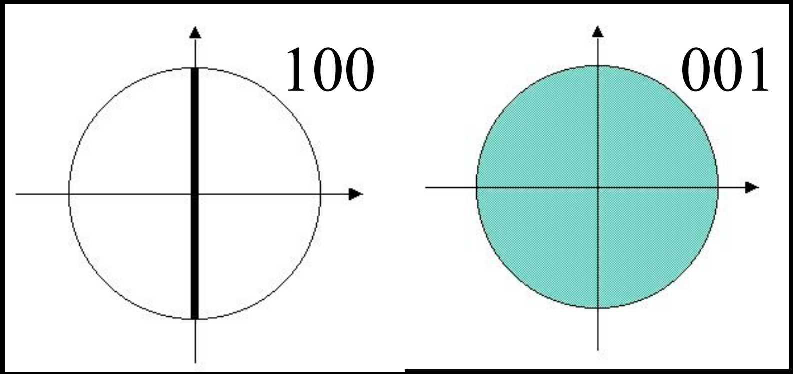

Planar texture

2 degrees of freedom
1 [hkl] at random in a plane

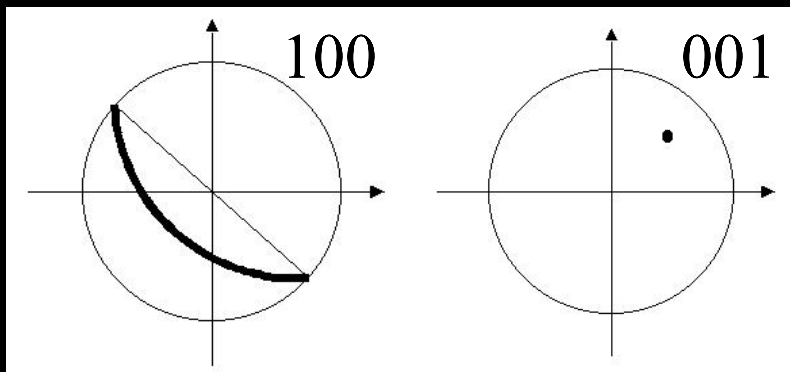

Fibre texture

1 degree of freedom
1 [hkl] along 1 **y** direction

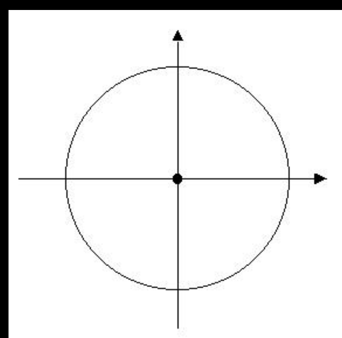

Cyclic-Fibre texture

$\mathbf{c}$ // Z_A

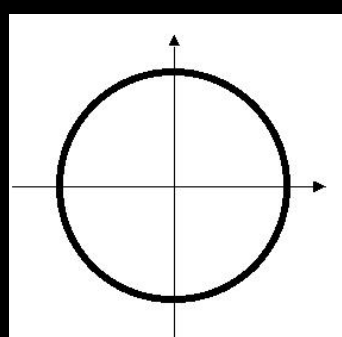

Cyclic-Planar texture

$\mathbf{c}$ // (X_A, Y_A)

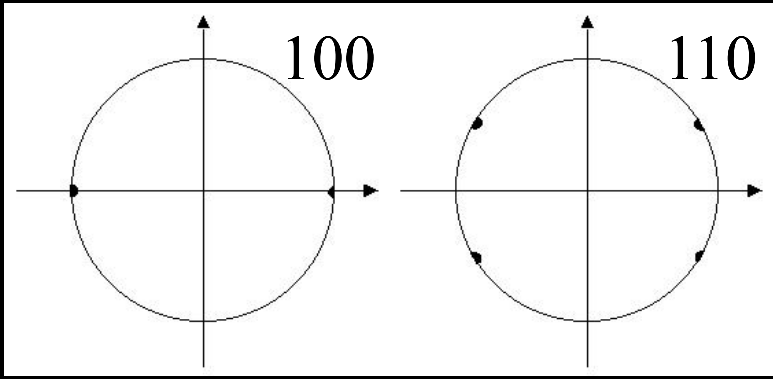

<u>Single crystal-like texture</u>

0 degree of freedom
2 [hkl]'s along 2 **y** directions

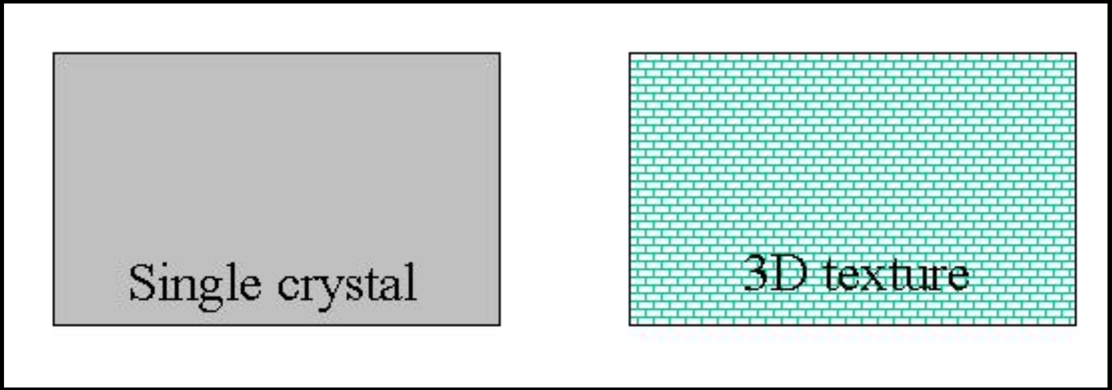

Single-crystal and perfect 3D orientation not distinguished

Pole figure and Orientation spaces

Pole figure expression:

$$\frac{dV(\mathbf{y})}{V} = \frac{1}{4\pi} P_{\mathbf{h}}(\mathbf{y})\, \mathbf{dy}$$

$\mathbf{dy} = \sin\vartheta_y \, d\vartheta_y \, d\varphi_y$

$$\int_{\varphi_y=0}^{2\pi} \int_{\vartheta_y=0}^{\pi/2} P_{\mathbf{h}}(\vartheta_y, \varphi_y) \sin\vartheta_y \, d\vartheta_y d\varphi_y = 4\pi$$

Orientation Distribution Function f(g):

$$\frac{dV(g)}{V} = \frac{1}{8\pi^2} f(g)\, dg$$

$dg = \sin(\beta) d\beta d\alpha d\gamma$

$$\int_{\alpha=0}^{2\pi} \int_{\beta=0}^{\pi/2} \int_{\gamma=0}^{2\pi} f(g)\, dg = 8\pi^2$$

From Pole figures to the ODF

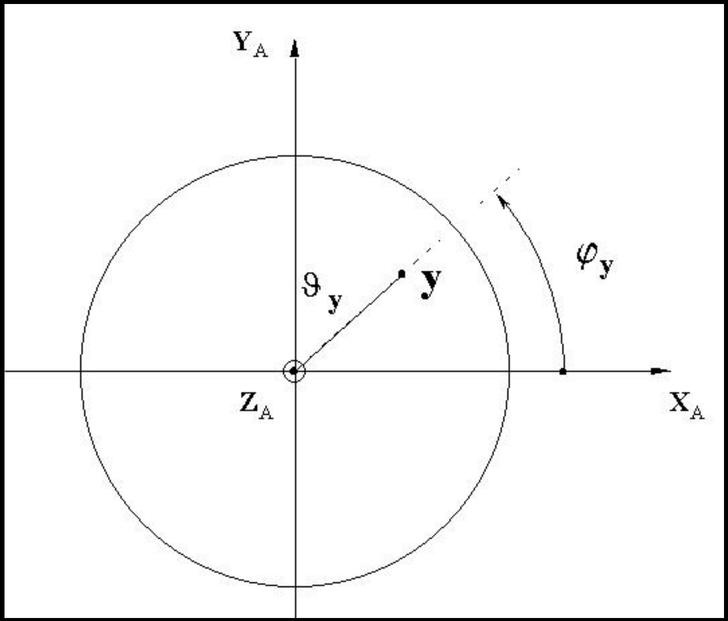

Pole figure: one direction fixed in K_A

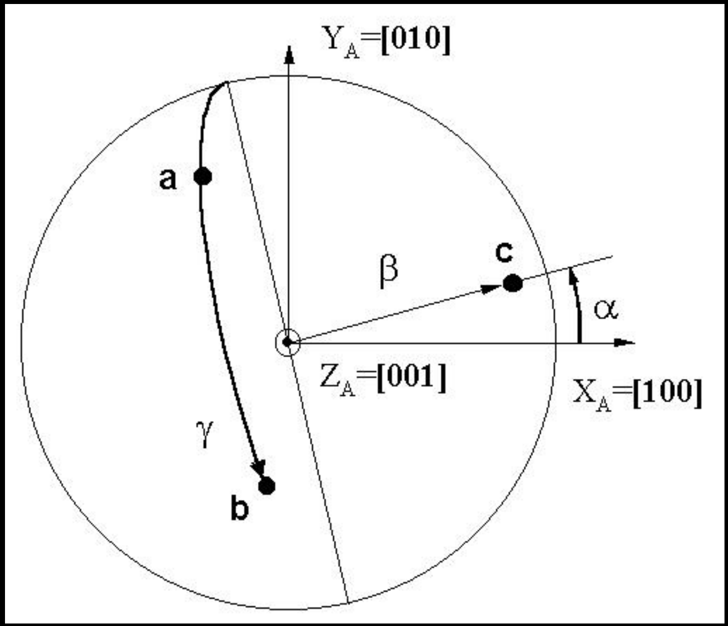

Orientation: two directions fixed in K_A

Fundamental Equation of QTA

$$P_{\mathbf{h}}(\mathbf{y}) = \frac{1}{2\pi} \int_{\mathbf{h}//\mathbf{y}} f(g)\, d\tilde{\varphi}$$

Needs several pole figures to construct f(g)

Pole figures from g

- Rotation of K_A about the axis Z_A through the angle α:
  [$K_A \mapsto K'_A$]; associated rotation $g_1 = \{\alpha,0,0\}$
- Rotation of K'_A about the axis Y'_A through the angle β:
  [$K'_A \mapsto K''_A$]; associated rotation $g_2 = \{0,\beta,0\}$
- Rotation of K''_A about the axis Z''_A through the angle γ:
  [$K''_A \mapsto K'''_A // K_B$]; associated rotation $g_3 = \{0,0,\gamma\}$

finally: $g = g_1\, g_2\, g_3 = \{\alpha,0,0\}\, \{0,\beta,0\}\, \{0,0,\gamma\} = \{\alpha,\beta,\gamma\}$

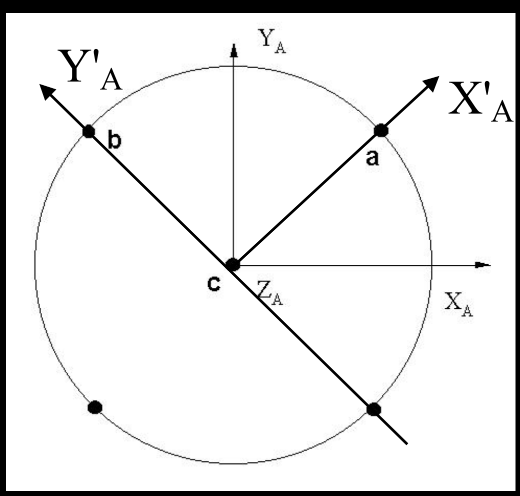

$g_1 = \{45,0,0\}$

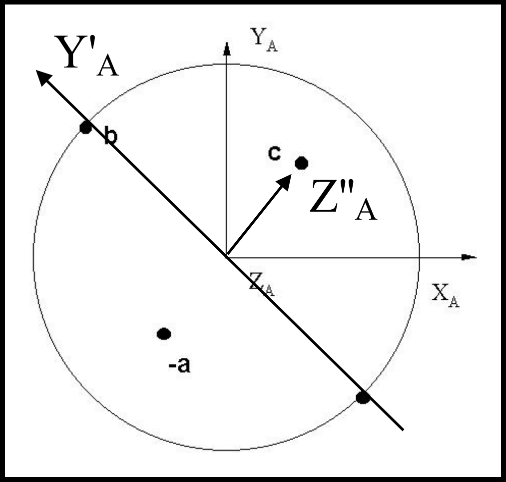

$g_2 = \{45,45,0\}$

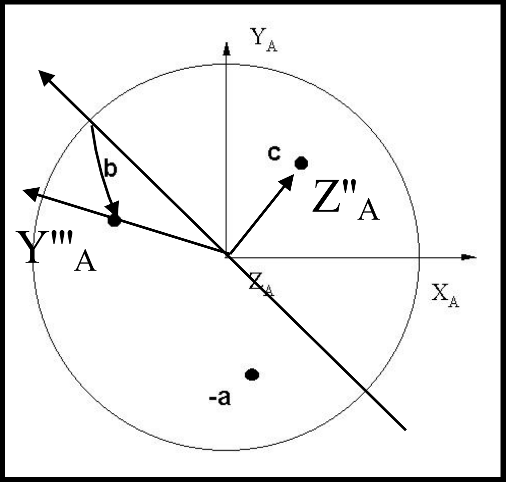

$g_3 = \{45,55,45\}$

Euler angles conventions

Matthies	Roe	Bunge	Canova	Kocks
α	Ψ	$\varphi_1 = \alpha + \pi/2$	$\omega = \pi/2 - \alpha$	Ψ
β	Θ	Φ	Θ	Θ
γ	Φ	$\varphi_2 = \gamma + 3\pi/2$	$\phi = 3\pi/2 - \gamma$	$\Phi = \pi - \gamma$

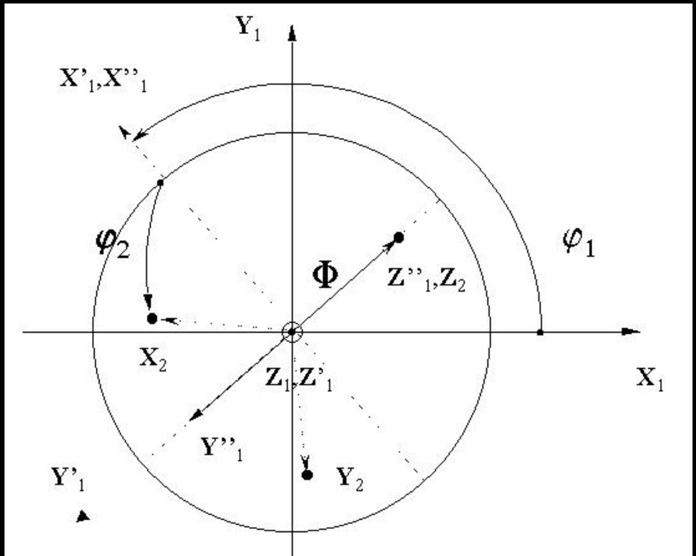

Bunge's convention

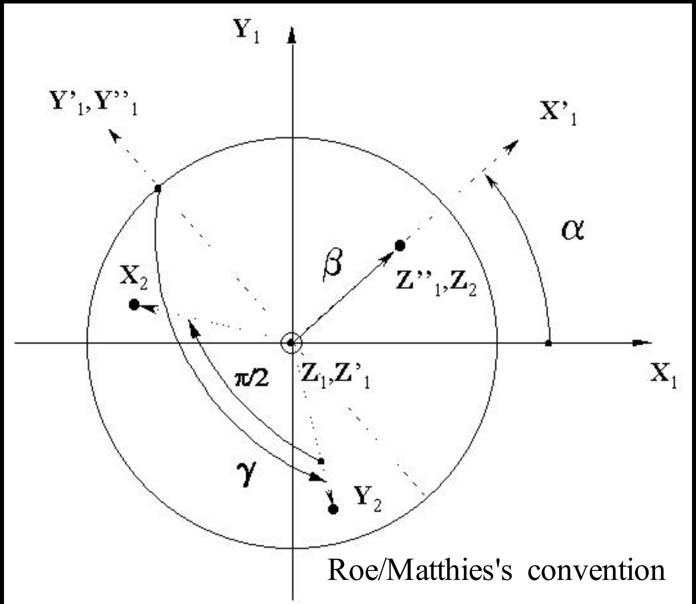

Roe/Matthies's convention

From f(g) to the pole figures

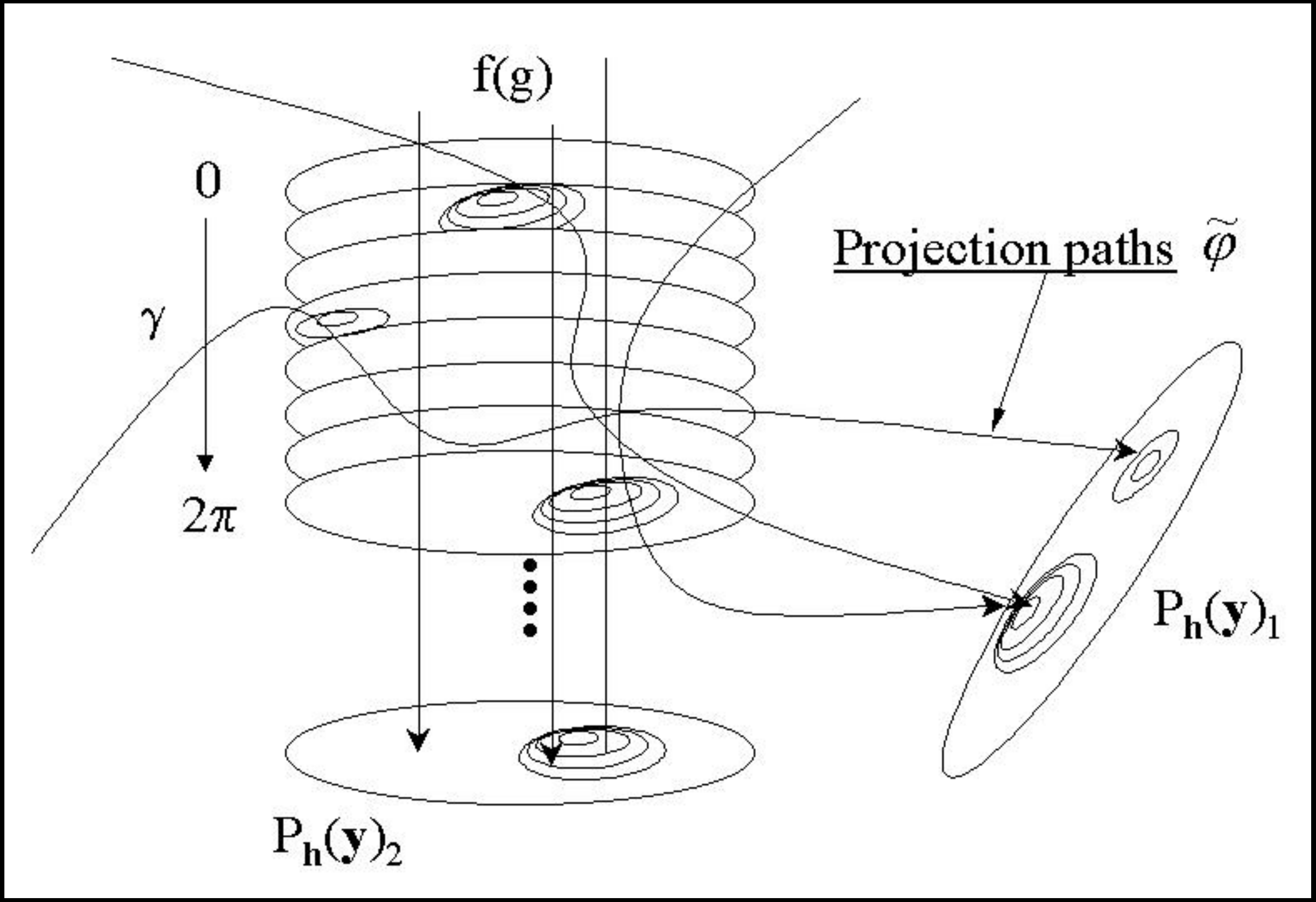

Deal with components in the ODF space

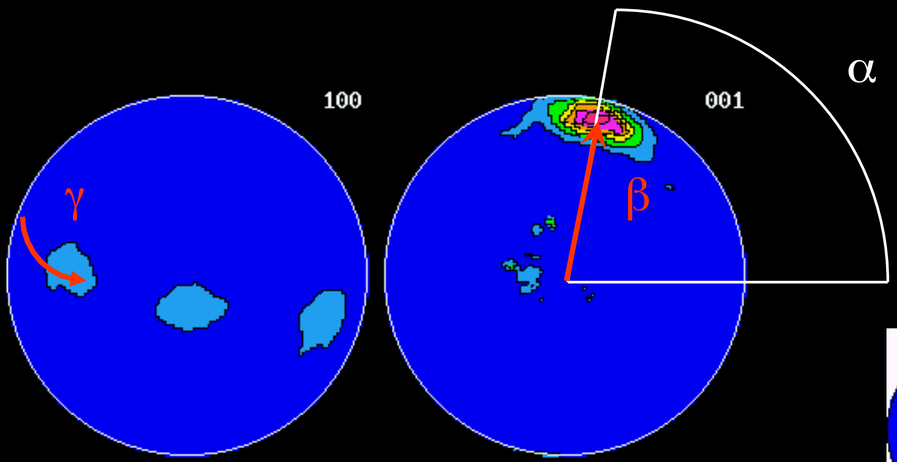

Pole figures

ODF γ-sections

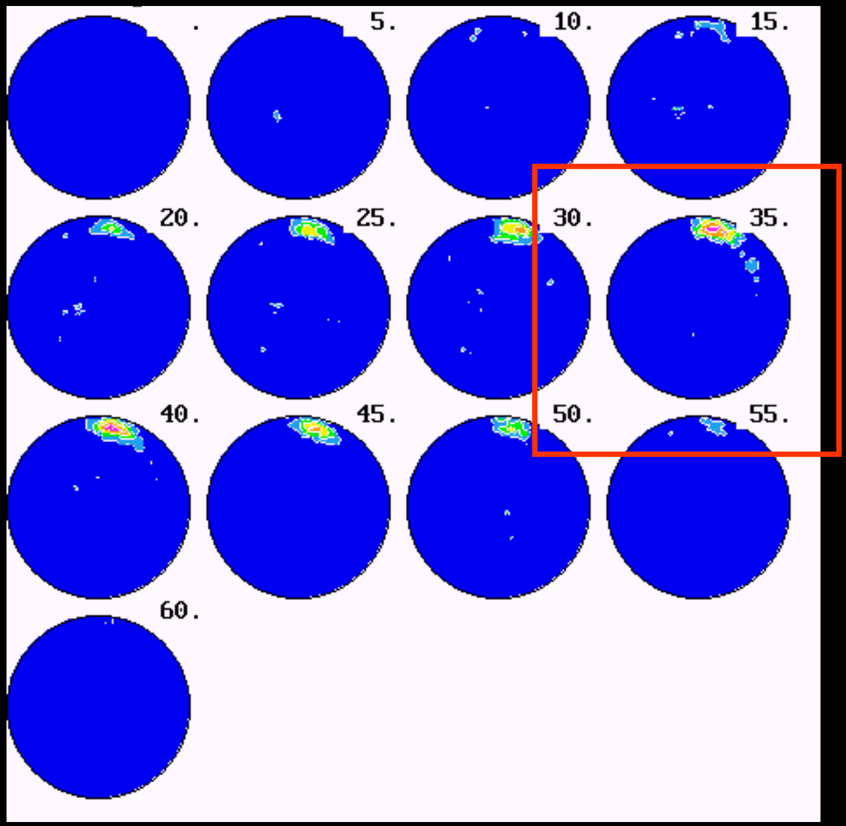

Component:
(Hexagonal system)
g = {85,80,35}

Plotting f(g)

A 3D plotting program: ODF plot

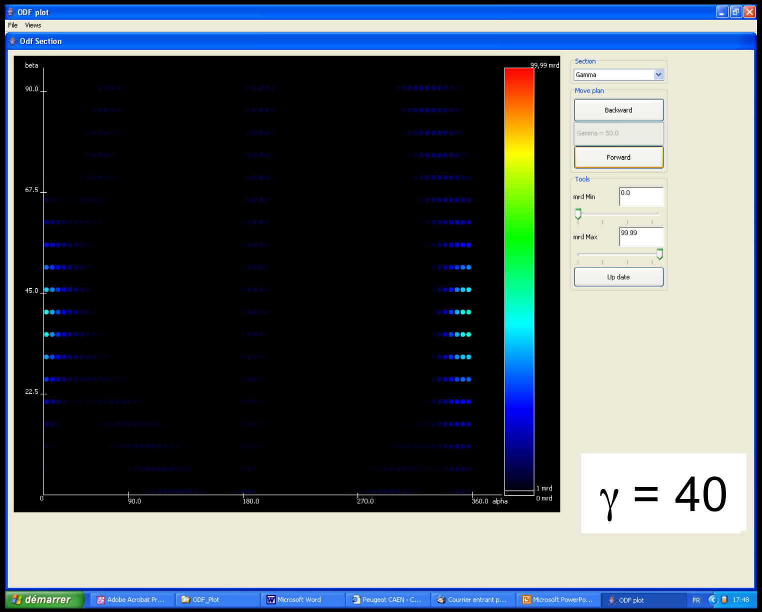

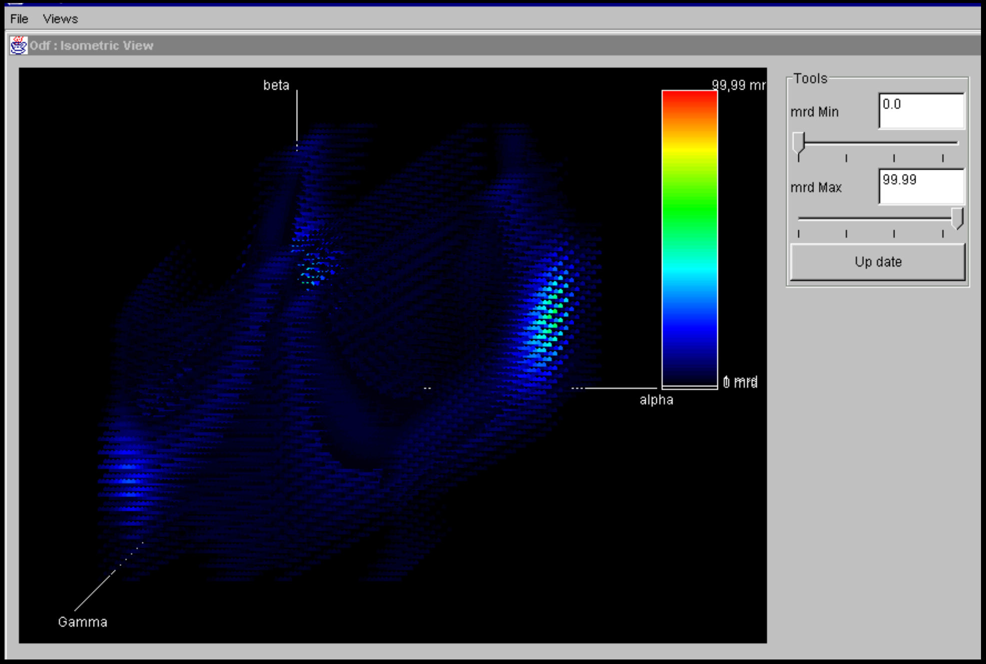

ODF sections (α, β, or γ)

ODF 3D-isometric view

Cartesian or Polar f(g) view

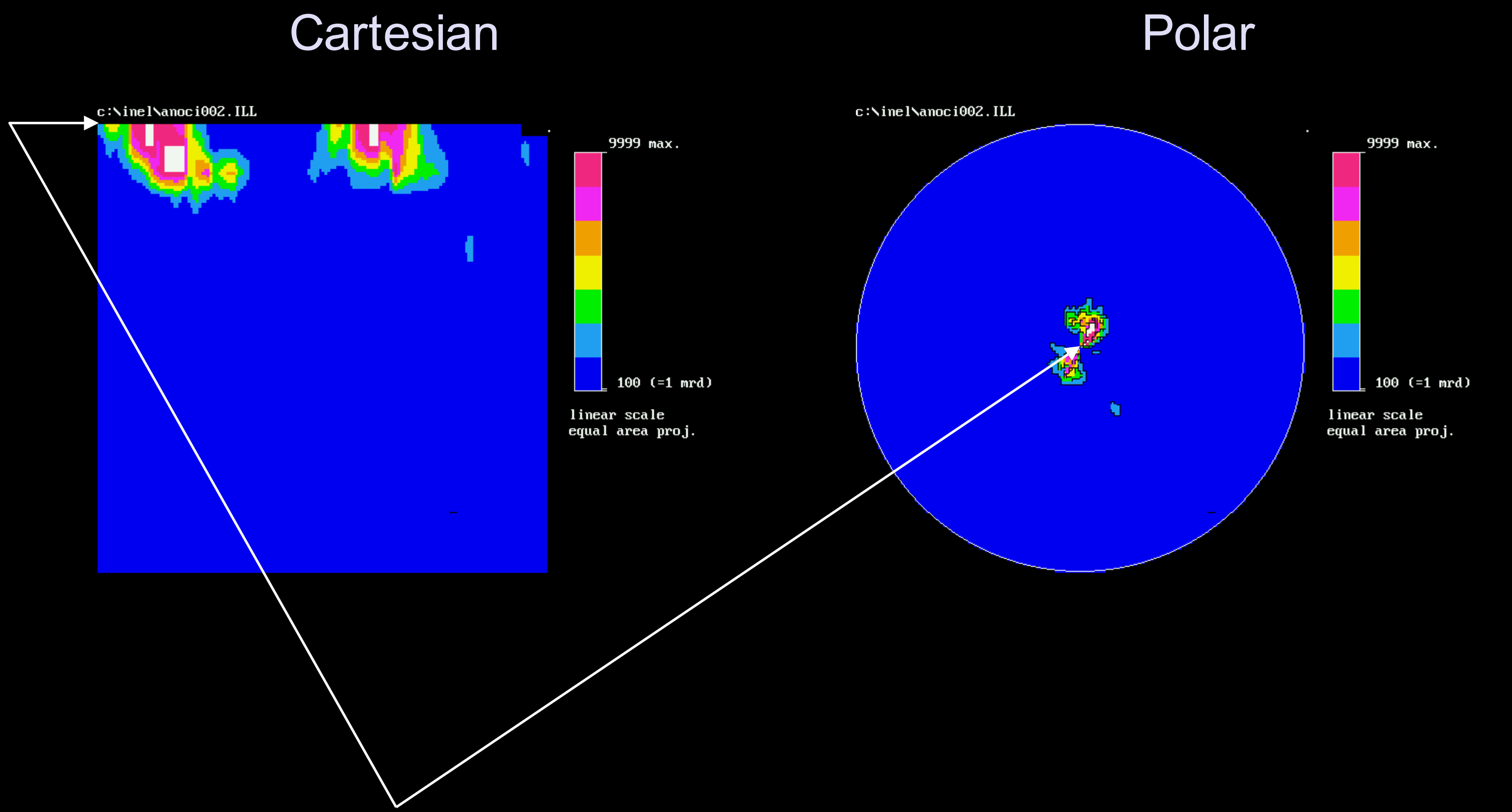

$\beta = 0$: space deformation

Inverse pole figures

$$P_{\mathbf{h}}(\mathbf{y}) = \frac{1}{2\pi} \int_{\mathbf{h}//\mathbf{y}} f(g)\, d\tilde{\varphi}$$

Pole figures

$$R_{\mathbf{y}}(\mathbf{h}) = \frac{1}{2\pi} \int_{\mathbf{y}//\mathbf{h}} f(g)\, d\tilde{\tilde{\varphi}}$$

Inverse Pole figures

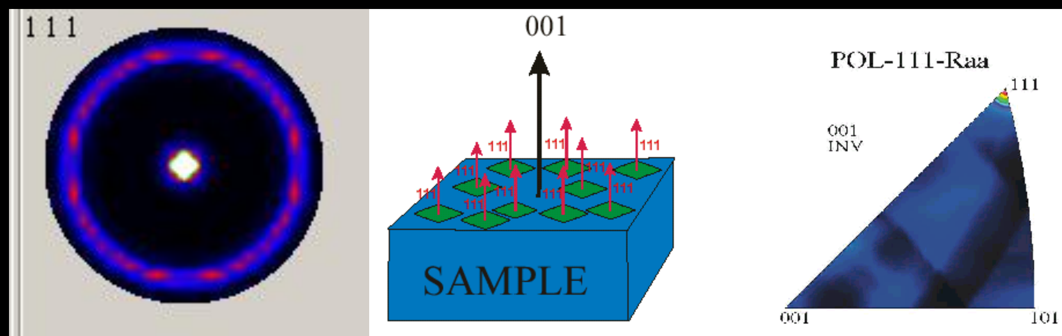

24 equivalent cubic sectors for the Inverse pole figure of a cubic system

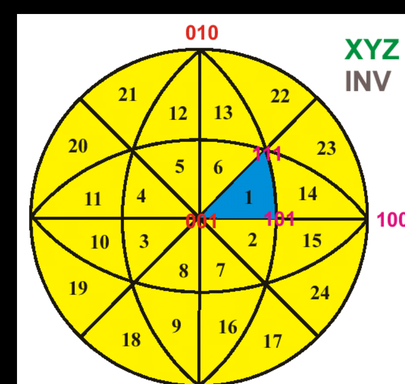

ODF refinement

One has to invert:

$$P_{\mathbf{h}}(\mathbf{y}) = \frac{1}{2\pi} \int_{\mathbf{h}//\mathbf{y}} f(g)\, d\tilde{\varphi}$$

- from Generalized Spherical Harmonics (Bunge):

$$f(g) = \sum_{l=0}^{\infty} \sum_{m,n=-l}^{l} C_l^{mn} T_l^{mn}(g)$$

$$P_{\mathbf{h}}(\mathbf{y}) = \sum_{l=0}^{\infty} \frac{1}{2l+1} \sum_{n=-l}^{l} k_l^n(\mathbf{y}) \sum_{m=-l}^{l} C_l^{mn} k_n^{*m}(\Theta_{\mathbf{h}} \phi_{\mathbf{h}})$$

Least-squares Refinement procedure $\sum_{\mathbf{h}} \sum_{\mathbf{y}} \left[I_{\mathbf{h}}(\mathbf{y}) - N_{\mathbf{h}} P_{\mathbf{h}}(\mathbf{y}) \right]^2 \mathbf{dy}$

But even orders are the only available parts: $f^e(g) = \sum_{\lambda=0(2)}^{\infty} \sum_{m,n=-\lambda}^{\lambda} C_\lambda^{mn} T_\lambda^{mn}(g)$

- from the WIMV iterative process (Williams-Imhof-Matthies-Vinel):

$$f^{n+1}(g) = N_n \frac{f^n(g) f^0(g)}{\left(\prod_{\mathbf{h}=1}^{I} \prod_{m=1}^{M_\mathbf{h}} P_\mathbf{h}^n(\mathbf{y}) \right)^{\frac{1}{IM_\mathbf{h}}}}$$

and

$$f^0(g) = N_0 \left(\prod_{\mathbf{h}=1}^{I} \prod_{m=1}^{M_\mathbf{h}} P_\mathbf{h}^{\exp}(\mathbf{y}) \right)^{\frac{1}{IM_\mathbf{h}}}$$

E-WIMV (Rietveld only):

with $0 < r_n < 1$, relaxation parameter,
M_h number of division points of the integral around k,
w_h reflection weight

$$f^{n+1}(g) = f^n(g) \prod_{m=1}^{M_\mathbf{h}} \left(\frac{P_\mathbf{h}(\mathbf{y})}{P_\mathbf{h}^n(\mathbf{y})} \right)^{r_n \frac{w_\mathbf{h}}{M_\mathbf{h}}}$$

- Entropy maximisation (Schaeben) and exponential harmonics (van Houtte):

$$f^{n+1}(g) = f^n(g) \prod_{m=1}^{M_\mathbf{h}} \left(\frac{P_\mathbf{h}(\mathbf{y})}{P_\mathbf{h}^n(\mathbf{y})} \right)^{\frac{r_\mathbf{n}}{M_\mathbf{h}}}$$

$$f_s(g) = e^{h(g)} \geq 0$$

$$C_{s\lambda}^{mn} = (2\lambda + 1) \int e^{h(g)} T_\lambda^{mn}(g) dg$$

- arbitrarily defined cells (ADC, Pawlik):

Very similar to E-WIMV, with integrals along path tubes

- Vector method (Ruer, Baro, Vadon):

I linear equations for J unknown quantities:

$$\mathbf{P_i(h) = [\sigma_{ij}(h)]\ f_j}$$

- Component method (Helming):

$$f(g) = F + \sum_c I^c f^c(g)$$

Gaussian component:

$$f(g, g^c) = f(\tilde{g}) = \frac{2\sqrt{\pi}}{\zeta\left\{1 - \exp\left(-\left(\frac{\zeta}{2}\right)^2\right)\right\}} \exp\left(-\left(\frac{\tilde{g}}{\zeta}\right)^2\right)$$

$$S = \frac{\ln 2}{1 - \cos\left(\frac{\zeta}{2}\right)} \qquad N(S) = \frac{1}{I_0(S) - I_1(S)}$$

Evaluation of the OD coverage

Say 20 measured (5° x 5°) complete pole figures:

= 20 x 1368 = 27360 experimental points

ODF (5° x 5° x 5°, triclinic): 98496 points to refine

{100} pole figure, measured up to χ = 45° :

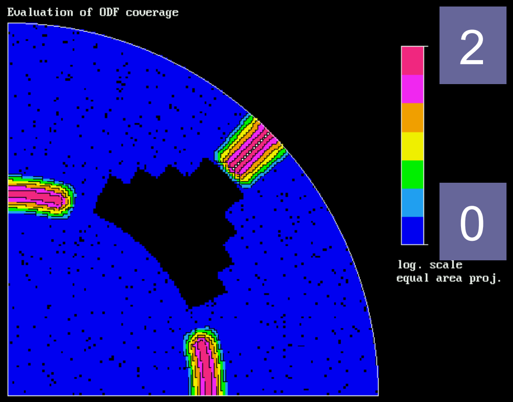

{100} + {110}, measured up to χ = 45° :

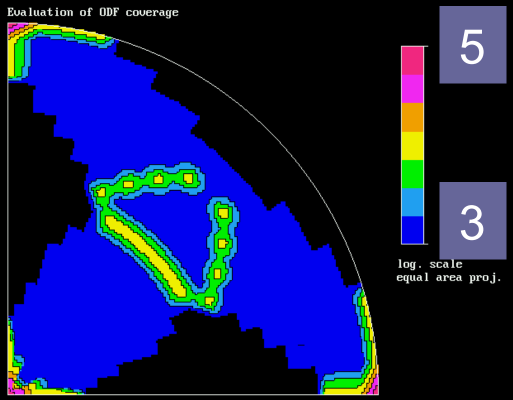

{100} + {110} + {111}, up to χ = 45° :

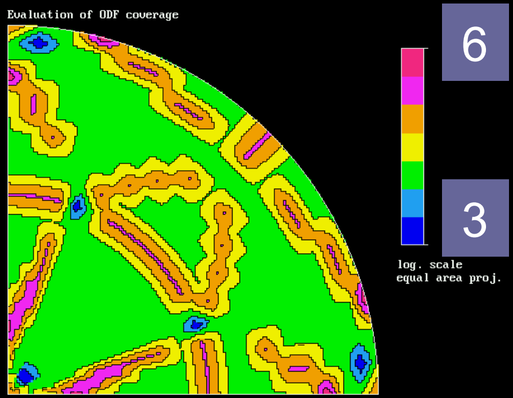

Estimators of Refinement Quality

Visual assessment

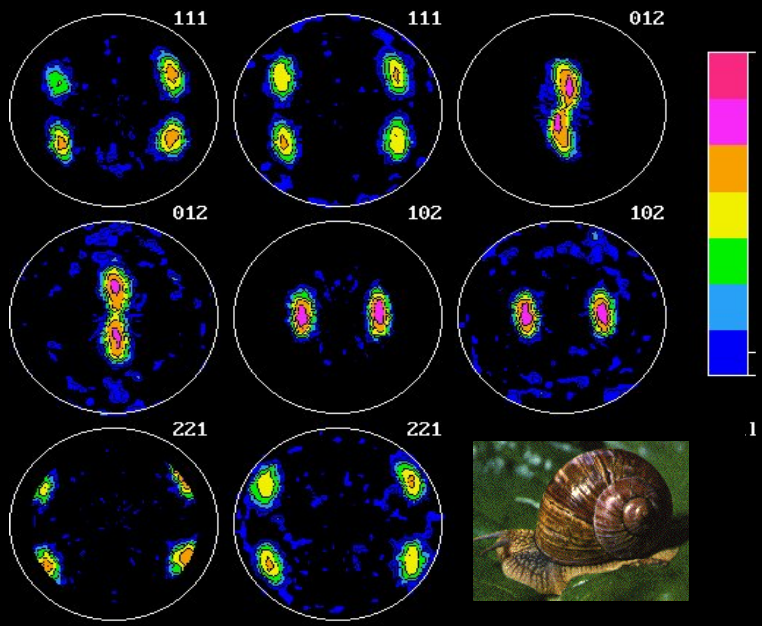

Helix pomatia (Burgundy land snail: Outer com. crossed lamellar layer)

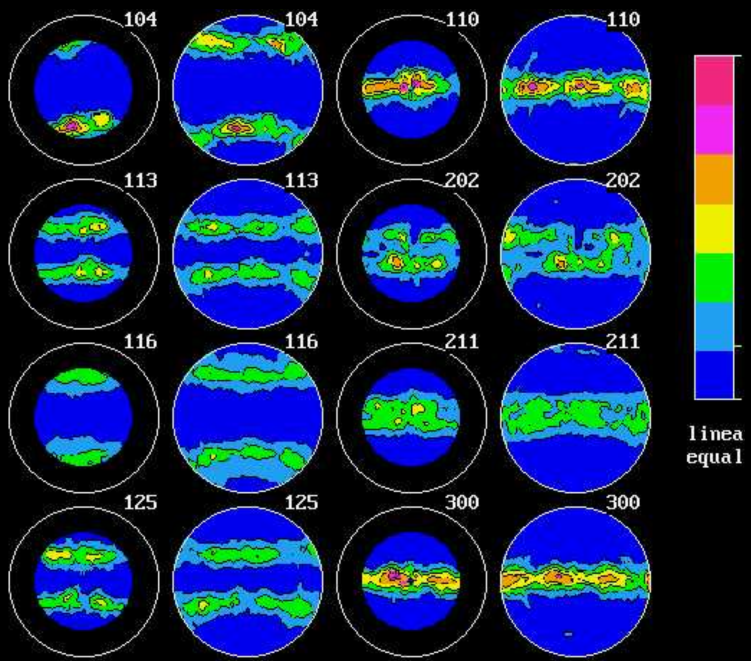

Bathymodiolus thermophilus (deep ocean mussel: Outer Prismatic layer)

RP Factors:

Individual pole figures:

$$RP_x(h_i) = \frac{\sum_{j=1}^{J} \left| \tilde{P}^o_{h_i}(y_j) - \tilde{P}^c_{h_i}(y_j) \right|}{\sum_{j=1}^{J} \tilde{P}^o_{h_i}(y_j)} \theta\left(x, \tilde{P}^o_{h_i}(y_j)\right)$$

$$\theta(x,t) = \begin{cases} 1 \text{ for } t > x \\ 0 \text{ for } t \leq x \end{cases}$$

$$x = \varepsilon, 1, 10 \ldots$$

Averaged on all pole figures:

$$\overline{RP}_x = \frac{1}{I} \sum_{i=1}^{I} RP_x(h_i)$$

Bragg R-Factors:

$$RB_x(h_i) = \frac{\sum_{j=1}^{J}\left[\widetilde{P}^{o}_{h_i}(y_j) - \widetilde{P}^{c}_{h_i}(y_j)\right]^2}{\sum_{j=1}^{J}\widetilde{P}^{o\,2}_{h_i}(y_j)}\,\theta\left(x, \widetilde{P}^{o}_{h_i}(y_j)\right)$$

Weighted Rw-Factors:

$$w_{ij} = \frac{1}{\sqrt{I^{o}_{h_i}(y_j)}}$$

$$Rw_x(h_i) = \frac{\sum_{j=1}^{J}\left[w^{o}_{ij}I^{o}_{h_i}(y_j) - w^{c}_{ij}I^{c}_{h_i}(y_j)\right]^2}{\sum_{j=1}^{J}w^{o}_{ij}I^{z\,2}_{h_i}(y_j)}\,\theta\left(x, \widetilde{P}^{o}_{h_i}(y_j)\right)$$

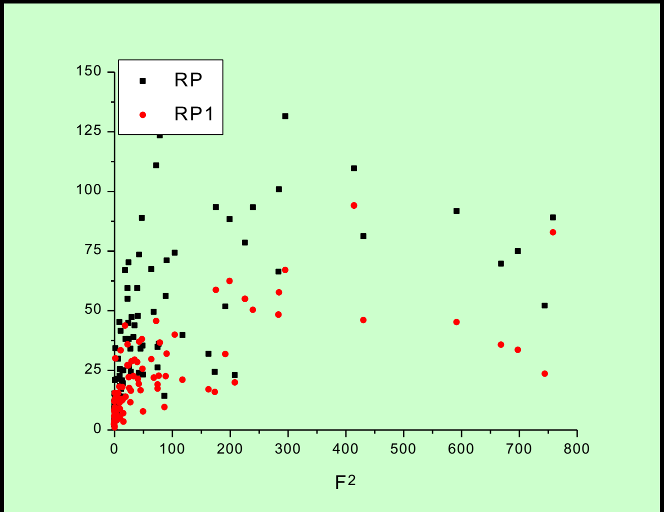

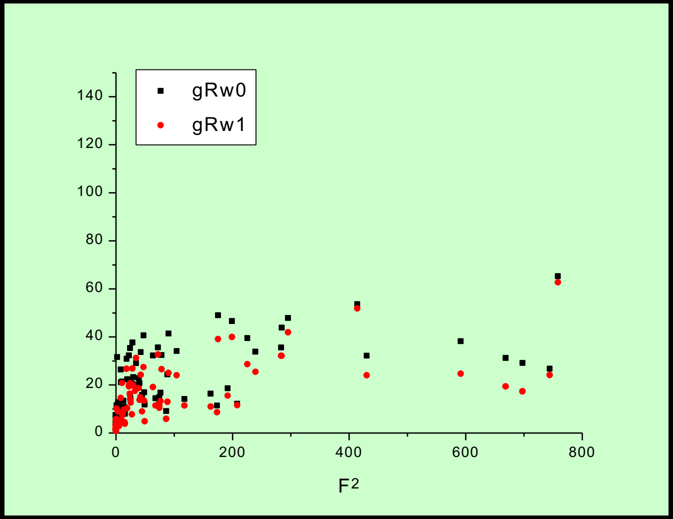

Texture strength estimators

ODF Texture Index:

$F^2 \in [1,\infty[$ $\quad > 1$ m.r.d^2

$= 1$: powder

$= \infty$: single crystal

$$F^2(\text{m.r.d.}^2) = \frac{1}{8\pi^2}\sum_i f^2(g_i)\Delta g_i$$

Discrete OD

$$F^2 = 1 + \sum_{\lambda=2}^{L}\left[\frac{1}{2\lambda+1}\right]\sum_{m=-\lambda}^{\lambda}\sum_{n=-\lambda}^{\lambda}\left|C_\lambda^{mn}\right|^2$$

Continuous ODF

Pole figures Texture Index:

$$J_{\mathbf{h}}^2 = \frac{1}{4\pi}\sum_i \left[P_h(\mathbf{y}_i)\right]^2 \Delta\mathbf{y}_i$$

Texture Entropy:

$S \in [0,-\infty[$ ≤ 0

$= 0$: powder

$= -\infty$: single crystal

$$S = \frac{-1}{8\pi^2} \sum_i f(g_i) \ln[f(g_i)] \Delta g_i$$

S - F^2:

Fon + smooth texture component(s)

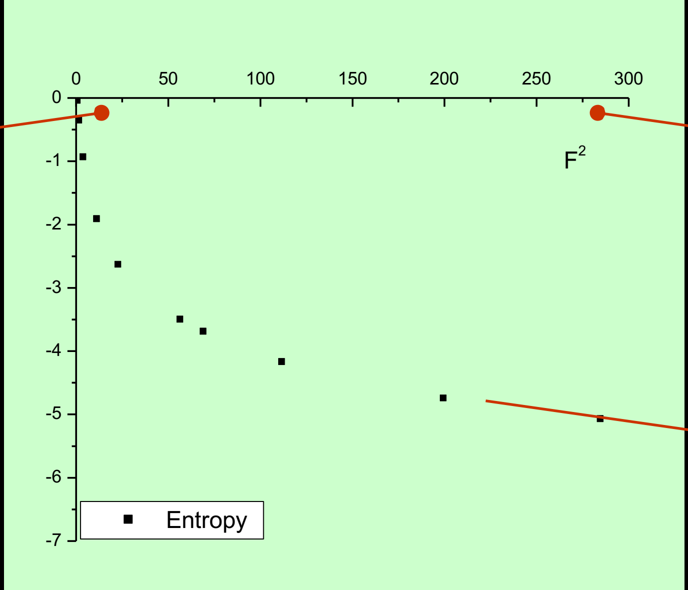

Fon + Dirac-like texture component

Lower bound: Fon = 0

Crystallographic texture

Diffraction Measurements
S space, $I(\chi,\varphi,\omega,\eta,2\theta)$

Corrections
(defocusing, localization,
Volume-absorption)

Pole figures
Y space, $I_h(y)$

Normalization
$P_h(y)$

Orientation Distribution Function
G space, f(g)

Macroscopic anisotropic properties $(M_i, C_{ijkl}, \sigma_{ij}, d_{ijk} \ldots)_M$
Elastic wave velocities (geophysics)
Anisotropic spectroscopies (P-EXAFS, ESR …)
Character analyses (phylogeny, palaeontology)
Art and Cultural Heritage

Magnetic QTA

$$I_{\vec{h}}(\vec{y},0) = I^{n}_{\vec{h}}(\vec{y},0) + I^{m}_{\vec{h}}(\vec{y},0)$$

$$I_{\vec{h}}(\vec{y},\vec{B}) = I^{n}_{\vec{h}}(\vec{y},0) + I^{m}_{\vec{h}}(\vec{y},\vec{B})$$

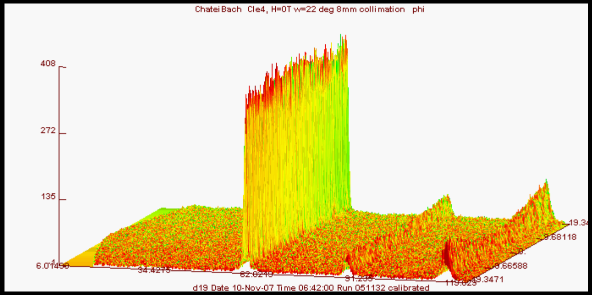

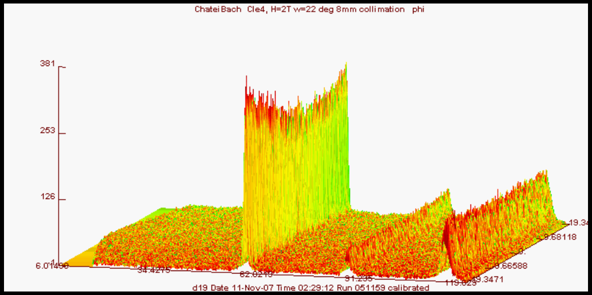

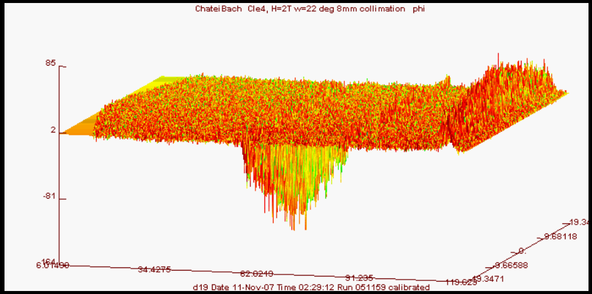

$$\Delta I^{m}_{\vec{h}}(\vec{y},\vec{B}) = I_{\vec{h}}(\vec{y},\vec{B}) - I_{\vec{h}}(\vec{y},0)$$

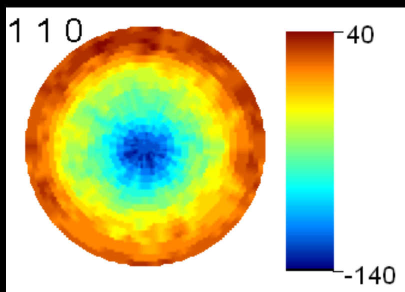

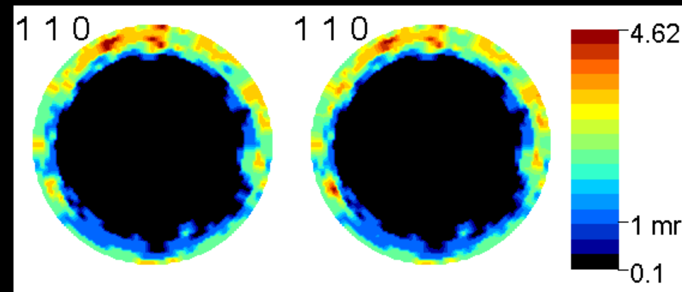

$$\Delta I_{\vec{h}}^{+p}(\vec{y},\vec{B})$$

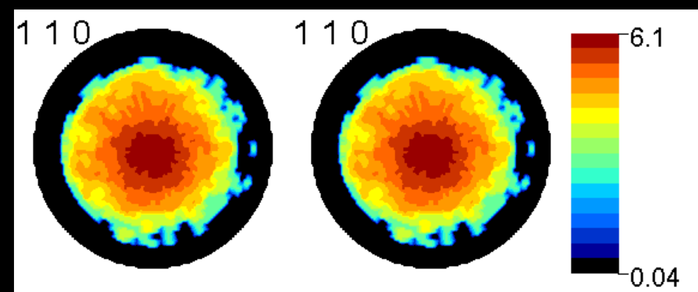

$$\Delta I_{\vec{h}}^{-p}(\vec{y},\vec{B})$$

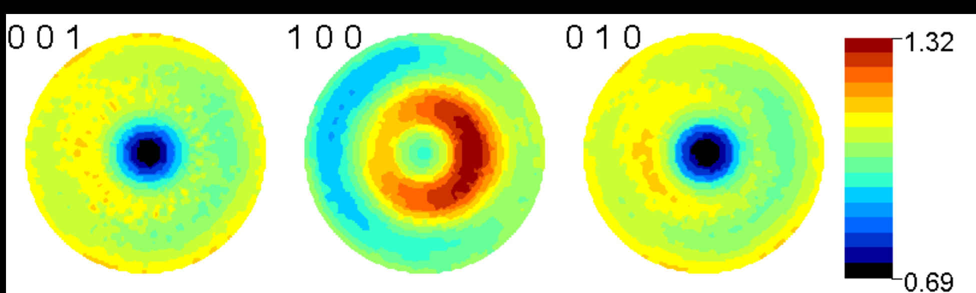

***** True iteration step #120 *****

ODF min max:	*0.64*	*2.26*
Texture Index (F^2)	*1.0294*	
Entropy	*-0.0144*	
Average RP	*0.2427*	
Average RP1	*0.3041*	

Why needing QTA

- Correct for QTA effects in XRD: structure analysis

QTA and structure correlations: yes, but

$f(g)$ and $|F_{\mathbf{h}}|^2$ are different !

Charonia lampas lampas

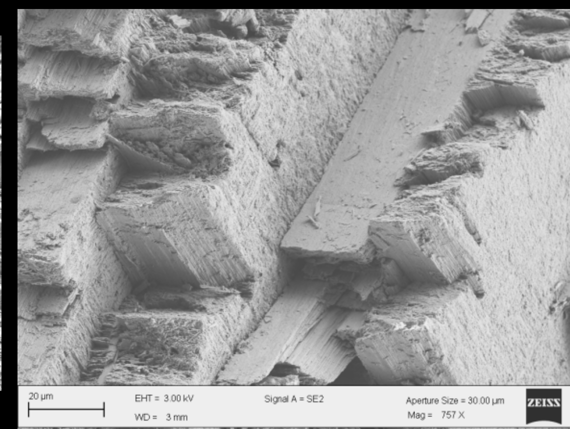

OD maximum (m.r.d.) **OD minimum (m.r.d.)**		299 0	196 0	2816 0
Texture index (m.r.d.^{2})		42.6	47	721
Texture reliability factors	**R_w (%)**	14.3	11.2	32.5
	R_B (%)	15.6	12.7	47.8
Rietveld reliability factors	**GoF (%)**	1.72	1.72	3.05
	R_w (%)	29.2	28.0	57.3
	R_B (%)	22.9	21.7	47.2
	R_{exp}(%)	22.2	21.3	32.8

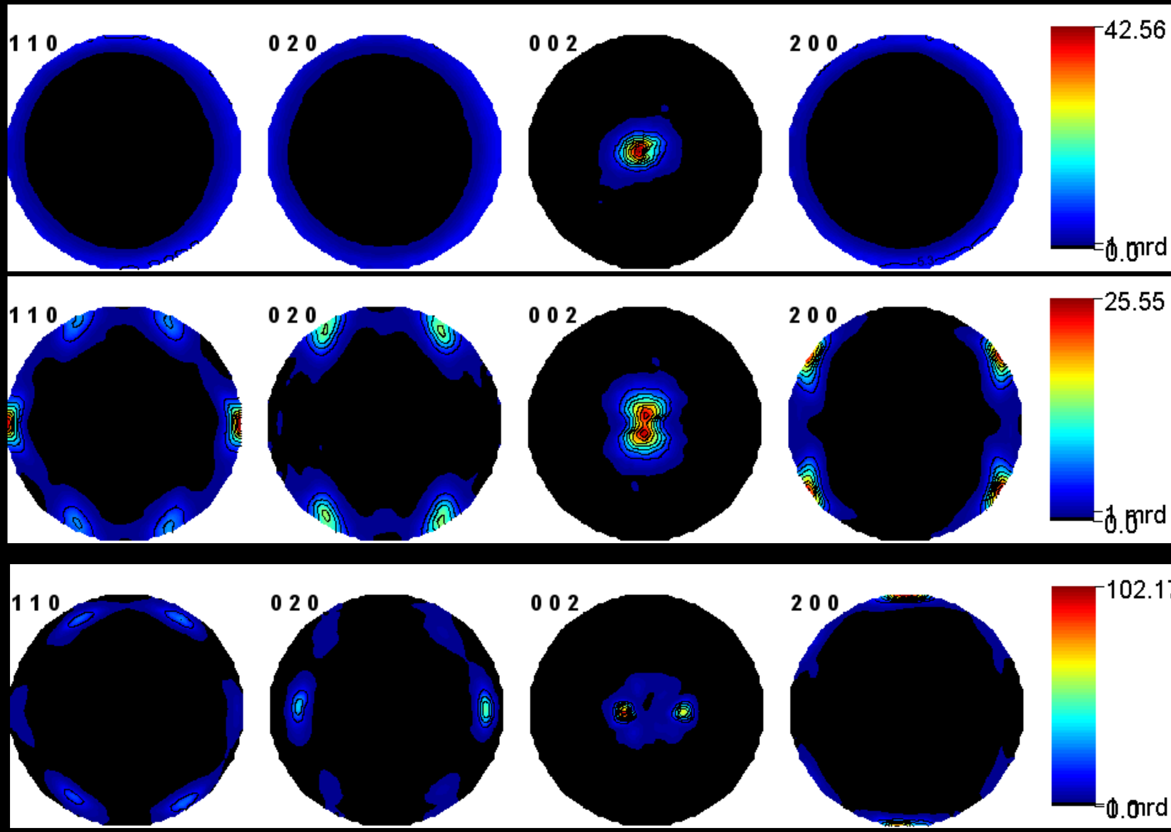
1 1 0
0 2 0
0 0 2
2 0 0
42.56
1 mrd
0.0
25.55
102.17

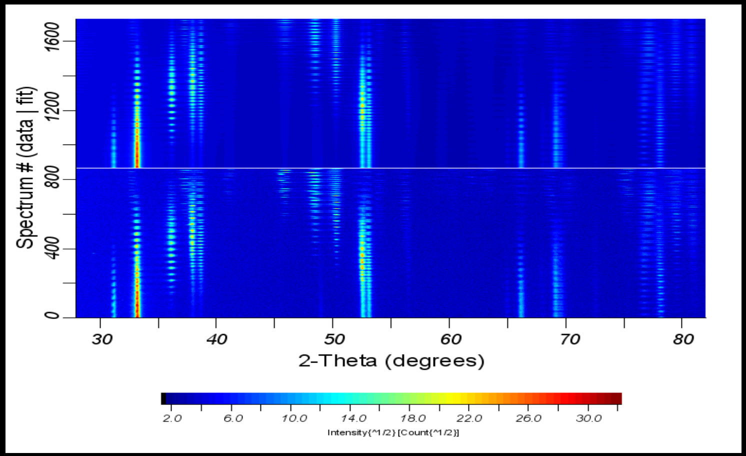
Spectrum # (data | fit)
0
400
800
1200
1600
30
40
50
60
70
80
2-Theta (degrees)
2.0
6.0
10.0
14.0
18.0
22.0
26.0
30.0
Intensity(^1/2) [Count(^1/2)]

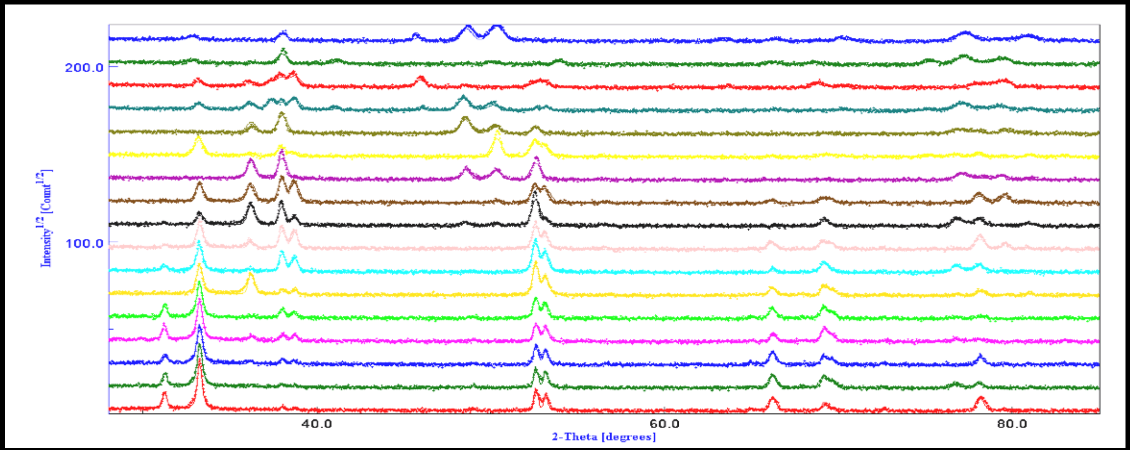
200.0
100.0
Intensity^1/2 [Count^1/2]
40.0
60.0
80.0
2-Theta [degrees]

		Geological reference	*Charonia lampas* OCL	*Charonia lampas* RCL	*Charonia lampas* ICCL	**Strombus decorus**
a (Å) b (Å) c (Å)		4.9623(3) 7.968(1) 5.7439(3)	4.98563(7) 8.0103(1) 5.74626(3)	4.97538(4) 7.98848(8) 5.74961(2)	4.9813(1) 7.9679(1) 5.76261(5)	4.9694(3) 7.9591(4) 5.7528(1)
Ca	y z	0.41500 0.75970	0.41418(5) 0.75939(3)	0.414071(4) 0.76057(2)	0.41276(9) 0.75818(8)	0.4135(7) 0.7601(8)
C	y z	0.76220 -0.08620	0.7628(2) -0.0920(1)	0.76341(2) -0.08702(9)	0.7356(4) -0.0833(2)	0.7607(4) -0.0851(7)
O1	y z	0.92250 -0.09620	0.9115(2) -0.09205(8)	0.9238(1) -0.09456(6)	0.8957(3) -0.1018(2)	0.9228(4) -0.0905(9)
O2	x y z	0.47360 0.68100 -0.08620	0.4768(1) 0.6826(1) -0.08368(6)	0.4754(1) 0.68332(9) -0.08473(5)	0.4864(3) 0.6834(2) -0.0926(1)	0.4763(6) 0.6833(3) -0.0863(7)
$\Delta Z_{C\text{-}O1}$ (Å)		0.05744	0.00029	0.04335	0.1066	0.031

Calcite: $\Delta Z = 0$

Biogenic intercrystalline effect

- Correct for QTA effects in XRD: QPA

QTA and QPA correlations: yes, but

f(g) and S_Φ are different !

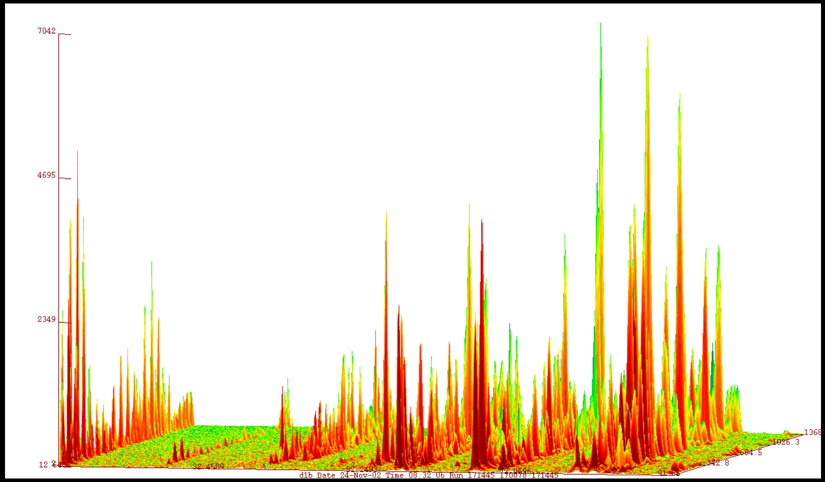

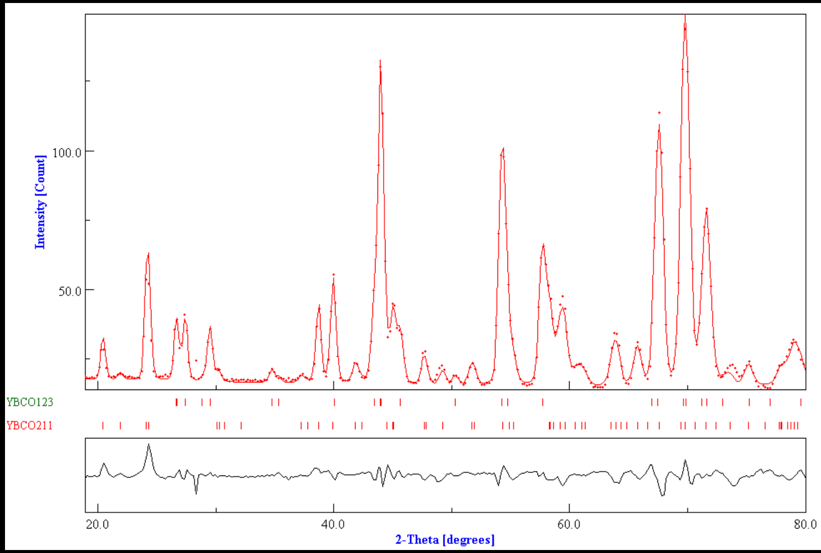

f(g) is on the individuals

S_Φ is on the sum

- Correct for QTA effects in spectroscopies: P-EXAFS on clays

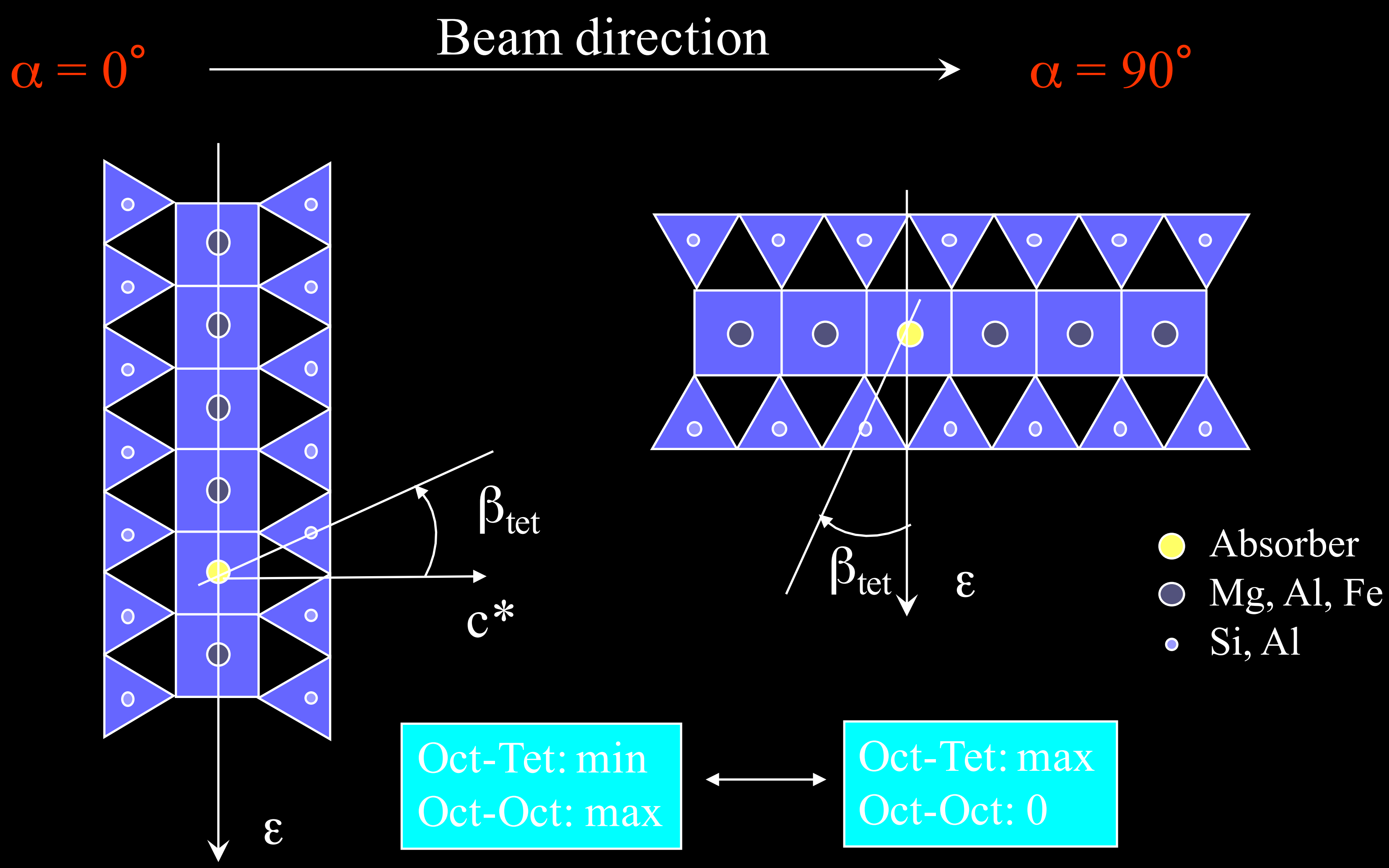

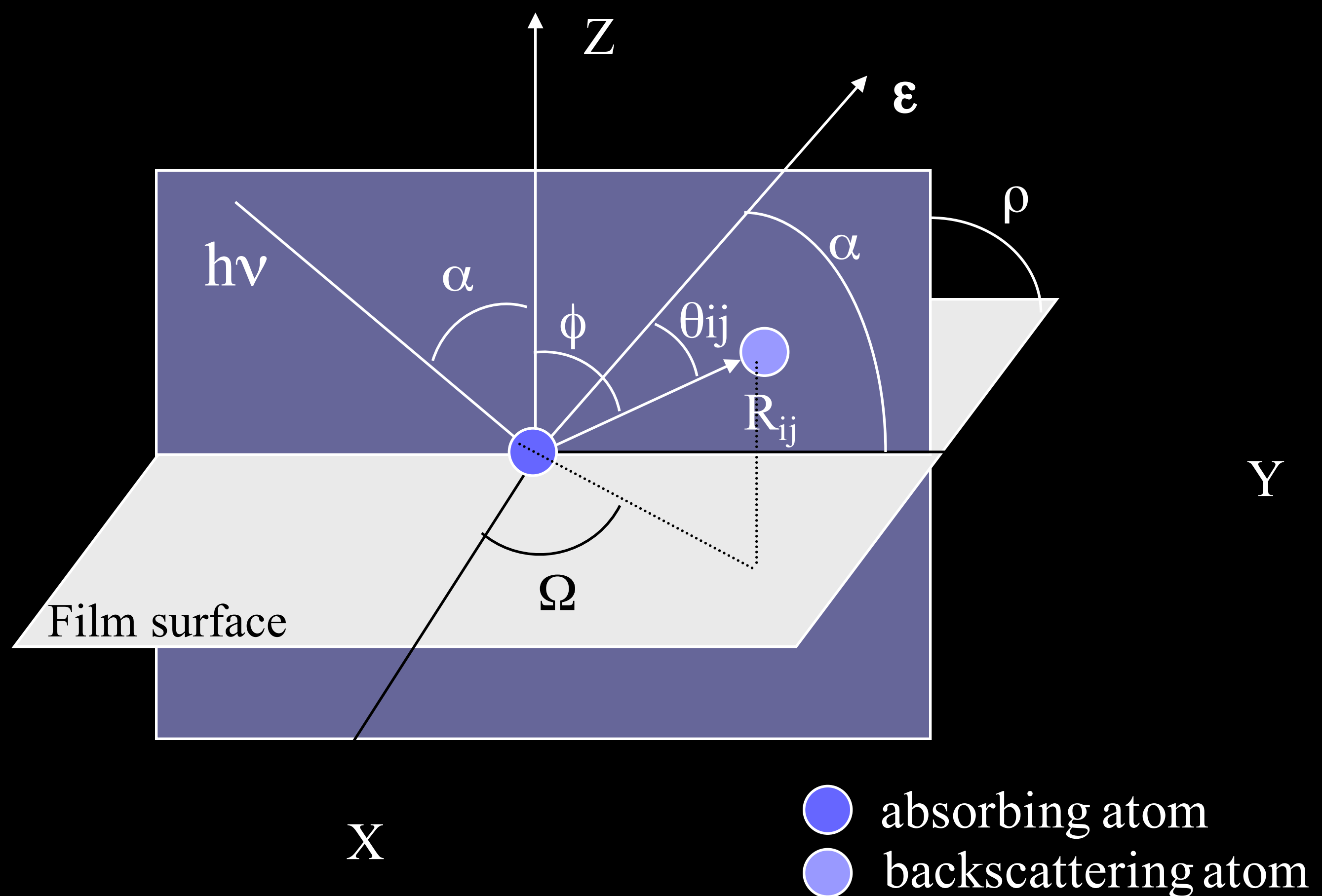

$$\left\langle \cos^2 \theta_{ij} \right\rangle = \frac{1}{2\pi} \int_0^{2\pi} \cos^2 \theta_{ij} d\Omega = \cos^2 \phi \sin^2 \alpha + \frac{\cos^2 \alpha \sin^2 \phi}{2}$$

Fe K-edge

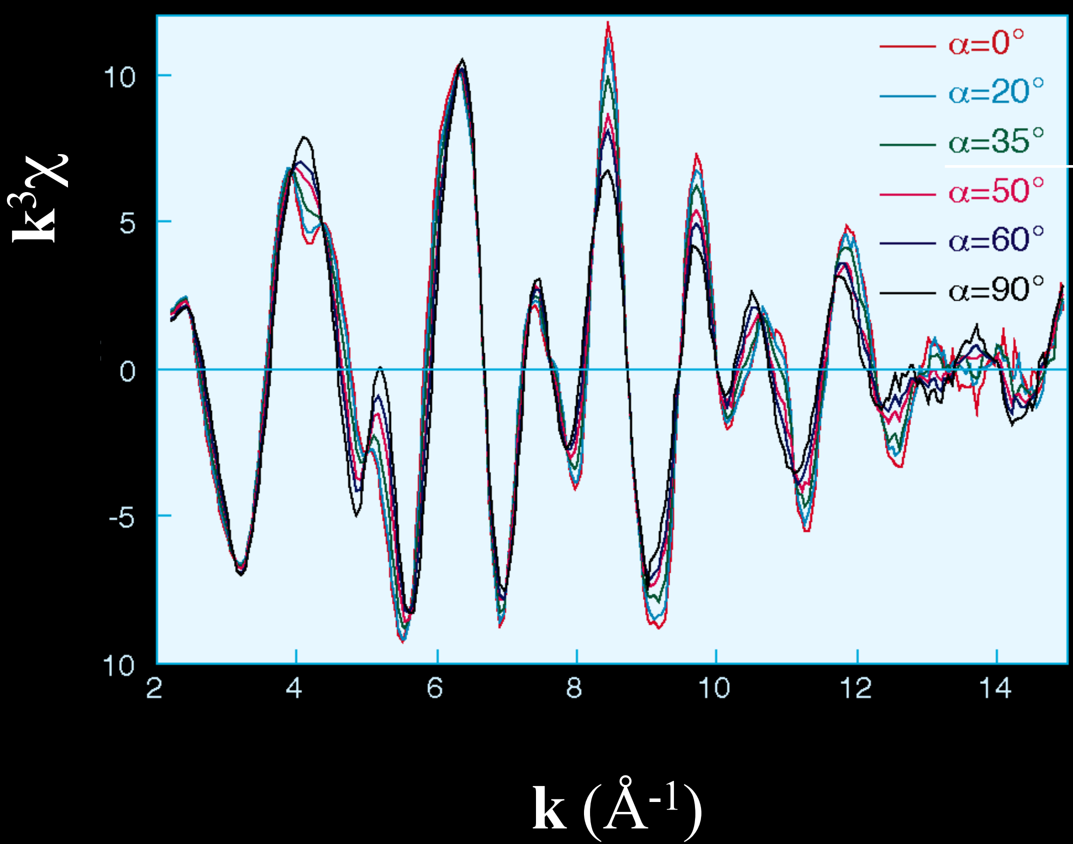

High quality range up to 14-15Å^{-1}

Powder spectra

Strong α dependence = strong texture

$$N_{obs} = 3N_{real}\left[\cos^2\phi\sin^2\alpha + \frac{\cos^2\alpha\sin^2\phi}{2}\right]$$

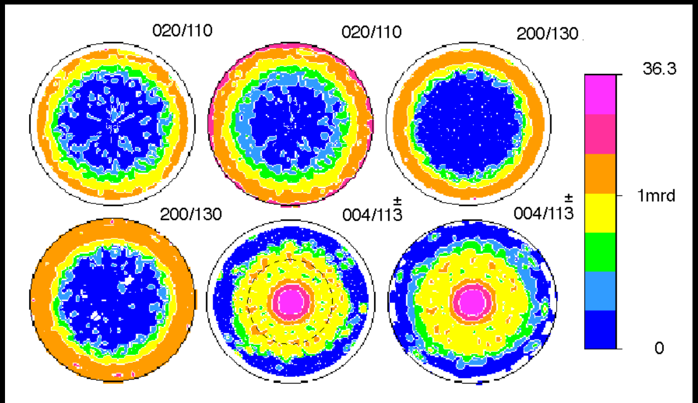

Experimental and recalculated pole figures

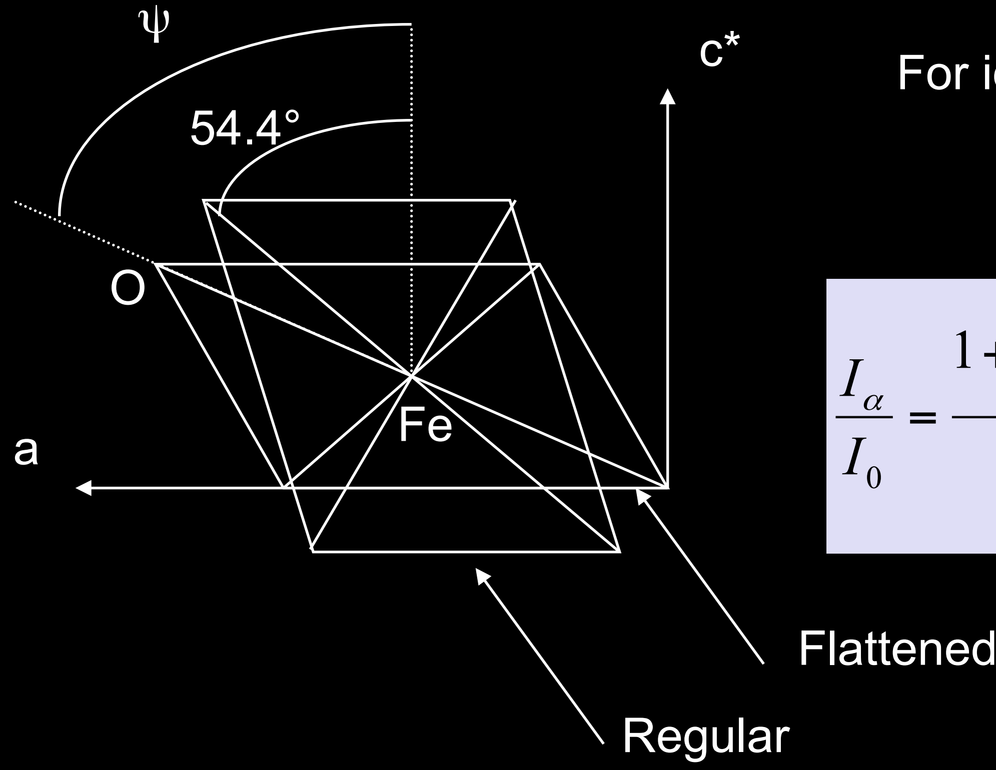

For ideally textured films:

$$\frac{I_\alpha}{I_0} = \frac{1 + \frac{1}{2}\left(3\sin^2\alpha - 1\right)\left(3\cos^2\psi - 1\right)}{1 - \frac{1}{2}\left(3\cos^2\psi - 1\right)}$$

- Mollusc shells and fossils: phylogeny

Closely related species, close textural characters, but significant variations: textural parameters can serve character analysis

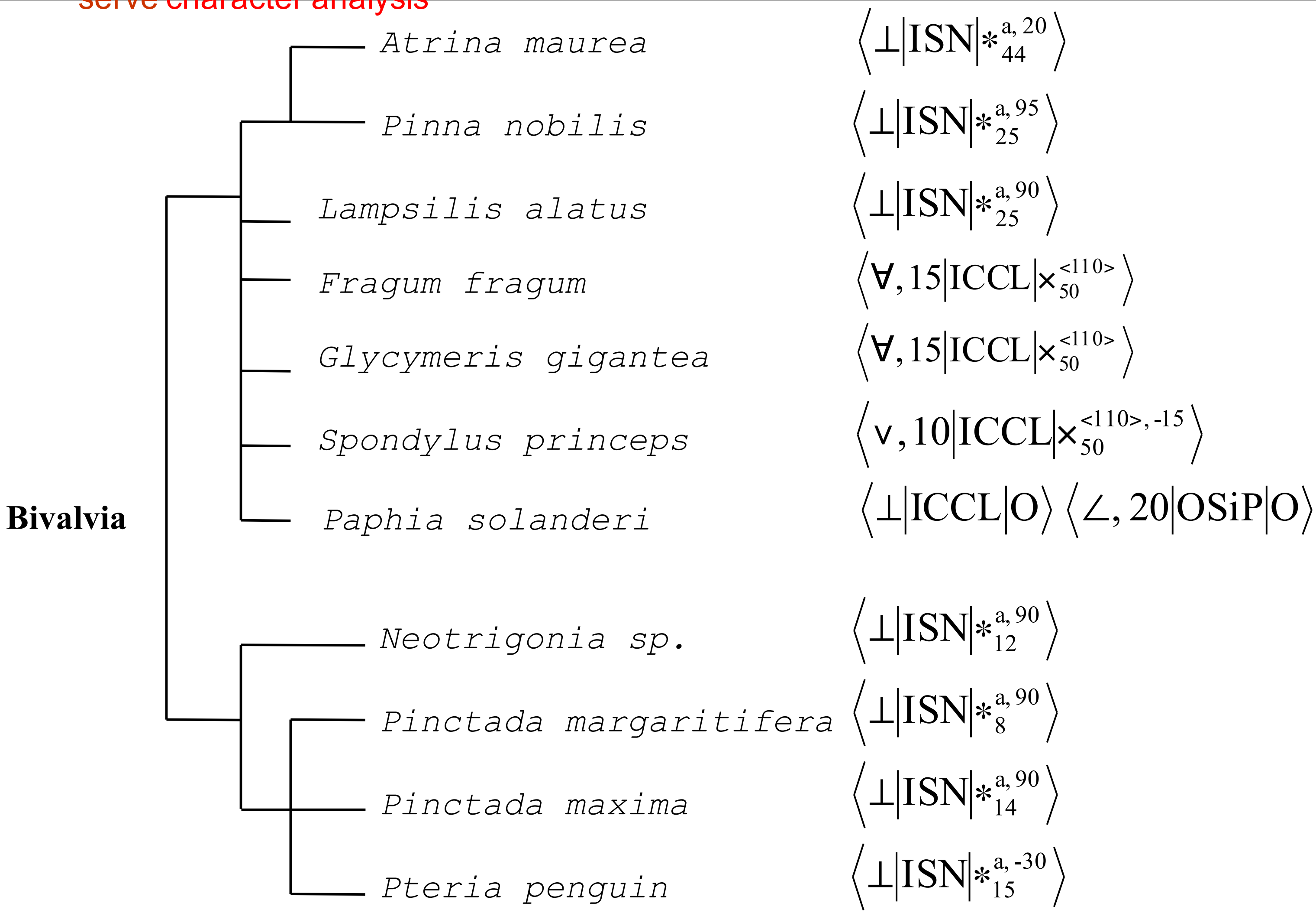

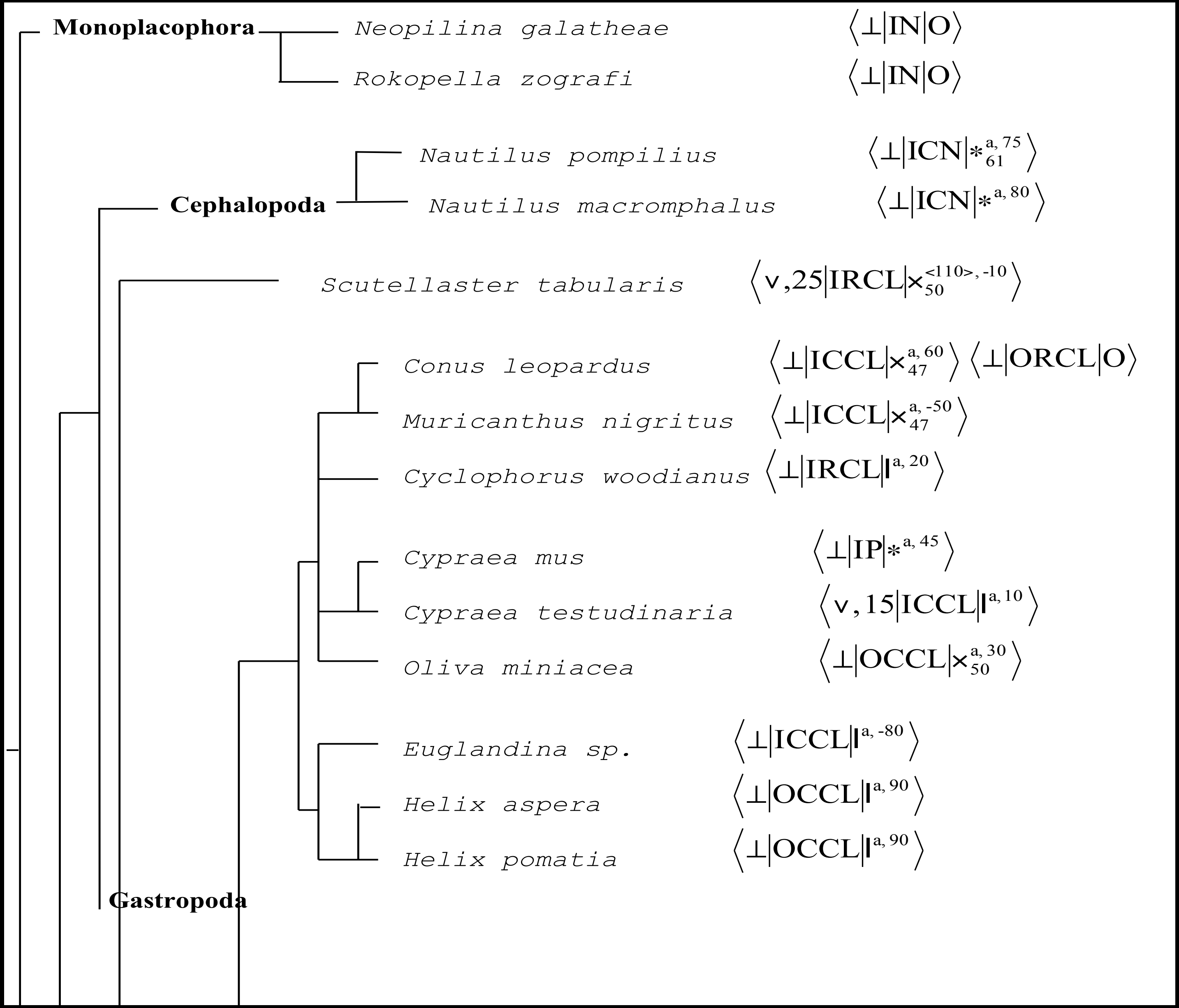
Monoplacophora
Neopilina galatheae
⟨⊥|IN|O⟩
Rokopella zografi
⟨⊥|IN|O⟩
Cephalopoda
Nautilus pompilius
⟨⊥|ICN|*a, 75 61⟩
Nautilus macromphalus
⟨⊥|ICN|*a, 80⟩
Scutellaster tabularis
⟨v,25|IRCL|×<110>, -10 50⟩
Conus leopardus
⟨⊥|ICCL|×a, 60 47⟩ ⟨⊥|ORCL|O⟩
Muricanthus nigritus
⟨⊥|ICCL|×a, -50 47⟩
Cyclophorus woodianus
⟨⊥|IRCL|Ia, 20⟩
Cypraea mus
⟨⊥|IP|*a, 45⟩
Cypraea testudinaria
⟨v,15|ICCL|Ia, 10⟩
Oliva miniacea
⟨⊥|OCCL|×a, 30 50⟩
Euglandina sp.
⟨⊥|ICCL|Ia, -80⟩
Helix aspera
⟨⊥|OCCL|Ia, 90⟩
Helix pomatia
⟨⊥|OCCL|Ia, 90⟩
Gastropoda

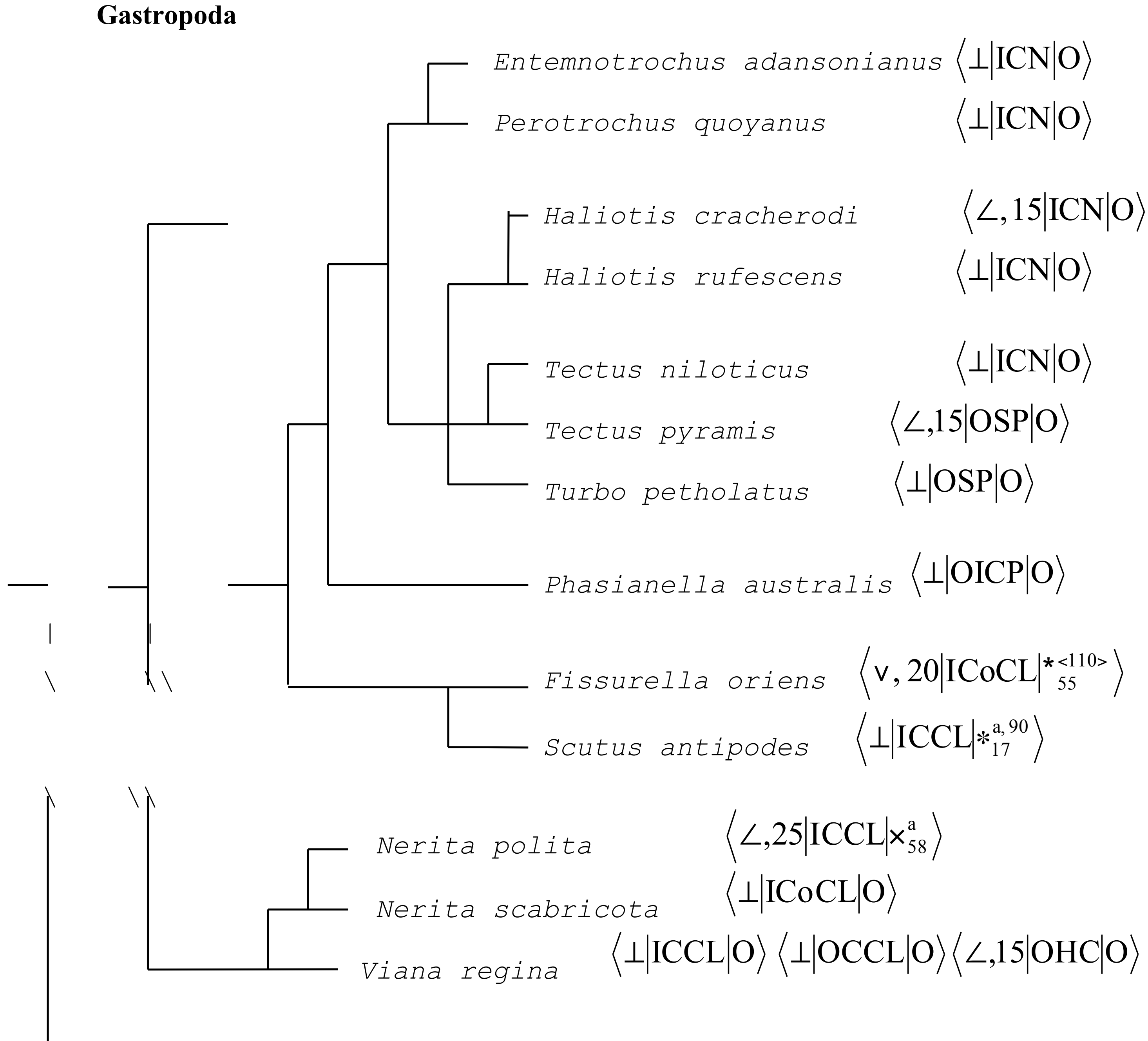
Gastropoda
Entemnotrochus adansonianus ⟨⊥|ICN|O⟩
Perotrochus quoyanus ⟨⊥|ICN|O⟩
Haliotis cracherodi ⟨∠, 15|ICN|O⟩
Haliotis rufescens ⟨⊥|ICN|O⟩
Tectus niloticus ⟨⊥|ICN|O⟩
Tectus pyramis ⟨∠,15|OSP|O⟩
Turbo petholatus ⟨⊥|OSP|O⟩
Phasianella australis ⟨⊥|OICP|O⟩
Fissurella oriens ⟨∨, 20|ICoCL|$*^{\langle 110\rangle}_{55}$⟩
Scutus antipodes ⟨⊥|ICCL|$*^{a,90}_{17}$⟩
Nerita polita ⟨∠,25|ICCL|$\times^{a}_{58}$⟩
Nerita scabricota ⟨⊥|ICoCL|O⟩
Viana regina ⟨⊥|ICCL|O⟩ ⟨⊥|OCCL|O⟩ ⟨∠,15|OHC|O⟩

Phylogenic interest: nacre = ancestral (Carter & Clarck, 1985)

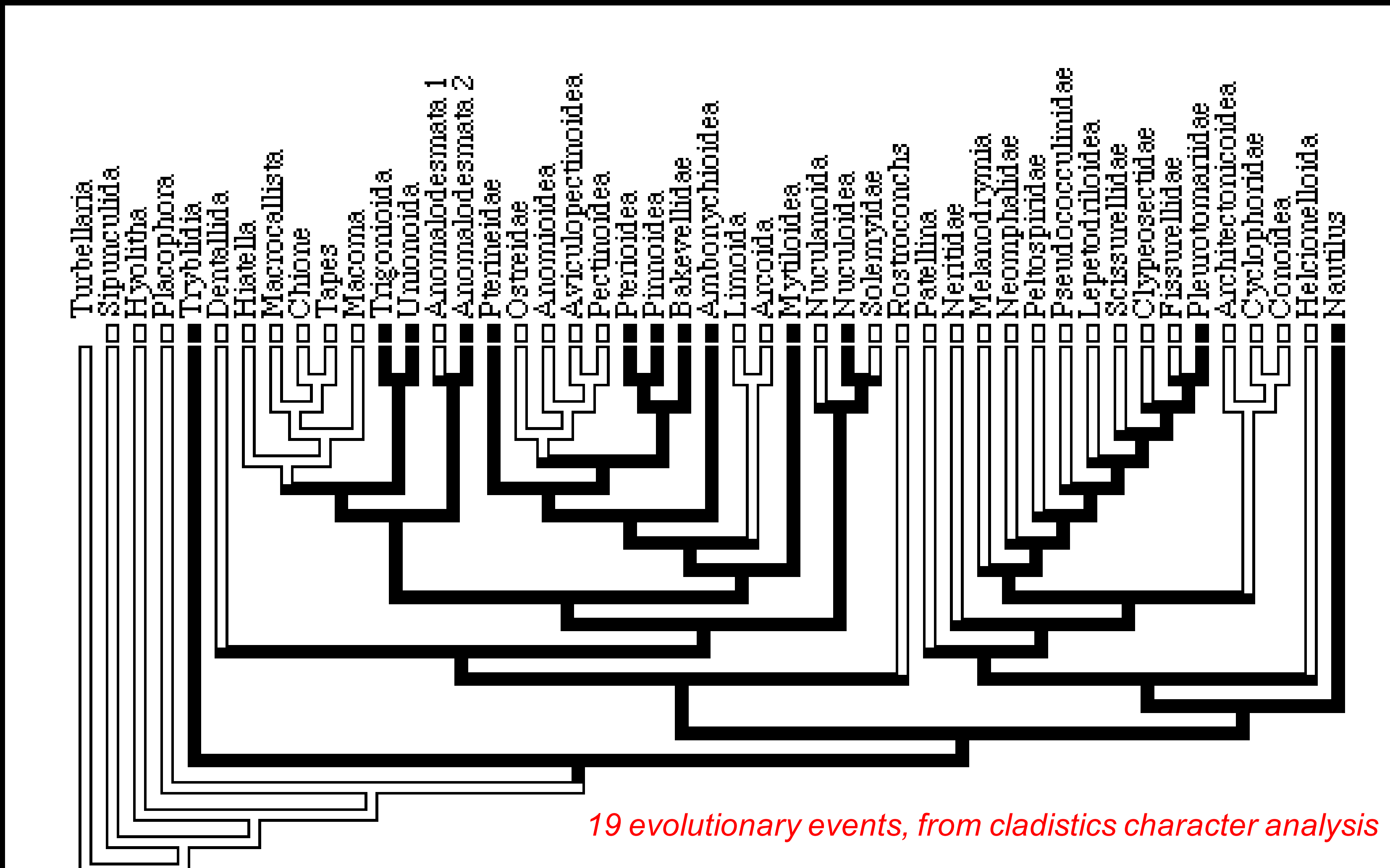

nacre not ancestral

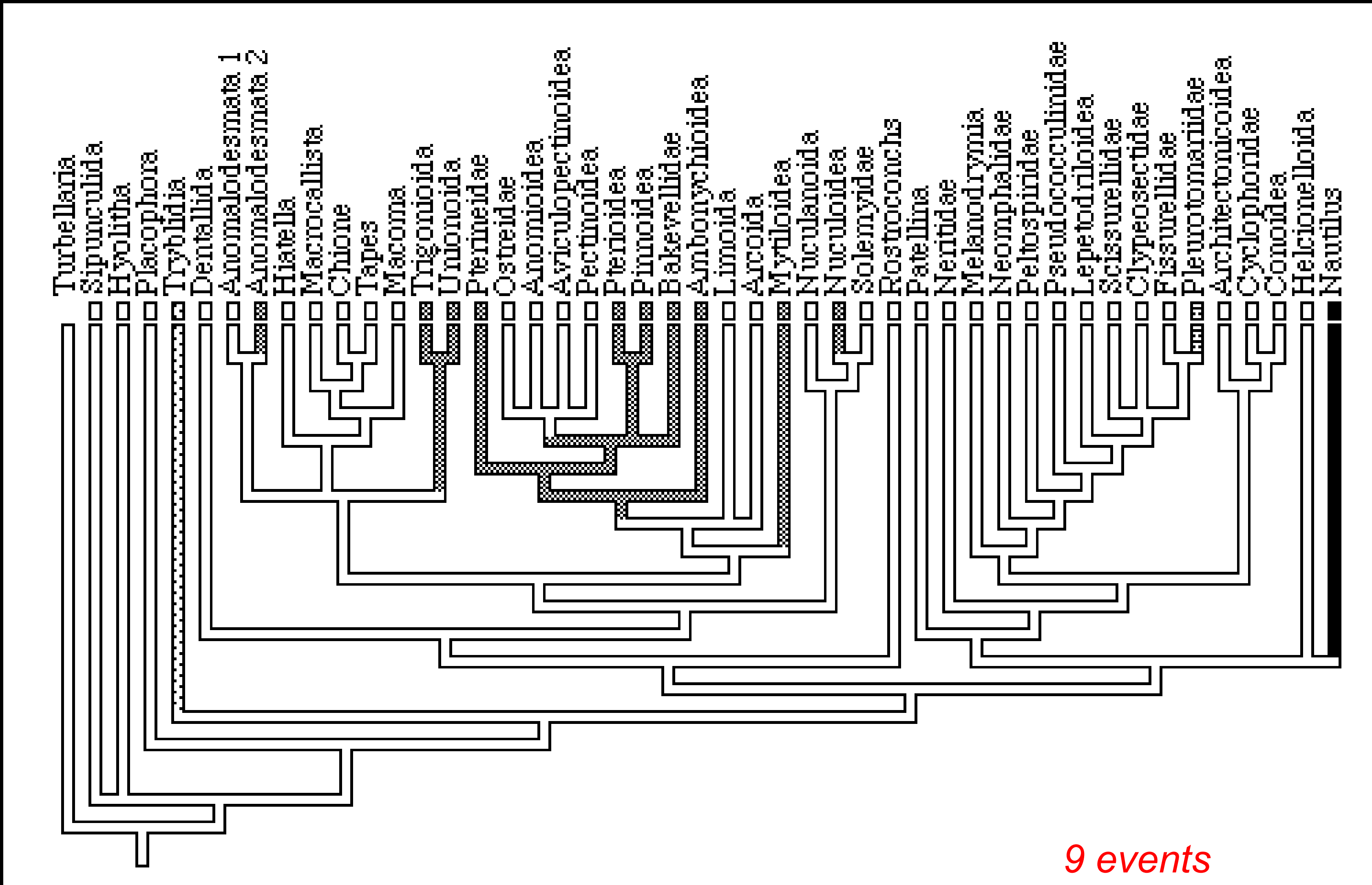

Calcitic fossils: trichites

	Layer type	ODF Max (mrd)	ODF min (mrd)	RP0 (%)	RP1 (%)	c-axis	a-axis	{001} Max (mrd)	F^2 (mrd^2)	- S
Pinna nobilis	OP	303	0	50	29	// N	random	68	29	2.3
Pteria penguin	OP	84	0	29	15	// N	random	31	13	1.9
Amussium parpiraceum	OP	330	0	53	33	// G	<110> // M	20	31	2.6
Bathymodiolus thermophilus	OP	63	0	25	18	// G	// M	27	13	1.9
Mytilus edulis	OP	207	0	41	25	75° from N	<110> // M	23	21	2.2
Trichites	P	390	0	52	28	15° from N	random	56	41	2.2
Crassostrea gigas	IF	908	0	45	31	35° from N	// M	>100	329	5.1

No DNA is available on fossils like Trichites, but Trichite's textural parameters are close to the ones of *pinnoids* or *pterioids*: interesting for the classification of extinct species

Calcitic fossils: *Belemnites*

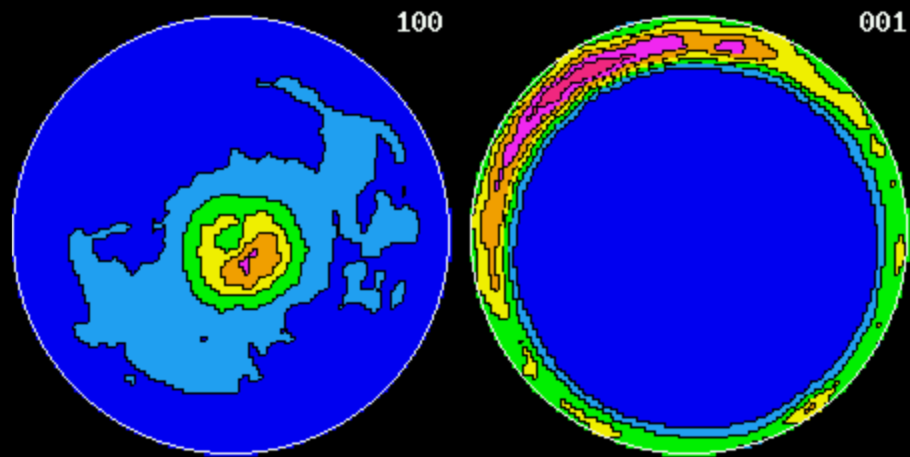

Belemnita mucronatus

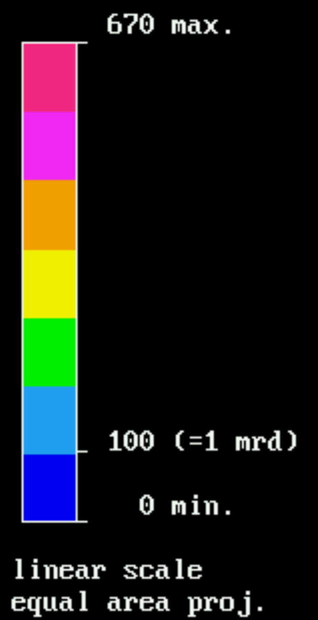

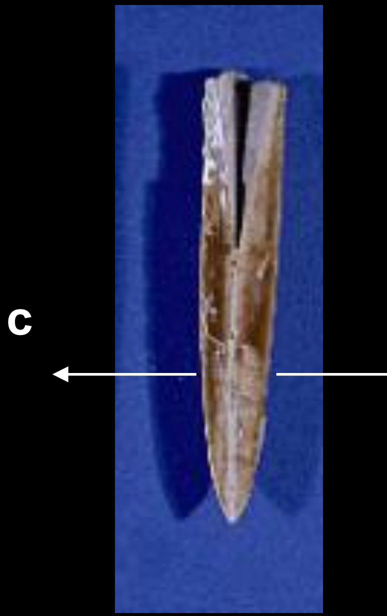

c-axes perp. to the shell: as in other cephalopods: nacre ancestral ?

Aragonitic fossils: *Baculities sp.*

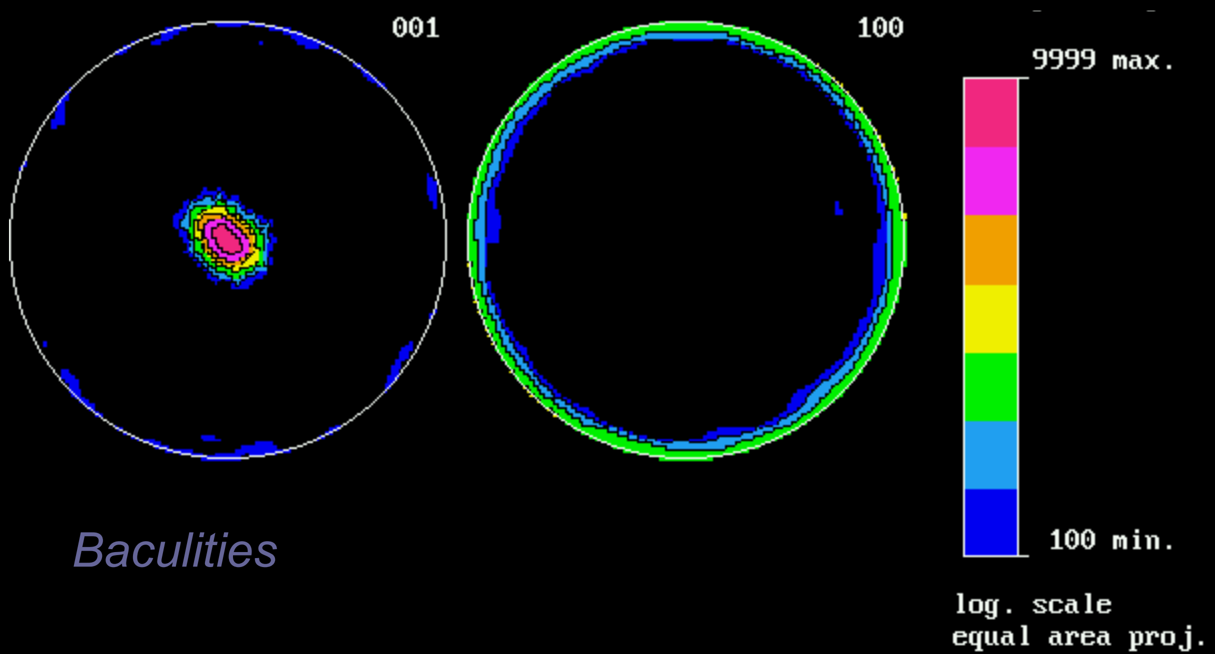

Baculities

c-axes perp. to the shell: as in other cephalopods, strong **c**-calcite to **c**-aragonite fossils interaction

- Predict macroscopic anisotropic properties: Elastic

Arithmetic average

$$\langle \mathcal{T} \rangle = \int_g \mathcal{T}(g)\, f(g)\, dg$$

$$\langle (\mathcal{T})^{-1} \rangle \neq \langle \mathcal{T} \rangle^{-1}$$

Voigt average
Homogeneous strain

$$C_{ijk\ell}^{M} = <C_{ijk\ell}>$$

Upper bound

Reuss average
Homogeneous stress

$$S_{ijk\ell}^{M} = <S_{ijk\ell}>$$

Lower bound

Geometric average

$$\lceil b \rceil = \prod_{k=1}^{N} b_k^{\,w_k} = \exp\left(\langle \ln b \rangle\right)$$

scalar

$$\langle \ln b \rangle = \sum_{k=1}^{N} \ln b_k \, w_k$$

$$\lceil T \rceil_{ij} = \exp(\langle \ln T \rangle_{i'j'})$$

tensor

$$\lceil \lambda_I \rceil = 1/\lceil 1/\lambda_I \rceil = \lceil \lambda_I^{-1} \rceil^{-1}$$

Eigenvalues of T_{ij}

$$\left\langle (C_{ijk\ell})^{-1} \right\rangle = \left\langle C_{ijk\ell} \right\rangle^{-1}$$

- Predict macroscopic anisotropic properties: Electric polarisation

$$\langle \mathbf{p}_h \rangle = \frac{\iint_{\mathbf{y}} \mathbf{p}_h P_h(\mathbf{y})\, \mathbf{dy}}{\iint_{\mathbf{y}} P_h(\mathbf{y})\, \mathbf{dy}}$$

- Predict macroscopic anisotropic properties: BAW

Propagation equation

$$\rho \frac{\partial^2 u^i}{\partial t^2} = \left[\mathrm{C}^{i\ell mn} \right] \frac{\partial^2 u_n}{\partial x^m \partial x^\ell}$$

Propagation direction	V_P	V_{S1}	V_{S2}
[100]	$\sqrt{\frac{c^M{}_{11}}{\rho}}$	$\sqrt{\frac{c^M{}_{44}}{\rho}}$	$\sqrt{\frac{c^M{}_{44}}{\rho}}$
[110]	$\sqrt{\frac{c^M{}_{11} + 2c^M{}_{44} + c^M{}_{12}}{2\rho}}$	$\sqrt{\frac{c^M{}_{11} - c^M{}_{12}}{2\rho}}$	$\sqrt{\frac{c^M{}_{44}}{\rho}}$
[111]	$\sqrt{\frac{c^M{}_{11} + 4c^M{}_{44} + 2c^M{}_{12}}{3\rho}}$	$\sqrt{\frac{c^M{}_{11} + c^M{}_{44} - c^M{}_{12}}{3\rho}}$	$\sqrt{\frac{c^M{}_{11} + c^M{}_{44} - c^M{}_{12}}{3\rho}}$

Cubic crystal system

	c_{11} or c_{11}^M	c_{12} or c_{12}^M	c_{13} or c_{13}^M	c_{14} or c_{14}^M	c_{33} or c_{33}^M	c_{44} or c_{44}^M
Single crystal	201	54.52	71.43	8.4	246.5	60.55
$LiNbO_3$/Si	206.4	68.5	67.6	0.48	216.5	64
$LiNbO_3$/Al_2O_3	204	65.7	69.7	1.1	219.9	63.2

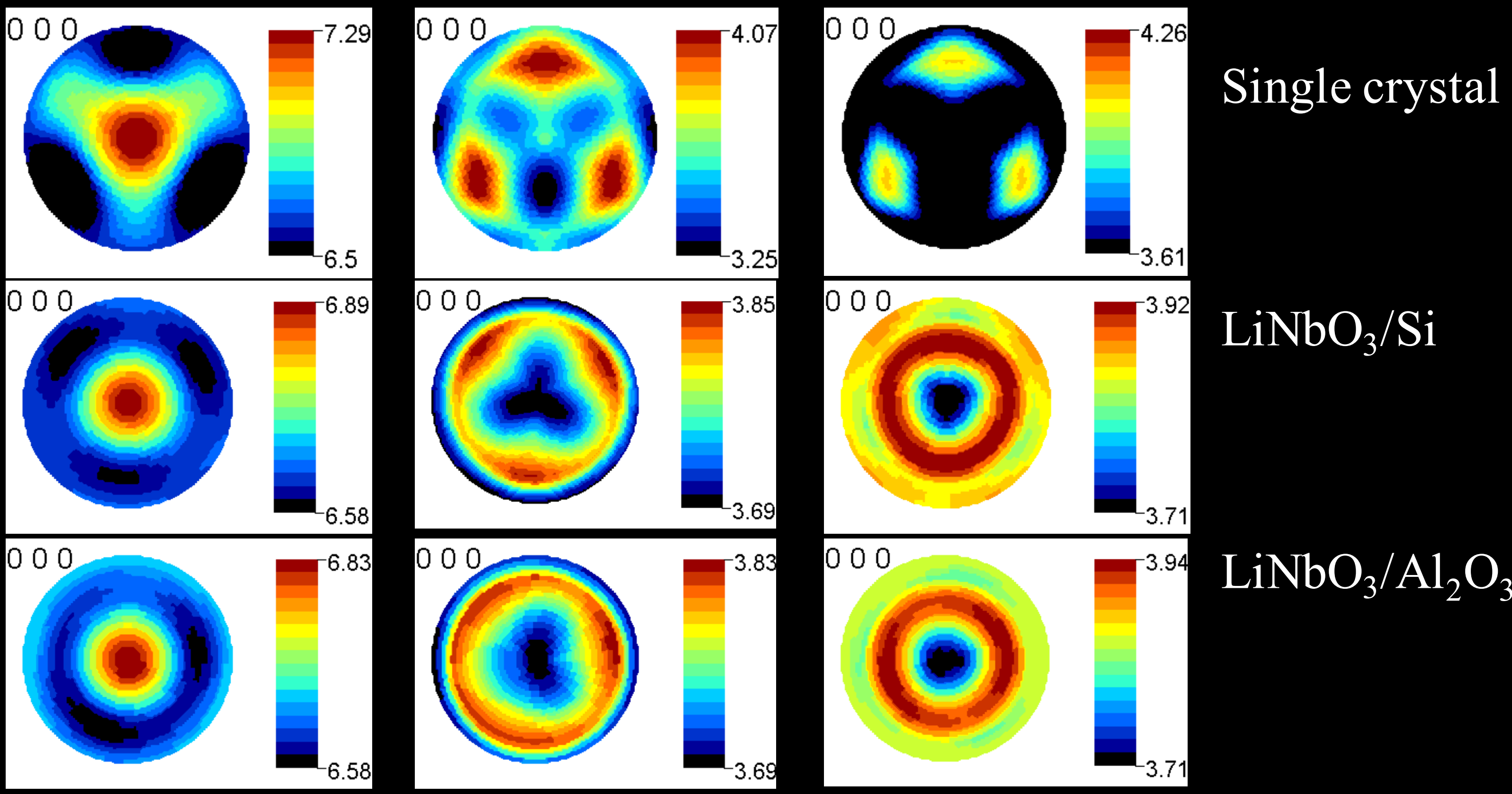

- Predict macroscopic anisotropic properties: Magnetisation

$$\frac{M_{\perp}}{M_S} = 2\pi\int_0^{\frac{\pi}{2}}(1-\rho_0)\,PV(\theta_g)\sin\theta_g\cos(\theta_g-\theta)\,d\theta_g + \rho_0 M_{random}$$

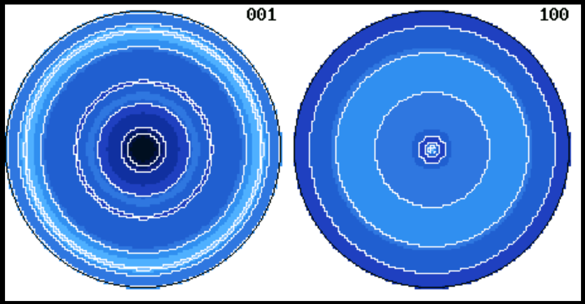

max {001}: 3.9 mrd
min: 0.5 mrd

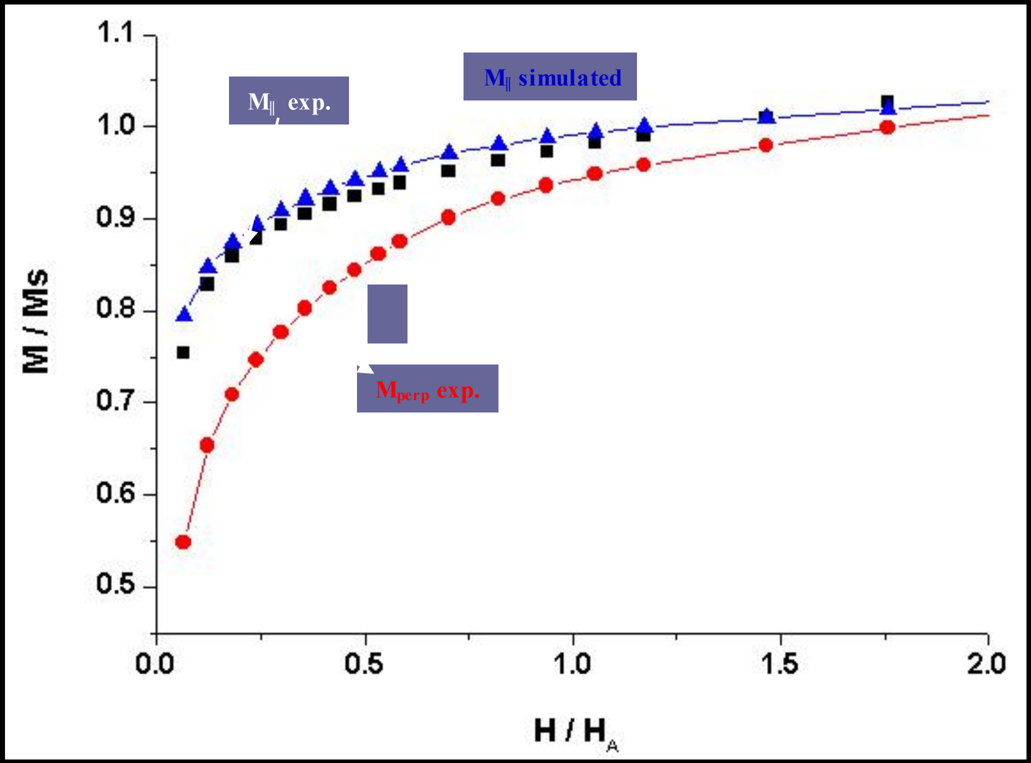

$ErMn_3Fe_9C$:
ODF + micros. → macros.

- Correlate macroscopic anisotropic properties: Thermoelectric PF

9.8 MPa for 2 h

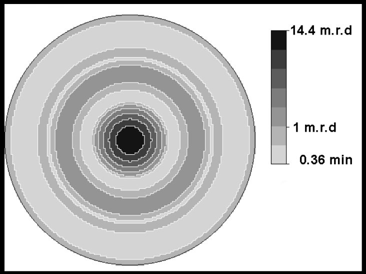

19.6 MPa for 6 h

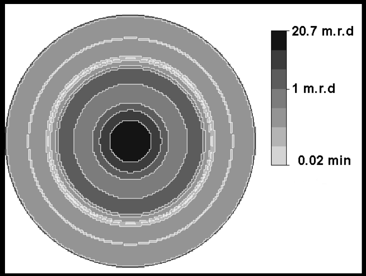

19.6 MPa for 20 h

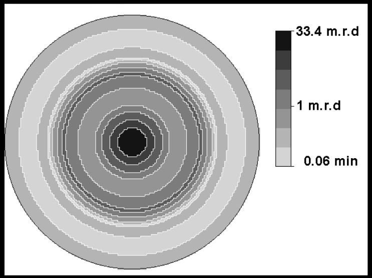

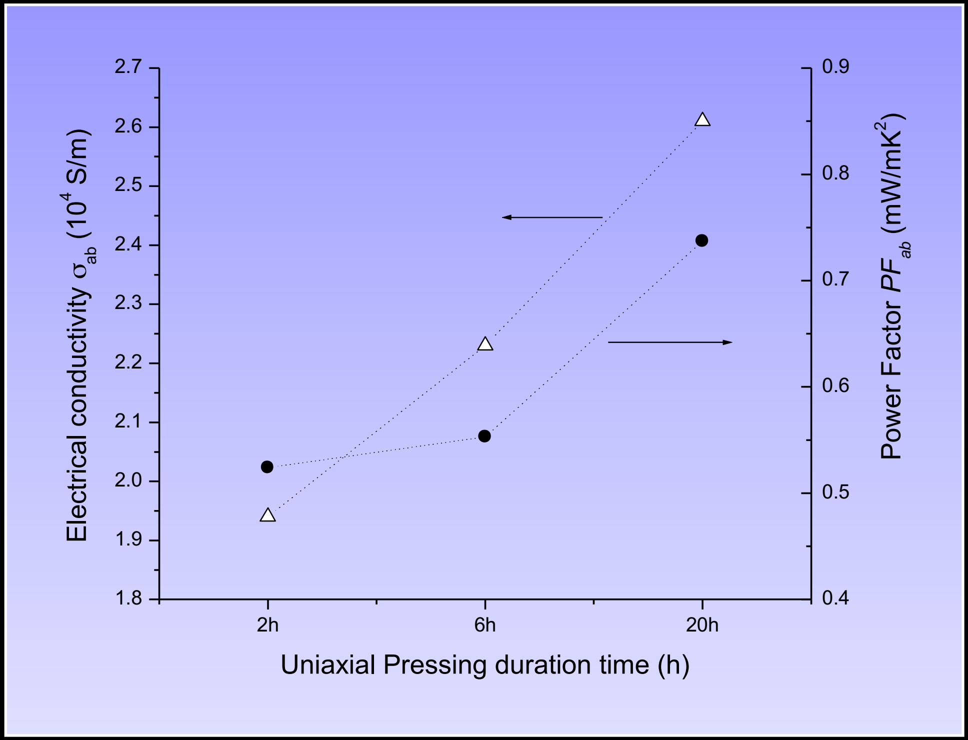

- Correlate macroscopic anisotropic properties: Pyroelectric coefficient

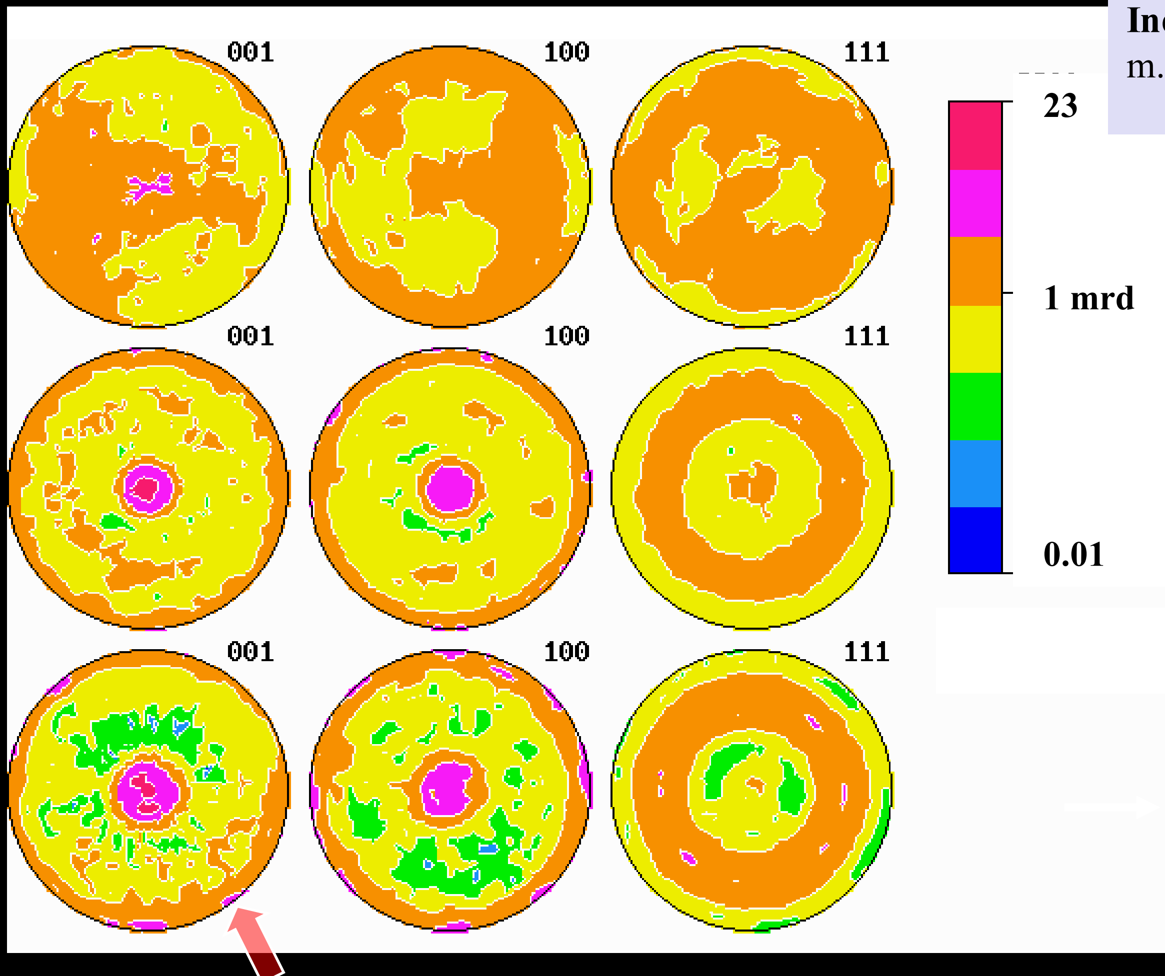

Sample	Texture Index m.r.d.[2]	Pyroelectric Coefficient 10^{-8}C cm^{-2} K^{-1}
PCT on Pt/TiO_2/(100)Si	2.1	0.3
PCT on Pt/(100)MgO	5.1	1.5
PCT on Pt/(100)$SrTiO_3$	7.9	1.1

Enhancement of <001> texture

- Correlate macroscopic anisotropic properties: Tauc gap in nano-Si

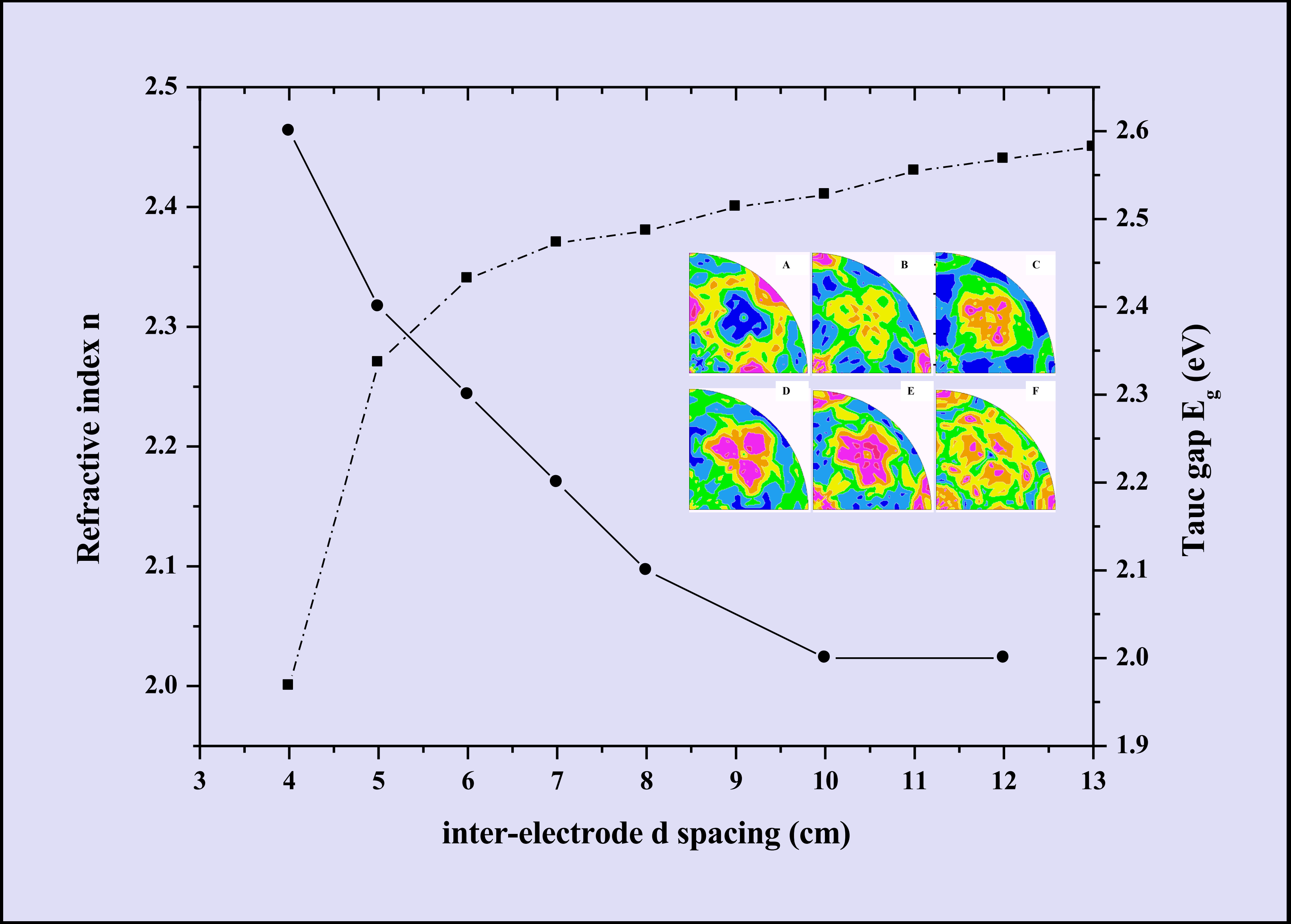

-Correlate macroscopic anisotropic properties: Bi-2223 / Bi-2212 superconducting Jc's

Sinter-forging dwell time (h)	*Orientation Distribution Max (m.r.d.)*		*RP0 (%)*	*RP1 (%)*	*J_c (A/cm^2)*
	Bi2212	*Bi2223*			
20	21.8	20.7	17.74	10.56	12500
50	24.1	24.4	17.05	11.04	15000
100	31.5	25.2	13.54	9.31	19000
150	65.4	27.2	16.24	12.25	20000

Sinter-forging Time

Texture strength

% Bi2223

Crystallite Size

J_c

-Correlate macroscopic anisotropic properties: Levitation force and trapped flux in MTG-YBCO

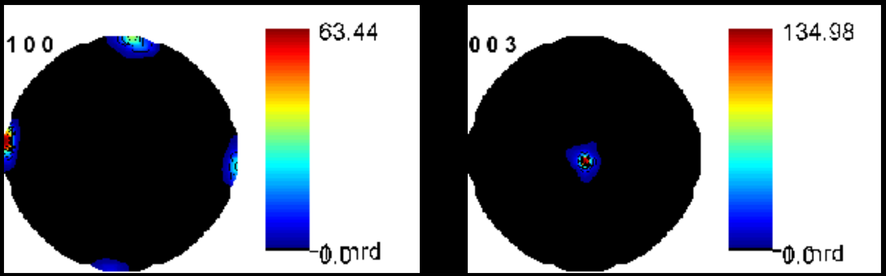

Neutron pole figures (D1B-ILL)

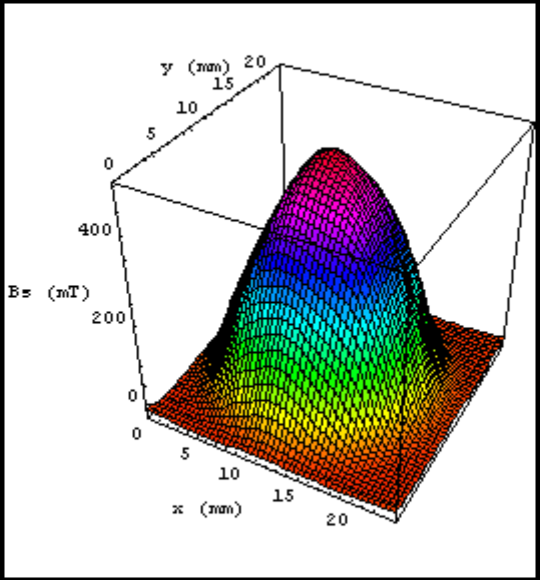

and trapped flux

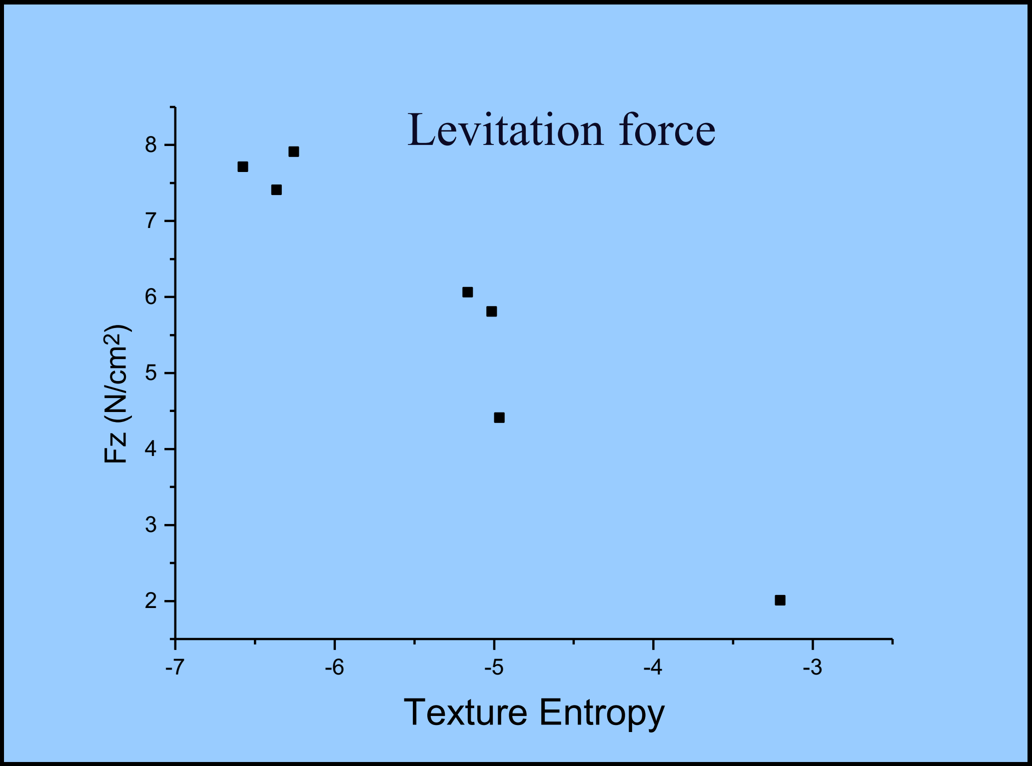

Models ?

Why needing combined analysis

- Solve the peak-overlap problems (intra- and inter-phases)

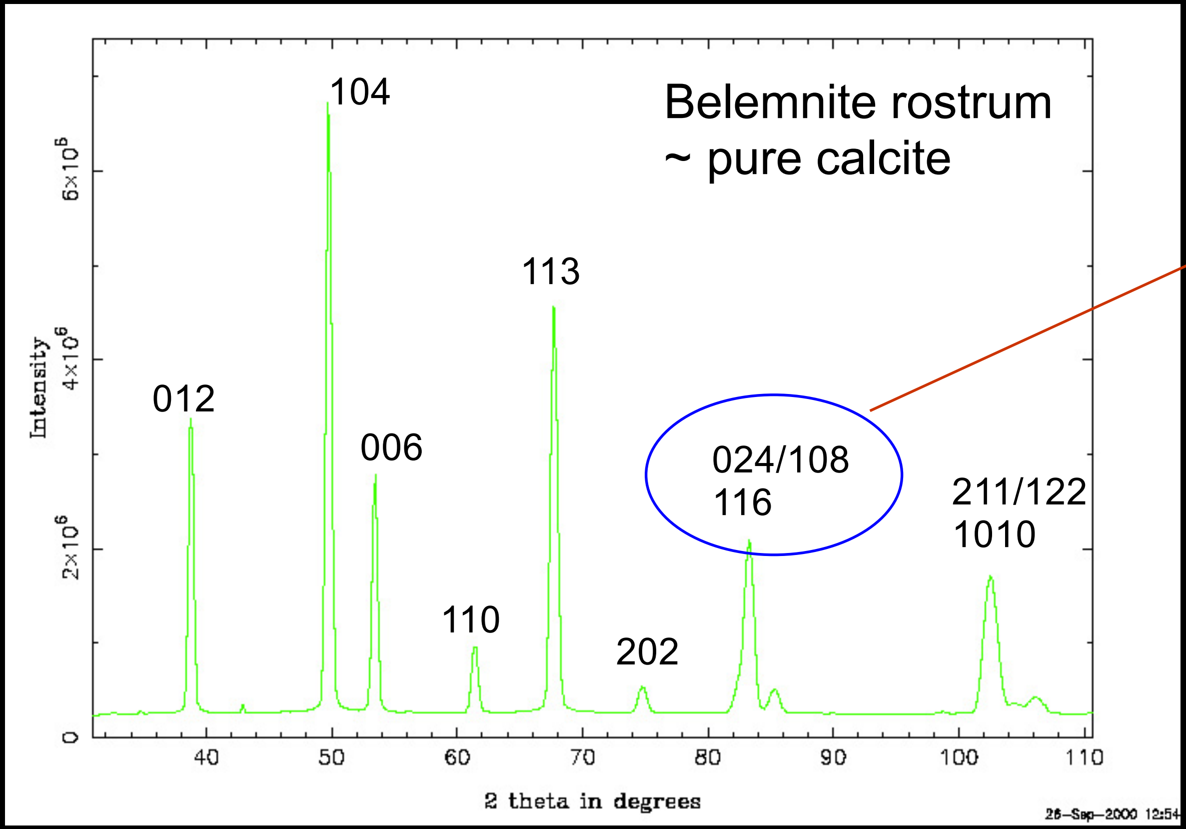

Resolved during ODF refinement

Polyphased Mylonite (Palm Canyon, CA)

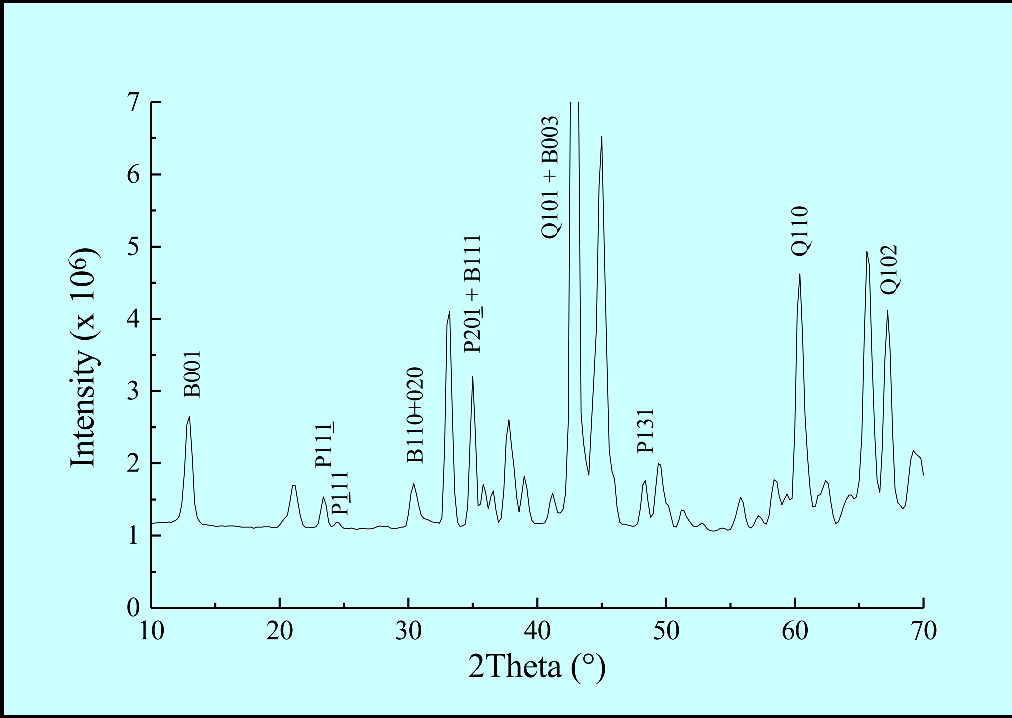

Using 0D detector hardly manageable

Space group	C2/m	R3	C-1

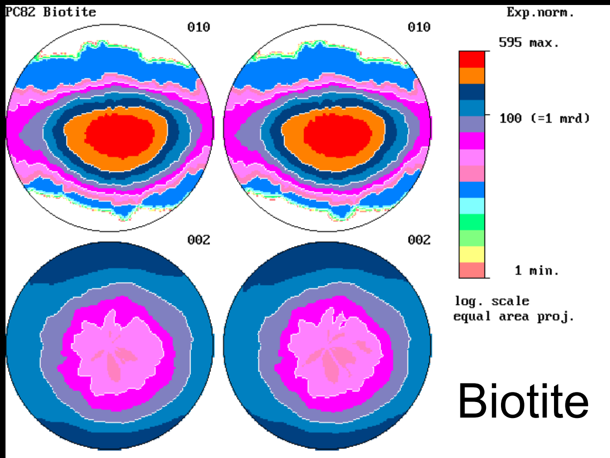
PC82 Biotite
010
010
Exp.norm.
595 max.
100 (=1 mrd)
002
002
1 min.
log. scale
equal area proj.
Biotite

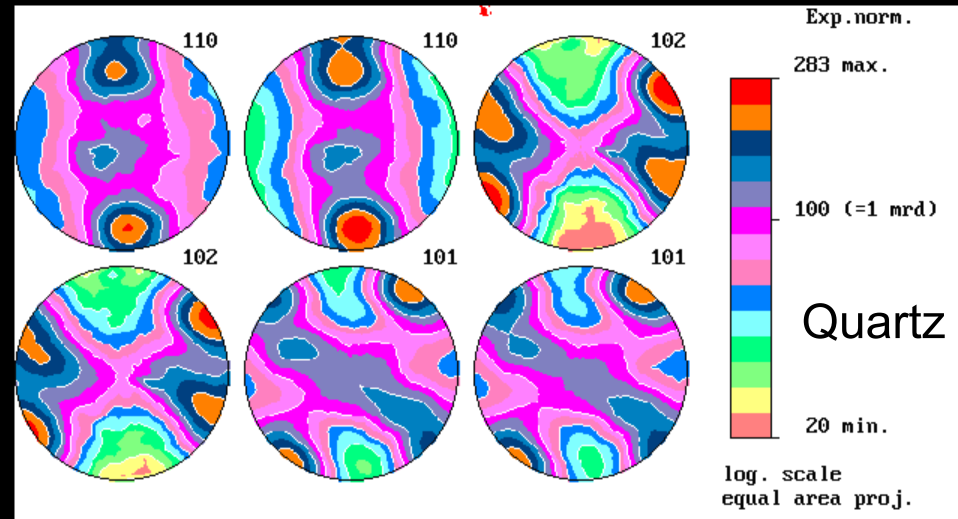
110
110
102
Exp.norm.
283 max.
100 (=1 mrd)
102
101
101
Quartz
20 min.
log. scale
equal area proj.

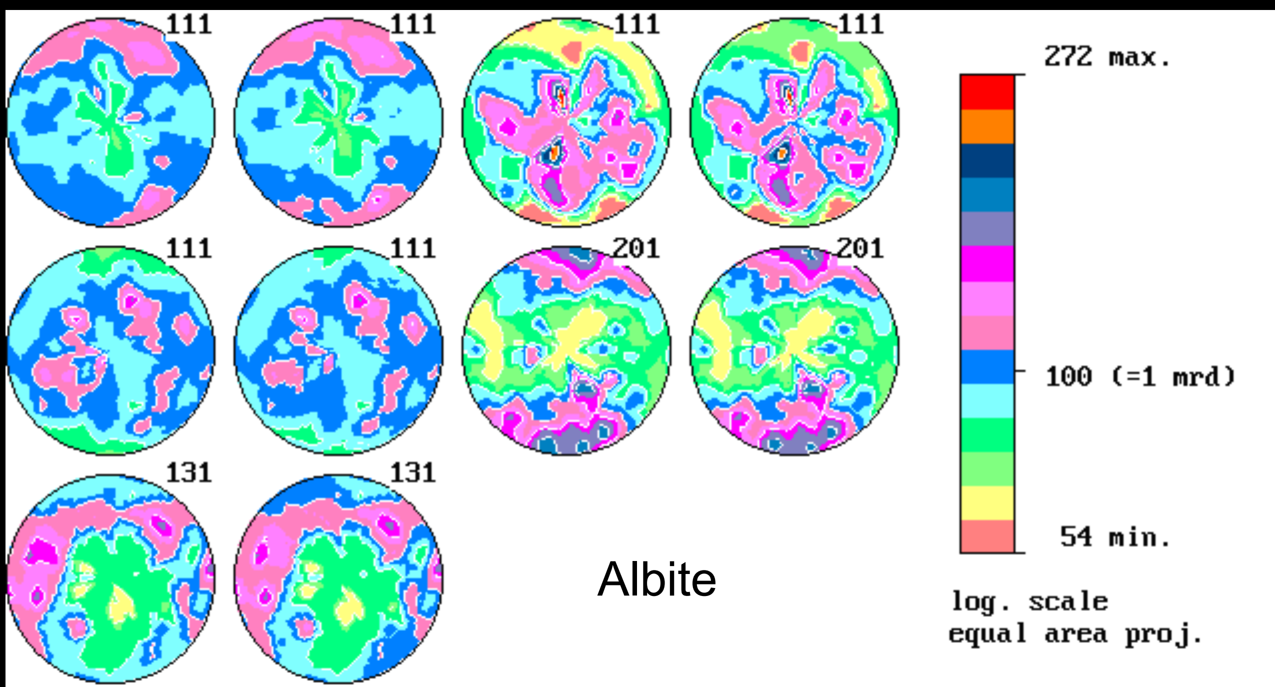
111
111
111
111
272 max.
111
111
201
201
100 (=1 mrd)
131
131
Albite
54 min.
log. scale
equal area proj.

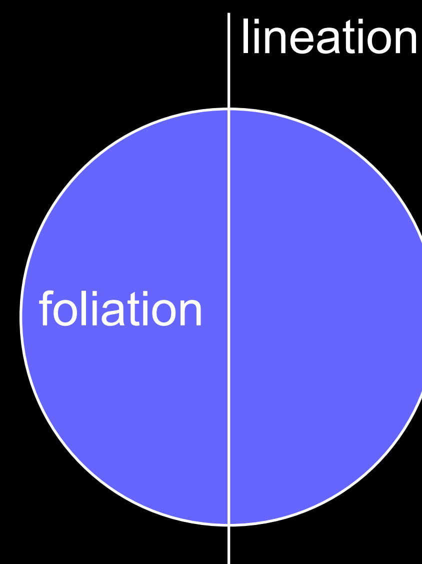
lineation
foliation

Plasma-treated polypropylene films

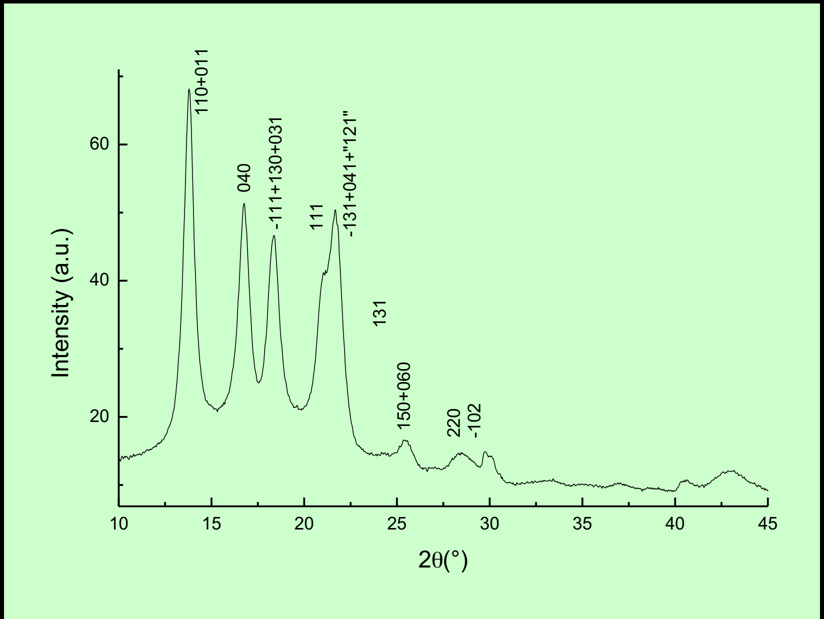

Large broadening + overlaps + amorphous phase

PCT ferroelectric films

Substrate influence:
Interphase overlaps of reflections from the film and the substrate

Intraphase overlaps

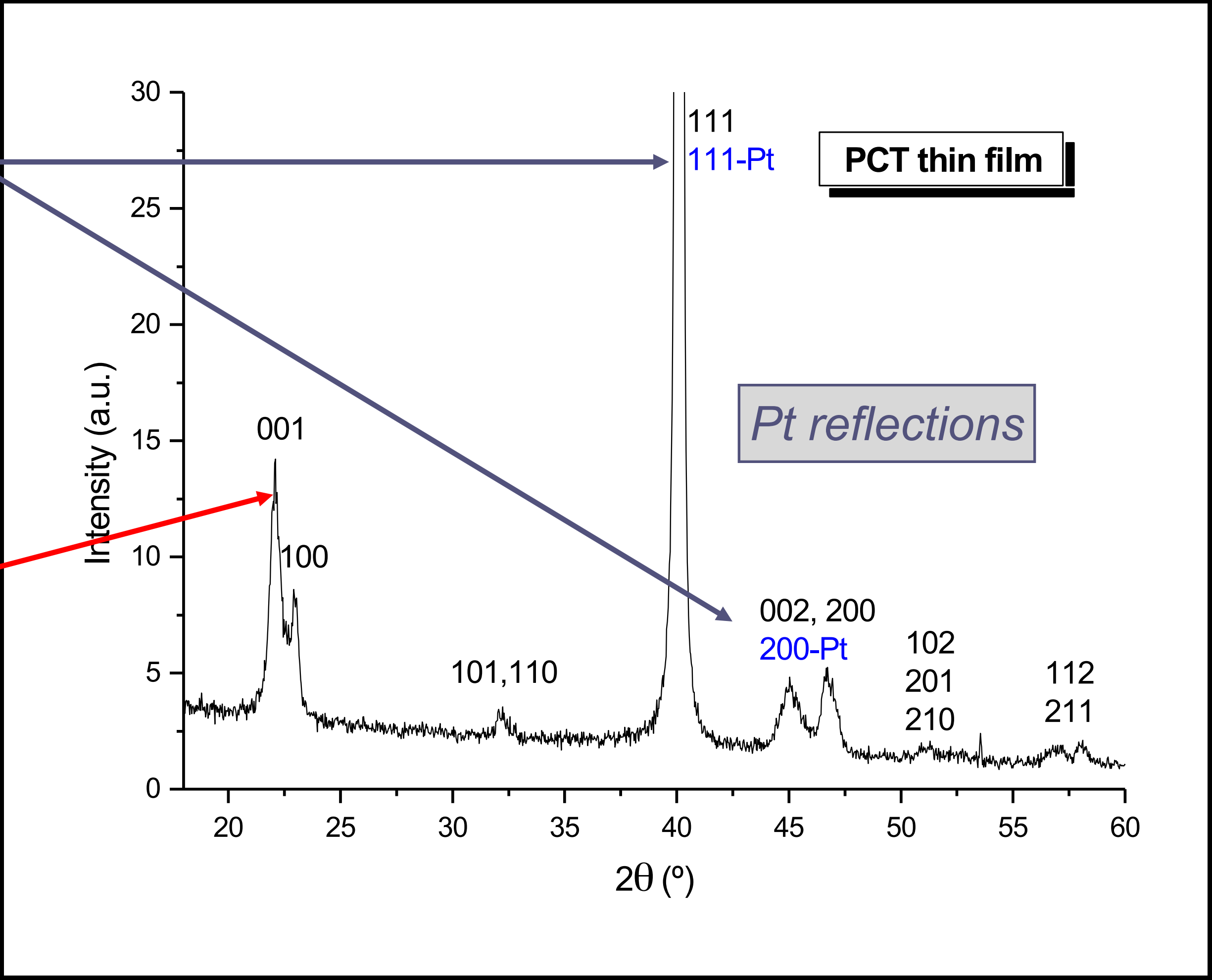

Minimum experimental requirements

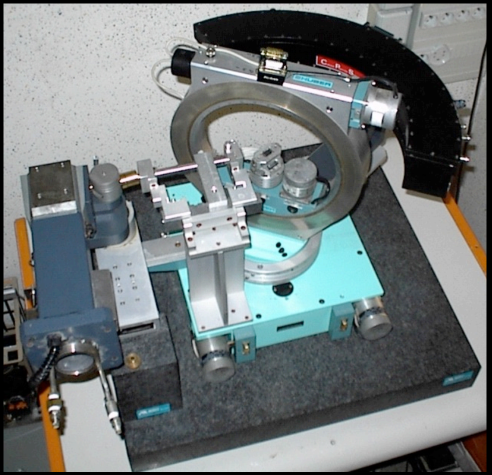

1D or 2D Detector + 4-circle diffractometer
(X-rays and neutrons)
CRISMAT, ILL

+

~1000 experiments (2θ diagrams)
in as many sample orientations

+

Instrument calibration
(peaks widths and shapes,
misalignments, defocusing …)

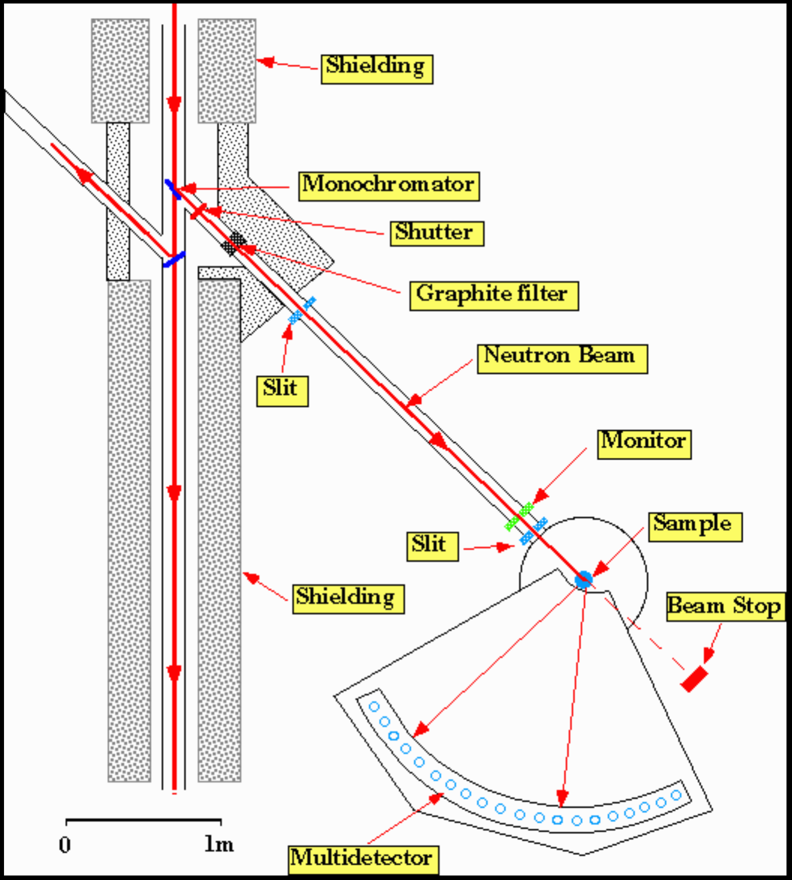

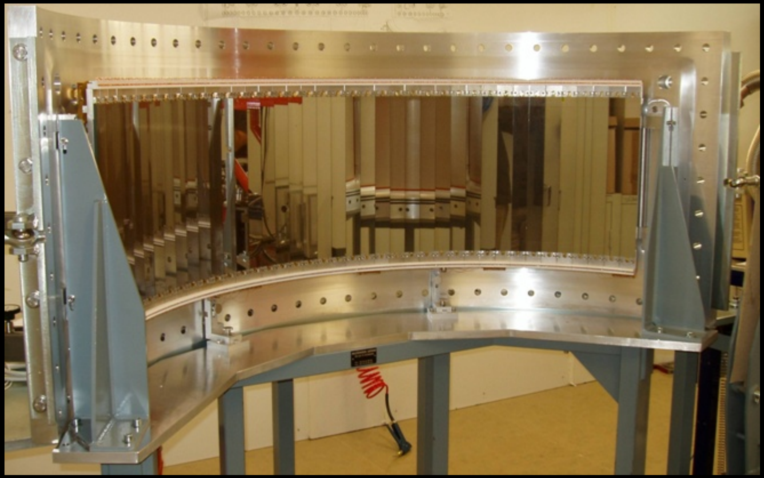

2D Curved Area Position Sensitive Detector

D19 - ILL

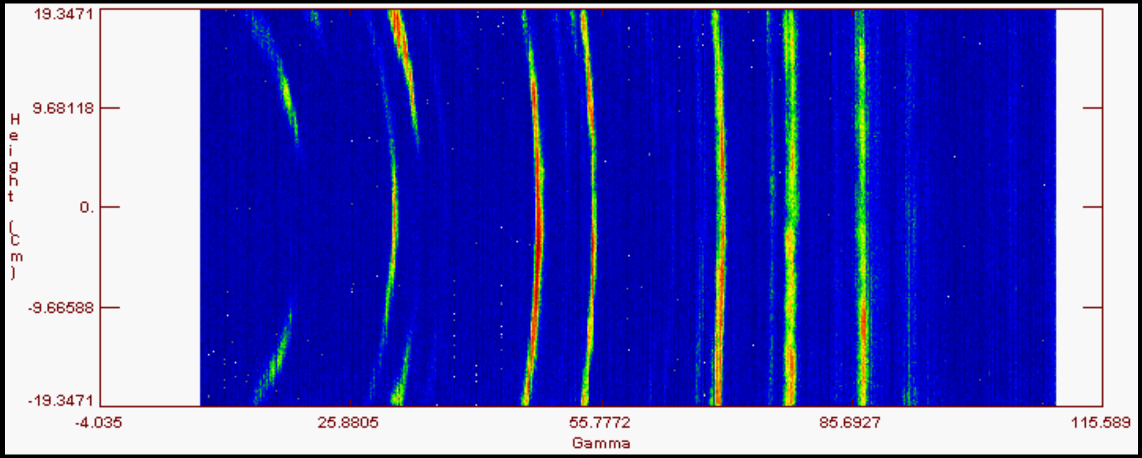

Belemnite sp.

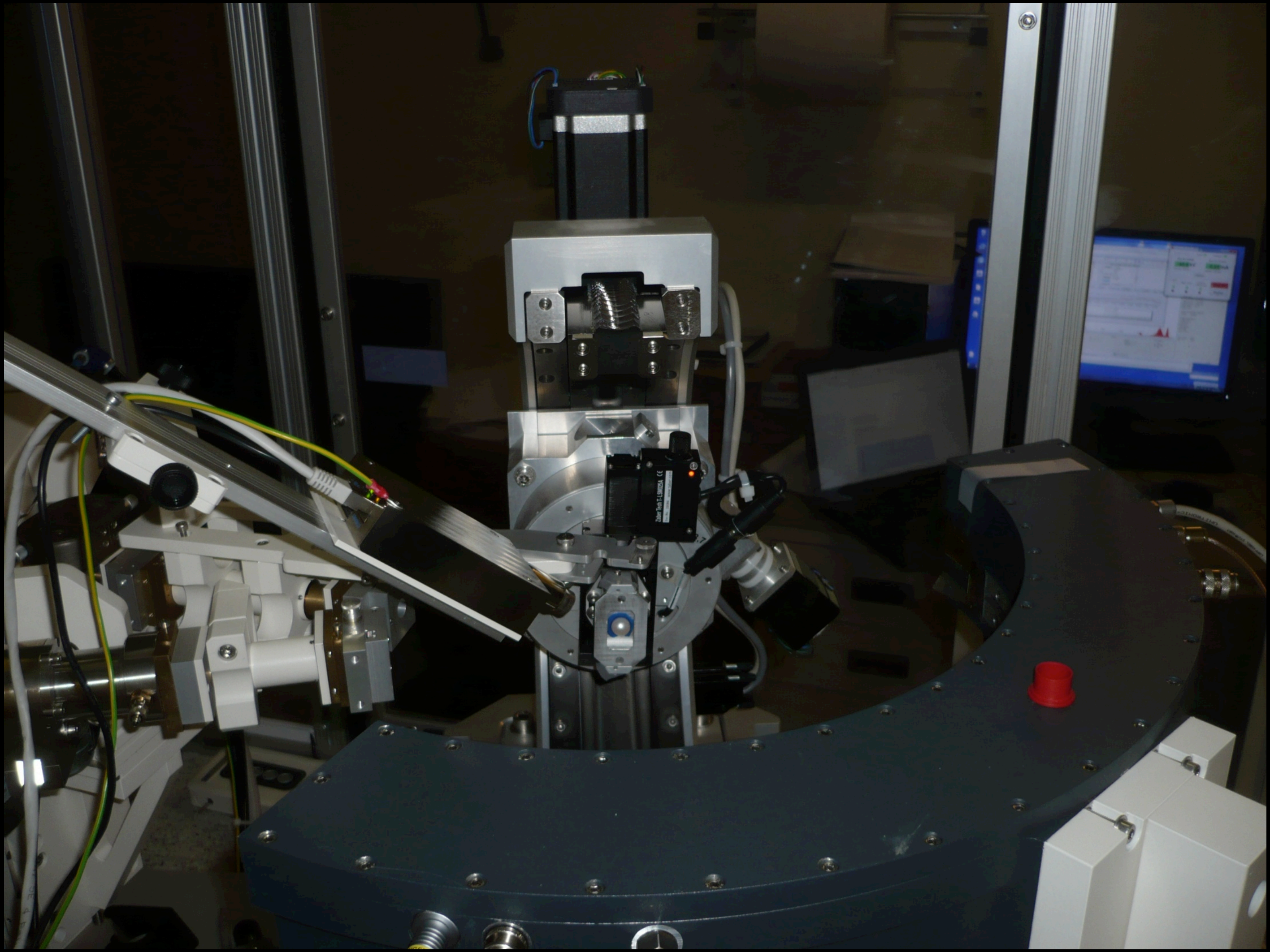

1D CPS + 2 Ips + XRF

With 2 sources (Mo + Cu)

Calibration

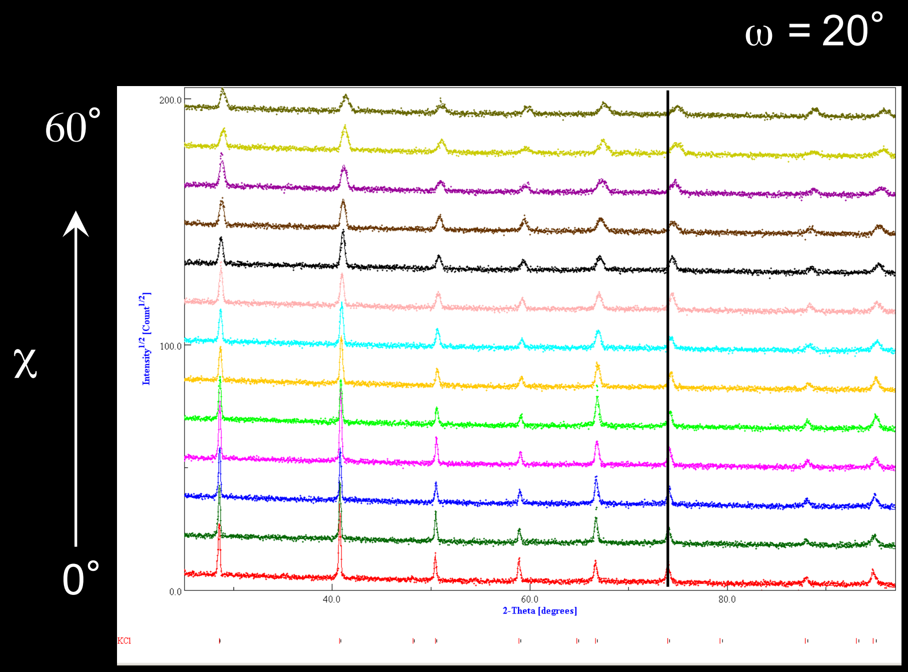

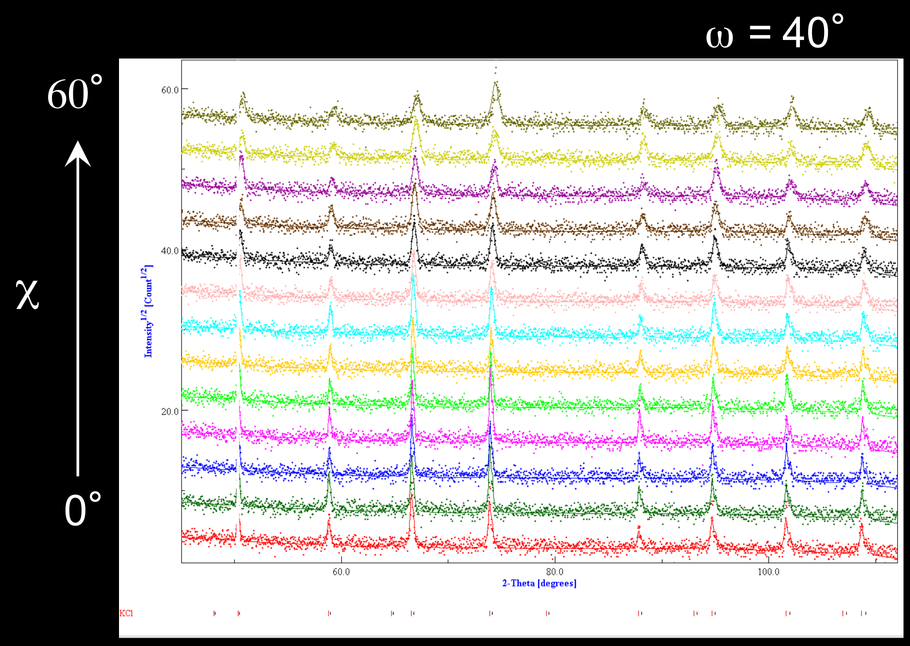

KCl, LaB_6 …

FWHM (ω, χ, 2θ …)
2θ shift
gaussianity
asymmetry
misalignments …

Combined Analysis approach

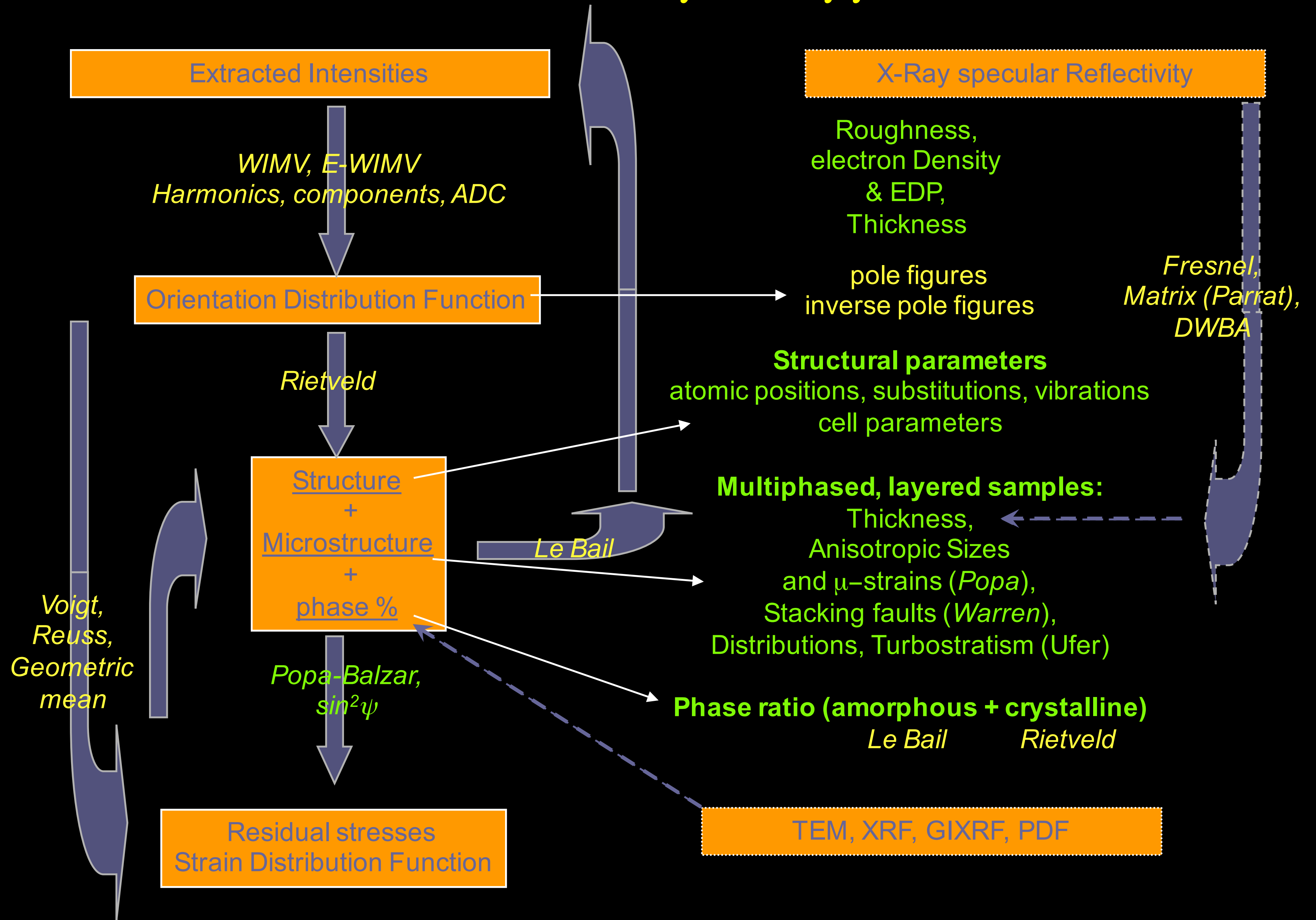

Why not more ?

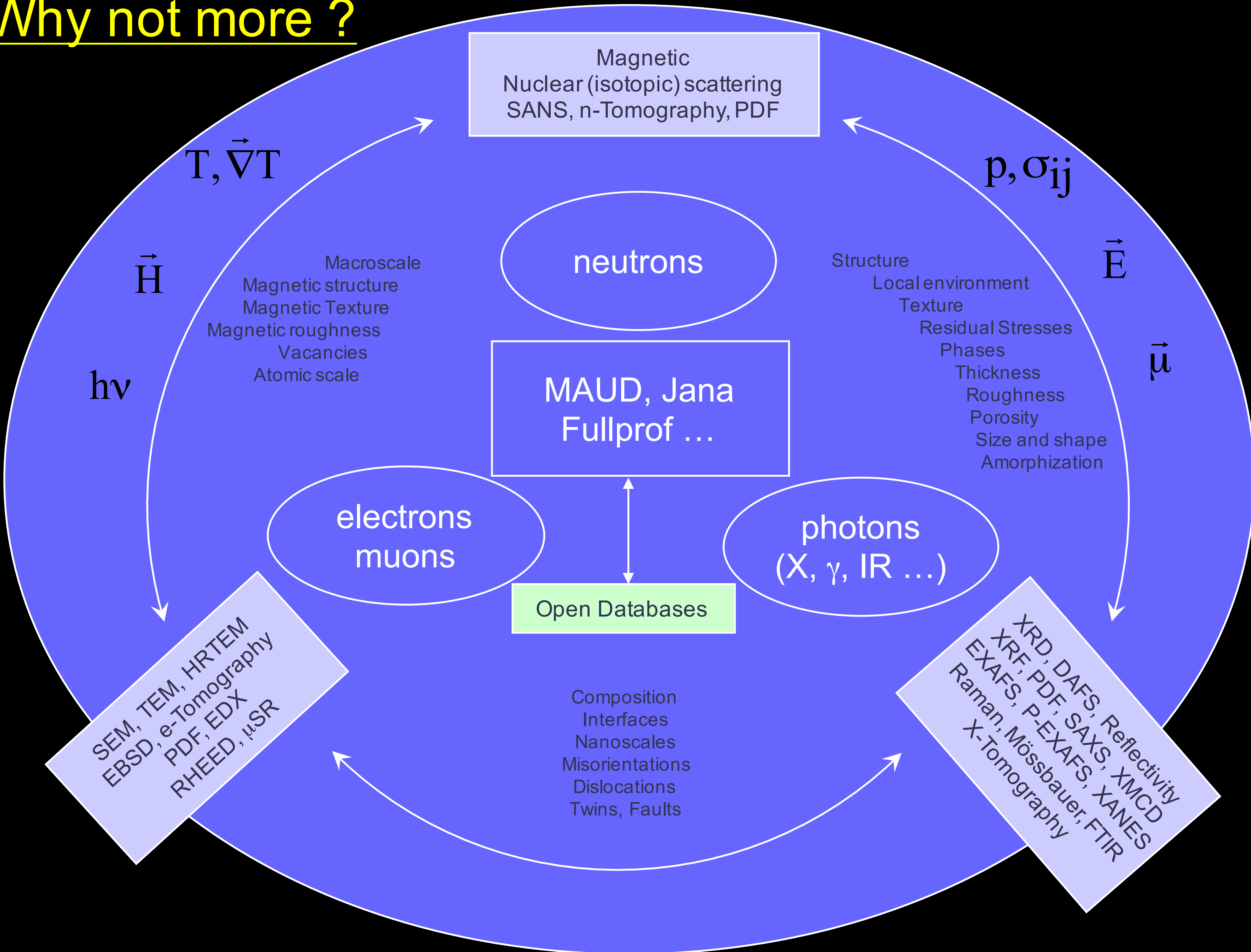
Magnetic
Nuclear (isotopic) scattering
SANS, n-Tomography, PDF
$T, \vec{\nabla}T$
p, σ_{ij}
$\vec{H}$
$\vec{E}$
$h\nu$
$\vec{\mu}$
neutrons
Macroscale
Magnetic structure
Magnetic Texture
Magnetic roughness
Vacancies
Atomic scale
Structure
Local environment
Texture
Residual Stresses
Phases
Thickness
Roughness
Porosity
Size and shape
Amorphization
MAUD, Jana
Fullprof …
electrons
muons
photons
(X, γ, IR …)
Open Databases
SEM, TEM, HRTEM
EBSD, e-Tomography
PDF, EDX
RHEED, μSR
XRD, DAFS, Reflectivity
XRF, PDF, SAXS, XMCD
EXAFS, P-EXAFS, XANES
Raman, Mössbauer, FTIR
X-Tomography
Composition
Interfaces
Nanoscales
Misorientations
Dislocations
Twins, Faults

- Don't want or can't powderise your sample:
  - . Rare: Ice from deep cores, meteorite rocks ...
  - . Expensive: high-tech materials
  - . Impossible: hard materials, polymers, thin structures ...

- Decreases instrument time:
  - . 5° x 5° grid = 1368 points / pole figure
  - . ODF: needs as much pole figures as possible

- Access to other parameters:
  - . crystal sizes, micro-strains, stacking faults + twins (QMA)
  - . residual strains and stresses (QSA)
  - . Structure determination
  - . Phase proportions (QPA)
  - . Thicknesses, roughnesses (XRR)

- Avoid false minima due to parameter correlation:
    . phase and texture
    . Structure and texture
    . Structure and strains
    . Thickness and phase
    …

- Benefit of these correlation to access "true" values
    Textured materials: between powder and single-crystal, angular discrimination

- Easier to practice !